BIODEGRADATION OF PARAQUAT BY BACTERIA-IMMOBILIZED BIOCHAR IN AQUEOUS SOLUTION

NGUYEN CHI TOAN

A Thesis Submitted to the Graduate School of Naresuan University
in Partial Fulfillment of the Requirements
for the Doctor of Philosophy in Environmental Engineering
2022

BIODEGRADATION OF PARAQUAT BY BACTERIA-IMMOBILIZED BIOCHAR IN AQUEOUS SOLUTION

NGUYEN CHI TOAN

A Thesis Submitted to the Graduate School of Naresuan University
in Partial Fulfillment of the Requirements
for the Doctor of Philosophy in Environmental Engineering
2022

Thesis entitled "BIODEGRADATION OF PARAQUAT BY BACTERIA-IMMOBILIZED BIOCHAR IN AQUEOUS SOLUTION"

By Nguyen Chi toan

has been approved by the Graduate School as partial fulfillment of the requirements for the Doctor of Philosophy in Environmental Engineering of Naresuan University

Oral Defense Committee

..... Chair
(Associate Professor Wanpen Wirojanagud, Ph.D.)

..... Advisor
(Associate Professor Dondej Tungtakanpoung, Ph.D.)

..... Co Advisor
(Professor Puangrat Kaewlom, Ph.D.)

..... Internal Examiner
(Assistant Professor Pajaree Thongsanit, Ph.D.)

Approved

.....
(Associate Professor Krongkarn Chootip, Ph.D.)
Dean of the Graduate School

Title	BIODEGRADATION OF PARAQUAT BY BACTERIA-IMMOBILIZED BIOCHAR IN AQUEOUS SOLUTION
Author	Nguyen Chi toan
Advisor	Associate Professor Dondej Tungtakanpoung, Ph.D.
Co-Advisor	Professor Puangrat Kaewlom, Ph.D.
Academic Paper	Ph.D. Dissertation in Environmental Engineering, Naresuan University, 2022
Keywords	Adsorption, Paraquat, Biochar, Bacteria, Biodegradation

ABSTRACT

The work studied the isotherm, kinetic and mechanism of Paraquat adsorption in aqueous solution by using corncob biochar produced from different pyrolysis temperatures and times. The kinetic and isotherm data was fitted by the Pseudo-second-order and Langmuir models. These results showed that the adsorption capacity decreased with increasing pyrolysis temperatures during 6 hours in the order 200, 300, 400, 500, 600^{o}C and decreasing pyrolysis time in the order 2, 3, 4, 5, 6 hours, respectively at 200^{o}C. The mechanisms possibly contributed to hydrogen bonding and pore filling while π-π interaction was minor contributor in the adsorption process. Therefore, the corn cob biochar can become an alternative and promising adsorbent for Paraquat removal from an aqueous solution.

Furthermore, the study explored the isotherm, kinetic and mechanism of paraquat adsorption in aqueous solution by coconut fiber (CFB), corn cob (CCB), bagasse (BGB) and rice husk (RHB) biochars.The biochar characteristics were identified using SEM, BET, and FTIR. Kinetic and isotherm data were followed the Pseudo-second-order and Langmuir models. The biochars were arranged according to their capacity: CFB (12, 72 mg/g), CCB (10.27 mg/g), RHB (9.72 mg/g), BGB (7.79 mg/g) where specific surface area and pore volume determined the adsorption capacity. The intraparticle diffusion model was used to assess the kinetic rate of the adsorption process, which indicates the rate constant of the external diffusion phase where Kip1 was higher than the Kip2 and Kip3 phases. Film diffusion played a major role in the adsorption process. Pore filling, diffusion, hydrogen bonding, π-π and

electrostatic interactions contributed to the mechanism of adsorption. CFB has the highest adsorption capacity (12.72 mg/g), and can be an alternative adsorbent.

From this work, the study aims to explore the isotherm, kinetic and mechanism of paraquat adsorption in aqueous solution by free and immobilized cells of *Pseudomonas putida* on corn cob biochar using three methods: the adsorption method, the covalent bonding method and the entrapment method. The characteristics of bacteria and biochar were studied using SEM, BET. The results shown that kinetic and isotherm data were followed the Pseudo-second-order and Langmuir models. The covalent bonding method was the best immobilization cell method with PQ removal at 4.21 mg/g. Moreover, the PQ adsorption capacity of living cells (3.15 mg/g) is higher than the PQ adsorption capacity of dying cells (2.41 mg/g). The intermediate products such as 4,4-bipyridyl (*m*/*z* 155) and malic acid (*m*/*z* 133) are detected in the effluent of samples (free cells, fixed cells on CCB, CFB, BGB, RHB using entrapment, covalent binding and adsorption methods) was collected at 35 h experimental period for analysis Paraquat products by GC/MS. The experiment was set up at the optimal operational concentration of Paraquat being 25.73 mg/L. The study encircles biodegradation of paraquat by bacteria immobilized biochar in aqueous solution. The discovery of these intermediate products sheds light on the specific degradation pathways of paraquat and may provide valuable information for developing effective strategies for the remediation of paraquat contaminated environments.

ACKNOWLEDGEMENTS

First of all, I would like to express my gratitude to Professor Dr. Puangrat Kajitvichyanukul for the supervision and her helps. Moreover, I am also grateful to Associate Professor Dr. Dondej Tungtakanpoung for his guidance, supports and helps. I would like to thank to Associate Professor Dr. Wapen Wirojanagud, Assistant Professor Dr.Pajaree Thongsanit, thesis committee members, for useful discussion, comments and advice.

I sincerely thank to all members of CERI lab, Naresuan University for their kind assistance throughout my study period (2015-2022). I also especially thank Ms. Manee Jindakaraked (Rammy) for her enthusiastic help in the first days at Naresuan University in Thailand. Moreover, I am grateful to all technical and staff in the Department of Civil Engineering. In particular, I would like to thank Ms. Witchaya Imkrajang (P' Tuk) and Ms. Nipawan Chanthakhun (Biew) who helped me to borrow lab instruments. I also specially thank Professor Thammarat Koottatep at AIT, Associate Professor Dr.Bui Xuan Thanh at Ho Chi Minh City University of Technology and Dr.Tra Van Tung for encouragement me to study at Naresuan University, Thailand.

I sincerely thank Naresuan University's scholarship for the financial support that allowed me to complete my Ph.D. program at Naresuan University. Moreover, I have special thanks to Ms. Thatsaporn Kanokphara and Ms. Sukairaito Akatsukinosora who kept in touch with me and maintained my student status in order to try to finish my PhD program.

I am especially expressing my profound gratitude to my parents, my family members and friends for their infinite love and nonstop encouragement during my study period. Furthermore, I am grateful to my uncle Dr. Le Nhu Linh – President & CEO of Petro Vietnam Power Corporation, who always supports and encourages me to complete my PhD program.

Finally, I would like to dedicate this work to my wife Ms.Nguyen Thi Hai Ha and my son Nguyen Tien Dung (Pooh) who always stand side by side with me, share both the joy and sadness, the source of continuous in completing this work.

Nguyen Chi toan

TABLE OF CONTENTS

Page

LIST OF TABLE

Page

LIST OF FIGURE

Page

ABBREVIATION

PQ	=	Paraquat
CCB	=	Corn cob biochar
CFB	=	Coconut fiber biochar
BGB	=	Bagasse biochar
RHB	=	Rice husk biochar
SEM	=	Scanning electron microscope
FTIR	=	Fourier Transform Infrared spectroscopy
BET	=	Brunauer Emmett Teller
pHpzc	=	pH point of zero charge
SSA	=	Specific Surface Area
TPV	=	Total Pore Volume
BC200-6	=	Biochar was produced pyrolysis temperature at 200^0C in 6 hours
BC300-6	=	Biochar was produced pyrolysis temperature at 300^0C in 6 hours
BC400-6	=	Biochar was produced pyrolysis temperature at 400^0C in 6 hours
BC500-6	=	Biochar was produced pyrolysis temperature at 500^0C in 6 hours
BC600-6	=	Biochar was produced pyrolysis temperature at 600^0C in 6 hours
BC200-5	=	Biochar was produced pyrolysis temperature at 200^0C in 5 hours
BC200-4	=	Biochar was produced pyrolysis temperature at 200^0C in 4 hours
BC200-3	=	Biochar was produced pyrolysis temperature at 200^0C in 3 hours
BC200-2	=	Biochar was produced pyrolysis temperature at 200^0C in 2 hours

CHAPTER I

INTRODUCTION

Background of study

The Food and Agricultural Organization of the United Nations, defines a pesticide as “any substance or mixture of substances intended to prevent, destroy or control any pest, including vectors of human or animal disease, unwanted species of plants or animals causing harm during or otherwise interfering with the production, processing, storage, transportation or marketing of food, agricultural commodities, wood and wood products or animal feedstuffs, or substances which may be administered to animals for the control of insects, arachnids or other pests in or on their bodies” (FAO, 2002).

Historically, global pesticide use increased rapidly after the World War II as wartime technological advances were applied to peacetime production (Murray et al.2000). First DDT and then an array of other organochlorine and organophosphate compounds were introduced into US agriculture and later into farming systems around the world. Perkins et al. (1982) indicated that chemical manufacturing became “the premier industry in the US” in the post war period. In addition, pesticide sales increased steadily over the ensuing half century, reaching $ 32 billion annually by 1997 (Agrow, 1998). To be more specific, Marcus et al. (1980) reported that Rachel Carson in her classic work, *Silent Spring* in 1964 played a crucial role in inspiring government regulation including the creation of the Environmental Protection Agency (EPA). The EPA grew directly out of growing public awareness of pesticide problems. More seriously, the problem of acute pesticide illnesses grew to a level of 2-3 million poisonings worldwide annually, mostly in the developing world, by the end of the 1980s (WHO, 1990). Then the study by Wolff et al. (1993) implicated pesticides in the rising rate of breast cancer and studies by Rosenstock et al. (1991) and McConell et al. (1993) implicated pesticides in neurological damage experienced by agricultural workers and a range of problems associated with disruptions of the endocrine system (Colburn et al. 1996).

Technology related to the removal of pesticides are necessary to prevent the leaching of pesticides, into water sources, as well as the treatment of contaminated water sources. Pesticide removal technology are needed to meet environmental standards and improve the ecosystem and the environment for aquatic organisms and plants. The European standards permit the maximum concentration of pesticide or paraquat in drinking water is 0.3 µg/L and in 1-3 µg/L for surface water (Nanseu-Njiki et al., 2010).

In recent years, biochar is seen as a promising adsorbent with many applications in the environment. Low cost biochar which is relatively abundant and has comparable adsorptive abilities and is considered to be a potential substitute for commercial adsorbents such as activated carbon which is too expensive for use in environmental remediation and water treatment; including, wastewater treatment applications in low-income and remote communities in developing regions (Kearns, Wellborn, Summers, & Knappe, 2014).

Several microorganisms have been isolated which are able to utilize pesticides as a source of energy. There are some examples of fungi including *Trametes hirsutus, Phanerochaete chrysosporium, Phanerochaete sordia and Cyathus bulleri* that are able to degrade lindane and other pesticides (Singh and Kuhad, 1999, 2000). According to Tu, & Bollen (1968), *Aerobacter aerogenes, Agrobacterium tumefaciens, Pseudomonas fluorescens* and *Bacillus cereus* were able to utilize PQ as carbon and nitrogen sources in synthetic media. Moreover, Martani et al. (2006) investigated the role of bacterial inoculation on acceleration of PQ degradation in peat soil. They indicated that *Micrococcus sp. and Achromonas sp.* were able to degrade paraquat around 25% in undecomposed peat soil containing 20 ppm PQ. Therefore, *Pseudomonas putida* is a promising degrader in the biodegradation process. Specifically, *Pseudomonas putida* is a bacterium of the family of *Pseudomonadacease*, genus of *Pseudomonas spp*. It is a gram-negative, mesophilic, aerobic bacterium commonly present throughout the environment which can degrade various natural and synthetic compounds (Vizma Nikolajeva et al., 2012). Therefore, suitable pesticide treatment could be combinations of biological, chemical and physical processes.

Statement of the Problem

Presently, the alarming increase in the application of pesticides to control agricultural pests could cause environmental pollution and have adverse effects on human health, aquatic organisms and plants. They are toxic substances released into the environment as persistent organic pollutants (Gavrilescu, 2005). To be more specific, the fate and transport of paraquat are considered to be affected by its physical and chemical properties which can threaten groundwater, surface water and the soil. In addition, paraquat is a high risk to the ecosystem and human beings due to its high water solubility (Nanseu-Njiki et al., 2010). According to Weng (2014) and Wang (2015), adsorption is one of the most effective and suitable physical techniques for removing contaminants from water because the costs of this method is inexpensive and easy to implement**.** Moreover, one of the more interesting characteristics of biochar that makes it attractive for use is because it is a carbon-rich black solid material with high porosity and abundant functional groups and a high specific surface area (Zhu et al., 2005). In addition, biochar exhibits various physical and chemical properties depending on feedstock and pyrolysis conditions. Therefore, the removal of pesticides by investigating the feedstocks or biomass from various materials with different conditions of burning is necessary to find the best quality biochar at low cost and with high adsorption capacity.

Biodegradation has been useful in degrading residue pesticides in soil and water for human use (Singh et al. 2002, 2003a, b, 2004, 2005, 2006 and Xu et al. 2008). Moreover, immobilization of microbial cells have more advantages than free cell such as higher operational stability, reduce the costly processes of cell recycle and cell revovery, improve genetic stability, easier to use in reactors and faster degradation of toxic pollutants (Jianlong et al. 1995, 1997, 1999 and 2001; Singh and Balomajumder 2016). Immobilized cells have ways to protect themselves from direct contact with toxic pollutants (Felshia et al. 2017). The usage of immobilized cells can apply to enhance the retention time and existence of the bioremediation agents in the polluted sites (Singh and Balomajumder 2016).

Above all, this study addresses the "**Biodegradation of paraquat by bacteria-immobilized biochar in aqueous solution**."

Objectives of the study

This study was conducted to achieve the following of objectives:

The first objective was the synthesis of biochar in order to find a suitable biochar for the removal of paraquat and to characterize the properties of biochar in order to explain the interaction between biochar and paraquat. Adsorption studies explore isotherm adsorption to identify the adsorption capacity of biochar and paraquat; kinetic adsorption to determine the movement of paraquat into the biochar and mechanism adsorption of paraquat and biochar.

Second objective was to study free and fixed cells of *Pseudomonas putida* on the removal of PQ. The specific objectives of the experimental design were aimed at assessing the growth of free cells under different environmental conditions such as pH and various initial concentrations, compared to the efficiency of PQ removal by free and fixed cells of *Pseudomonas putida.*

Scope of the study

1. The materials were obtained from corn cob, coconut fiber, bagasse, and rice husk which were collected around Naresuan University and used to synthesize biochar.

2. Paraquat was selected as a pollutant in the synthesis of wastewater for lab scale of study.

3. The microorganism *Pseudomonas putida* which can degrade Paraquat, was chosen for this study.

4. Immobilization methods include the adsorption method, covalent binding method and the entrapment method.

5. The experiments were implemented in the lab scale of study for the contaminants in water at the Center of Excellent Research Innovation (CERI) lab, Naresuan University.

CHAPTER II

LITERATURE REVIEWS

Pesticide pollution

Overview of Pesticides

Presently, the purpose of modern pesticides are effective in smaller quantities, more target specific, and easy degradation in the environment. The study of Apiwat (2015) suggested that it is necessary to find biological agents to control agricultural pests for replacing chemical pesticides. According to standard classification criteria, pesticides can be categorized in two ways: chemical properties and target organism. The chemical classes are the basis of their physicochemical properties and behavior in water and soil as ionic and nonionic pesticides (Figure 2-1). Hence, classification can be explained as ionic pesticides: i) Acidic: dicamba, ioxynil, mecoprop; ii) Basic: atrazine, cyanazine, propazine; iii) Cationic: diquat, paraquat; iv) others: bromacil, cacodylic acid, isocil and nonionic pesticides: i) Carbanilates: chloropham, swep; of chloramben); Acetamides (CDAA); Carbothloates (molinate); Anilides (Alachlor); Methyl carbamates (carbaryl, terbutol) ; Urea (cyduron, linuron).ii) Dinitroanilides: benefin, trifluralin; i)Chlorinated HCs: endrin, lindane; iv) Organophosphate: ethion, parathion; v) Others: Benzonitriles (dichlobenil); Esters (methyl-ester)

Table 1 Classification of pesticides on the basis of their significant physicochemical properties and behavior in water and soil

Pesticides class	Chemical property	Some chemicals
Ionic pesticides	Cationic	Diquat, Paraquat, Mortamquat
	Basic	Ametryne, Atrazine, Cyanzine, Propazine
	Acidic	Dicamba, Ioxynil, 2,3,5-T, Fenac
	Miscellaneous	Bromacil, Isocil, Terbacil
Non-ionic pesticides	Chlorinated HCs	DDT, Endrin, Lindane, Methoxychlor
	Ops	Ethion, Parathion, Fenthion, Diazon
	Dinitroanilides	Benefin, Oryzalin, Isopropalin, Dinitramine
	Carbanilates	Chloropham, Swep, Prophan, Barban
	Benzonitriles	Dichlobent
	Esters	Isopropyl ester of 2,4-T, Methyl ester of Chloramben
	Anilindes	Alachlor, Propanil, Diphenamide, Propachlor
	Methyl carbamates	Carbaryl, Terbutol, Zetran
	Ures	Linuron, Diuron, Chloroxuror

Source: Gavrilescu, 2005

On the other hand, pesticides are generally classified according to the types of pests that they control (Table 2).

Table 2 Pesticide classification based on target organisms

Pesticides class	Target organisms	Some chemicals
Algicides or algaecides	Algae	Copper sulphate, Polyquat
Avicides	Birds	Strychnine, DRC-1339, CPTH, Avitrol
Bactericides	Bacteria	Hypochlorites, Chloramines, $HgCl_2$
Fungicides	Fungi and oomycetes	Barium polysulfide, Benalaxyl,

Pesticides class	Target organisms	Some chemicals
		Ampropylfos, Captafol, Dodicin
Herbicides	Weeds	2,4-D, Glyphosate, Atrazine, Agent Orange, Paraquat
Insecticides Ovicides Larvicides Adulticides	Insects Eggs Larve Adults	Organochlorines, Carbamates, DDT, Organophosphates, Pyrethroids, Arsenates, Sarin, Tabun, Soman
Miticides or acaricides	Mites	Fenazaquin, Propargite, Dicofol, Fenpropathrin, Etaxazole, Sulphur
Molluscicides	Slugs and snails	Tralopyriltrifenmorph, Methiocarb, AllicinTrimethacarb, Metaldehyde
Nematicides	Nematodes	Aldicarb, Furadan, Vydate, MocapStandak, Dasanit, Nemacur
Rodenticides	Rodents	Scilliroside, Strychnine, Mieshuan, Pindone
Virucides	Viruses	Bingqingxiao, Dufulin, Ribavirin, Xinjunan

Source: Gavrilescu, 2005

Current situation of pesticide pollution in Thailand

Global pesticide use increased rapidly after the World War II as wartime technological advances were applied to peacetime production. First DDT and then an array of other organochlorine and organophosphate compounds were introduced into farming systems around the world. Perkins et al. (1982) shown that chemical manufacturing became “the premier industry in the US” in the post war period. With the rise in pesticide use came highly effective promotional campaigns as the pesticide industry touted new products. When a pesticide is formulated, a lot of inert material is added along with the active ingredients. In 1987, a study by Jeyaratnam, indicated that the significance of acute pesticide poisoning among agricultural workers in Thailand was placed first out of 4 Asian countries which included Indonesia, Malaysia, Sri Lanka and Thailand.

Thailand is one of the most important agricultural countries of Asia. A lot of chemicals are imported for agricultural use. According to a report by Apiwat et al. (2015), expenditure by farmers on imported pesticides rose from 14,000 million Baht in 2007 to almost 24,000 million Baht in 2013 (Figure 1). This expenditure was as follows: herbicides formed the majority at (62-79%) followed by insecticides (12-23%) and fungicides (5-11%).

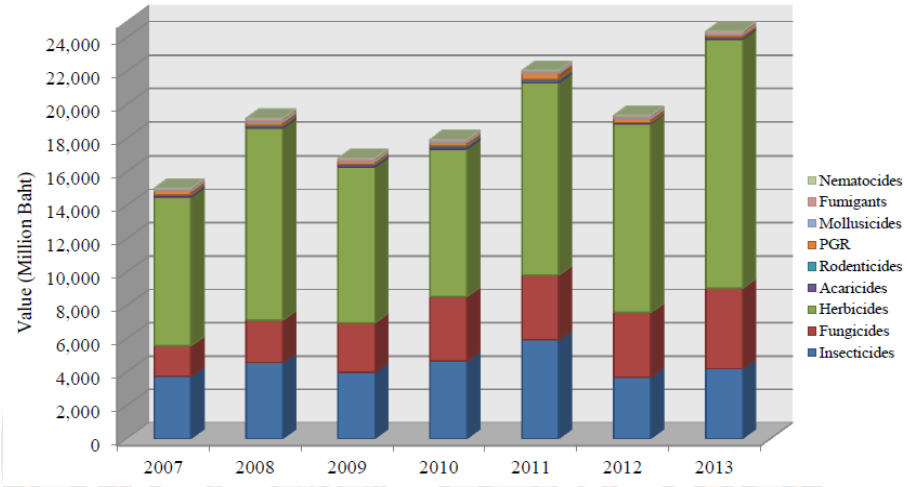

Figure 1 Pesticides import in value into Thailand 2007-2013

Source: Apiwat et al., 2015

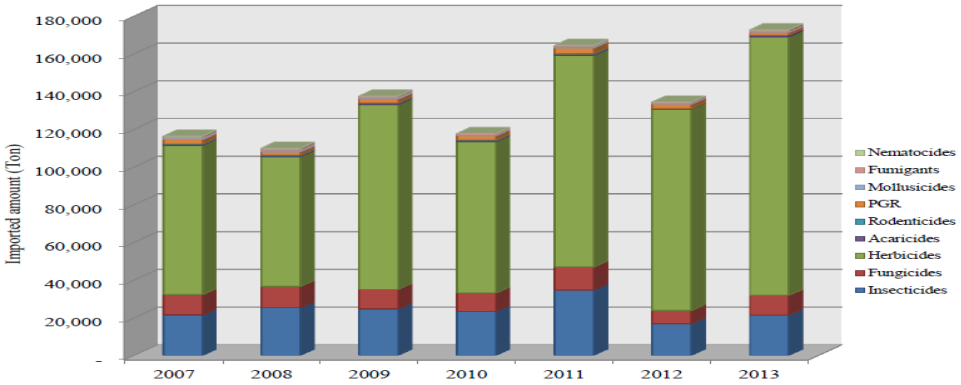

Figure 2 Demand for pesticides in the Thai agricultural sector

Source: Apiwat et al., 2015

There are many imports of toxic chemicals, which are mostly used in the agricultural sector, such as insecticides, herbicides and fungicides. Apiwat et al. (2015) indicate that from 2007 to 2013 there was an obviously increasing trend in the use of imported pesticides. Imports rose from about 110,000 tons in 2007 to approximately 172,000 tons in 2013 (Figure 2). In addition, this increase showed that pest control in Thai agriculture is mostly dependent on the use of pesticides to control pests in the agricultural sector.

Herbicides

Herbicides are defined as phytotoxic chemicals used to kill various types of weeds or interrupting their normal growth (Cobb, & Reade, 2010). They have different degrees of specificity. The work of Gupta (2004) reported that the use of herbicides on a global scale is 47.5% of the total pesticide usage. The consumption of herbicides in India is low because weed control is mainly done by hand weeding.

In his book, Weed Science Society of America, Senseman (2007), indicated that there are approximately 150 active chemical ingredients, which are formulated into hundreds of commercial herbicide products. The active ingredients are organic compounds which contain carbon, hydrogen, oxygen, and various other chemical elements.

The fate and transport of herbicides can be explained as follows in Figure 3 below.

Firstly, herbicides enter the soil and water as the result of direct application and runoff from plant surfaces. Secondly, a part of the herbicide can be transported and decomposed due to volatilization and photo decomposition. Thirdly, a residual part can be adsorbed into the soil, and is soluble in water. Herbicides can be subjected to biological degradation by microbial activity or chemical decomposition such as hydrolysis. Finally, the residue leaches into the ground water.

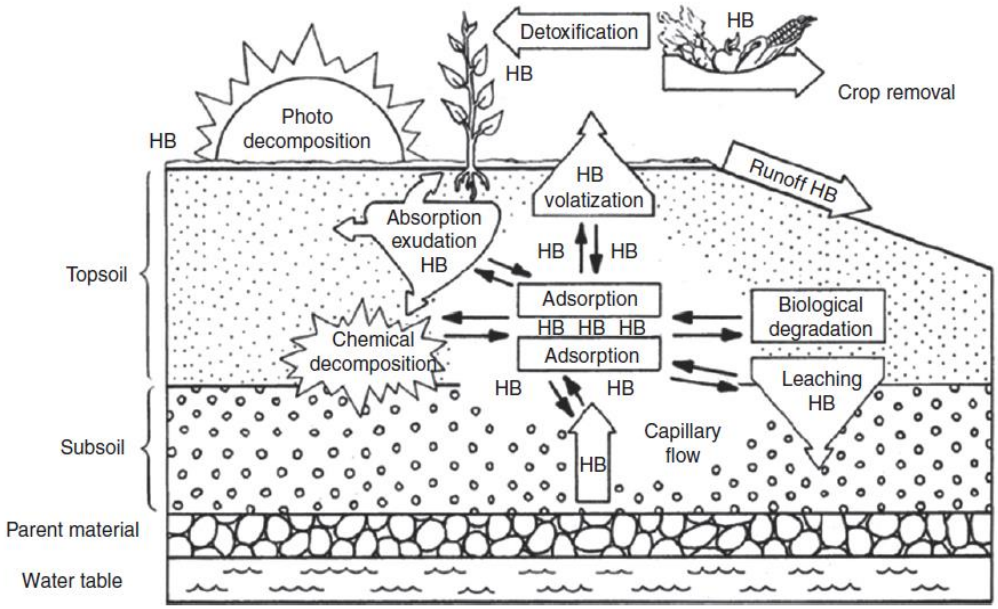

Figure 3 Fate and transport of herbicides in the environment

Source: Ross, & Lembi, 1999; Weber et al., 1974

Paraquat

Paraquat is a well-known herbicide in Thailand. It is a non-selective contact herbicide which kills all green plant tissues that it comes into contact with. It is effectively used for the control of broad-leafed weeds and grasses. According to Cheah et al., 1997, paraquat is often used in vegetable, rice paddy, rubber, palm oil and cocoa production in Malaysia. In the case of Thailand, a preliminary survey showed that it has been used to control weeds in the production of field crops such as chili, corn, soybean, sugarcane and fruit trees as oranges. Moreover, it has also been widely used in the control of aquatic weed. It should be sprayed when the weeds are young and less than 30 cm high.

Characteristics of paraquat

Paraquat has IUPAC name 1,1'-Dimethyl-4,4'-bipyridinium dichloride, molar mass (257 g/mol) and molecular structure in Figure 4.

Figure 4 Chemical structure of paraquat

The basic chemical properties of paraquat that are related to its fate and transport are solubility in water and its volatility. Based on a report of the National Institute for Occupational Safety and Health, authored by Husband (2001), the high solubility in water is 680 g/L at 200C and at pH 7.2; the vapor pressure is <10-7 mmHg (20^0 C). So Henry's Constant can be calculated as:

$H=VP/S = 5 \times 10^{-17}$ atm-m^3/mole

From Henry's law constant << 10-7 atm-m3/mole, paraquat is nonvolatile. Moreover, paraquat with log Kow = -4.5 at 25^0C. In other words, this means Kow = $10^{-4.5}$ and less than 10. Therefore, it can be said that paraquat is hydrophilic or soluble (like water).

Abiotic reaction(s): Chemical (Abiotic) degradation occurs by different reactions which include hydrolysis, oxidation-reduction, ionization and photolysis reactions. However, no hydrolysis was observed at pH 5, 7 or 9 and kept at 25 or 40^0 C (Upton, 1985). This suggests that the concentration of paraquat is stable and not subject to hydrolysis.

Oxidation-Reduction (Redox) reactions involve the transfer of electrons from the reduced species to the oxidized species in Figure 5.

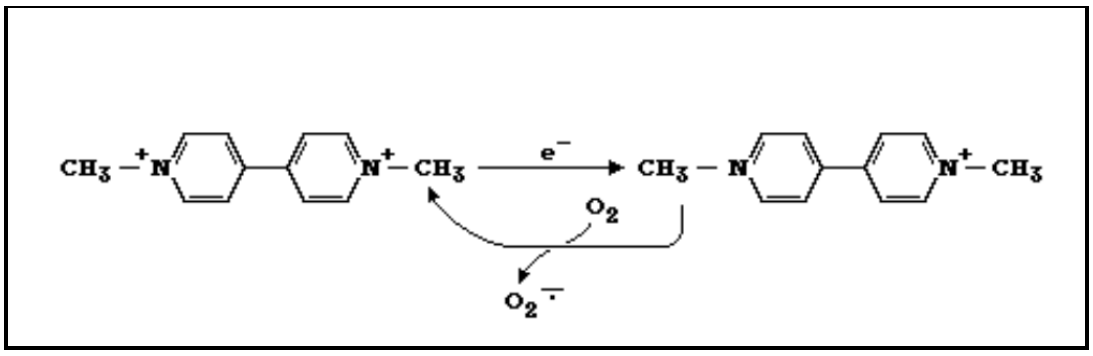

Figure 5 Paraquat reduction oxidation reaction

Source: WHO, 1984

Photolysis reaction is a chemical process by which paraquat is broken down into smaller units through the absorption or UV radiation in Figure 6.

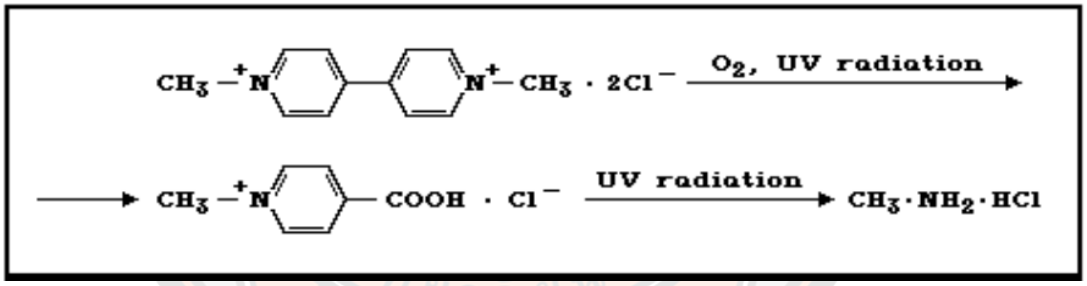

Figure 6 Photochemical paraquat dichloride degradation

Source: Slade, 1965

Fate and transport of paraquat in environment

According to Gavrilescu, M. (2005) the pesticides' characteristics are important in determining the fate and transport of the pesticide. The pesticides' characteristics include: solubility in water and a tendency to be adsorbed into the soil. To explain this statement, the concentration levels of the pesticide were, according to the annual Research Report of the Department of Agriculture, Bangkok, 2000, nearly as high in groundwater (1.5–18.9μgL-1) as in surface water (9.3–87.0μgL-1). In addition, paraquat, a polar organic compound, is very rapidly adsorbed in clay and

organic soil matter. Adsorption isotherm models have been employed and differentiated by measuring concentrations of paraquat remaining in the soil solution. The Langmuir equation describes paraquat sorption well at high concentrations approaching the soil cation exchange capacity (CEC), whereas the Freundlich model fits best at low concentrations.

Brownawell et al. (1990) suggests that paraquat sorption at less than 20% of CEC could be detected. Several soil constituents are known to influence paraquat adsorption. Clay and organic matter are among the leading factors governing electrostatic attraction and charge transfer. Thus the amount of adsorption is related to the CEC of clay, and sorption affinity is largely dependent on the type of clay minerals with montmorillonite a better sorbent than kaolinite, especially at high pH. Paraquat is more difficult to desorb from montmorillonite than from kaolinite or vermiculite, because interlayer adsorption in montmorillonite is stronger than surface adsorption.

Biochar

Selection of biochar (support materials)

Biochar is a recently coined term emerging in conjunction with the renewable fuel, soil amelioration, and carbon sequestration. Warnock et al. (2007) defined biochar to include char and charcoal, excluding fossil fuel products, produced by the partial combustion of carbonaceous organic materials like trees and plants. In the absence or partial supply of oxygen during combustion, the process inhibits complete combustion of the source material. According to Ahmad et al. (2013), biochar is somehow interrelated to each other in terms relating to its production and applications. It is critically important to differentiate between terminologies like biochar, charcoal, and hydrochar. The primary difference between these products lies in their fate. Charcoal is a carbon-rich solid product prepared via charring biomass and is used as a fuel source for producing energy where biochar is an alternative term for charcoal when it is used for a specific purpose, i.e. soil amendments (Lehmann et al., 2009). Typically, biochar is produced as a solid by-product material in a dry carbonization process like pyrolysis (Libra et al., 2011; Manya et al., 2012; Sohi et al., 2010; Brewer et al., 2009).

The selection of biochar can be according to the following: Firstly, the use of abundant biomass for the synthesis of biochar is increasing because of its availability in large quantities and at low cost. Secondly, biochar is characteristic i.e. specific physiochemical properties such as carbon-rich, porous with oxygen functional groups and a high surface area and a surface charge which are influential factors in controlling the sorption of organic contaminants (Zhu et al., 2005).

Biochar production

Biochar is normally produced by pyrolysis process. Pyrolysis is a thermochemical decomposition process of biomass which controls the temperature from 350 to 800^0C in the absence of oxygen. According to the studies of Brownsort (2009) and Mohan (2006), pyrolysis results are generated with the main properties of: a carbon-rich solid product (biochar), a volatile substance which can further be partially condensed to a liquid phase (bio-oil), and the remaining so-called "non-condensable" gases, like CO, CO_2, CH_4, and H_2 (syngas). Furthermore, there are three basic ways to produce biochar based on the products, yields and characteristics of biochar. They are slow pyrolysis, fast pyrolysis and gasification (Inyang. M and Dickenson. E., 2015). The characteristics of slow pyrolysis are temperature from 350 to 800^0C, holding time from minutes to days and no present oxygen. The characteristics of fast pyrolysis are temperature from 425 to 550^0c, a holding time of less than 2 seconds and no oxygen present. The characteristics of gasification are temperature more than 800^0C, holding time from seconds to hours, no oxygen present and sometimes steam or CO2.

Modified biochar

Modified biochar by acid washing after production aims to eliminate minerals which can block pores or the pore network on the surface of the biochar. In Figure 7, pore blocking limits the pollutants diffusing in to the pore network. In a study by Zhang et al., 2016, biochar produced from a giant reed (Arundo donax) was washed with 1 M HCl and 1M:1M HCl-HF solution to remove most of the minerals on biochar. According to Uchimiya et al., 2012, in order to remove excess ash, biochar was modified by 0.1 M HCl with a ratio of 27 g/l (w/v) for 1 hour. A report by Gai et al., 2014, the pores of biochar rinsed by 1 M H_2SO_4 were cleaner than those rinsed biochar by H_2O.

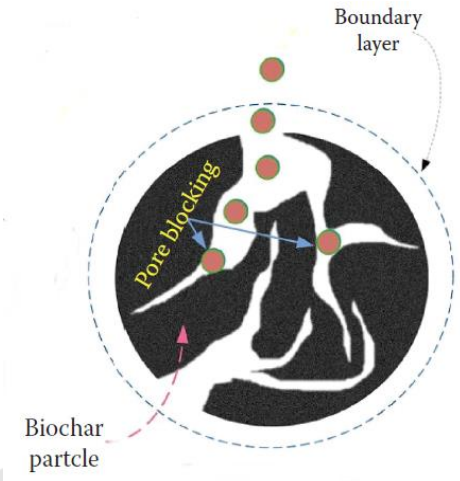

Figure 7 Pore blocking

Source: Tran et al., 2017b

Adsorption studies

Adsorption is known as a fundamental process. According to Scheele, C.W, the first adsorption phenomenon was quantitatively observed in 1773 through experiments of the absorption of gases by charcoals and clays derived from different sources. Adsorption is a process when atoms, ions, or molecules from a gas, liquid or dissolved solids, called adsorbate, accumulate and form a molecular or atomic film on the surface of the adsorbent. The most common high surface adsorbents are activated carbon, silica gel, and alumina. Activated carbon is produced by roasting organic material such as wood, shell and bone to granules of carbon. Silica gel is a matrix of hydrated silicon dioxide. Alumina is mined or precipitated aluminum oxide and hydroxide. The exact nature of the adsorbed material is generally classified as exhibiting physical and chemical adsorption. The adsorption is classified as follows: physical adsorption is a type of adsorption in which the adsorbate adhered to the surface through Van de Waals (weak intermolecular) interactions and chemical adsorption which is a type of adsorption whereby a molecule adheres to a surface through the formation of a chemical bond, driven by a chemical reaction occurring at the exposed surface. A new chemical species is generated at the adsorbent surface. The strong interaction between the adsorbate and the substrate surface creates new

types of electronic bonds-ionic or covalent, depending on the reactive chemical species involved.

Adsorption process

According to Weber (1984) who reported that adsorption is integral to a broad spectrum of physical, biological, and chemical processes and operations in the environmental field. Furthermore, the steps in the adsorption process (Figure 8) can occur as follows:

1. Film mass transfer of the reactant A, i.e. bulk diffution of A through the stagnant gas film on boundary layer surrounding the catalyst particle to the external catalyst surface.
2. Diffusion of species A (by either bulk or molecular diffusion) through the porous network of the catalyst to the catalytic surface.
3. Adsorption of A onto the catalyst surface.
4. Reaction of A to B on the catalytic sites of the catalyst surface.
5. Desorption of the product B molecules from the surface.
6. Diffusion of species B through the porous network to the pore mouth.
7. Film mass transfer of product B, i.e. bulk diffusion of B from the external catalyst surface though the stagnant gas film to the bulk gas stream.

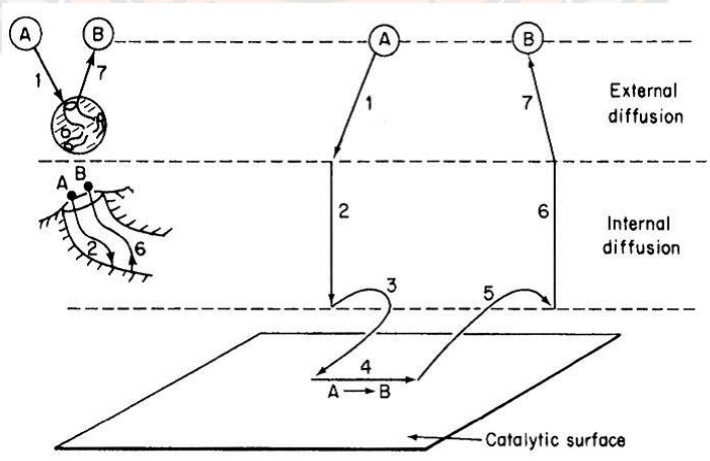

Figure 8 Steps of adsorption process

Source: Fogler, 1999

Isotherm study

Adsorption isotherm predict adsorption capacity of biochar at equilibrium. Basically, the two most well-known adsorption isotherm models are the Langmuir and Freundlich equations because of the simple application to compare the isotherm equations by calculating a correlation coefficient, R^2 (Shi et al., 2018).

The Langmuir isotherm is used to quantify the amount of paraquat adsorbed by the biochar as a function of the concentration at a given temperature. It considers the adsorption of an ideal pesticide onto an idealized biochar surface with the assumption that the surface of the biochar is homogeneous and no strong interaction takes place between the solvent and the pollutant to get equivalent biochar sites.

The Langmuir equation is written below (Weber et al. 1972):

$$\frac{C_e}{Q_e} = \frac{1}{bQ_o} + \frac{C_e}{Q_o}$$

Where Q_e is the weight of the paraquat adsorbed (adsorbent) per unit weight of the adsorbent (mg/g), C_e is the equilibrium concentration of paraquat in solution ((mg/L), Q_o is the maximum adsorption capacity for monolayer (mg/g) and b is constant which directly measures the affinity of the adsorption between an adsorbent and an adsorbate (L/mg) (Hamdaoui, O., 2006).

Several publications reported the fitting of paraquat adsorption with the Langmuir equation as the parameters given in Table 3. Based on previous studies, the Langmuir model can be used to evaluate paraquat adsorption on different adsorbents and to indicate the different adsorption capacities and different adsorbent ranges from 33.7 (mg/g) to 317.7 (mg/g).

Table 3 Langmuir isotherm parameters of paraquat adsorption on sorbents

Sorbents	qm(mg/g)	b (L/mg)	Reference
Activated bleaching earth	39.7	22.91	Tsai et al. (2003)
Activated carbon derived from used tires	33.7	0.014	Hamadi et al.(2004)
Methacrylic acid-modified rice hush	317.7	-	Hsu, & Pan. (2007)
Ayou (Triplochiton schleroxylon) sawdust	36.8	0.014	Nanseu-Njiki. (2010)

The Freundlich isotherm describes the equilibrium on the heterogeneous surface of the adsorbent. This equation is:

$$Q_e = K_F C_e^{1/n}$$

$$\text{Or } logQ_e = logK_F + \frac{1}{n} logC_e$$

Where Q_e is the weight of the adsorbate per unit of weight of the adsorbent (mg/g), C_e is the equilibrium concentration of the adsorbate in solution (mg/L), KF is a constant indicating the adsorption capacity of adsorbent and n is constant (Crini, G et al., 2008).

Q_e in both equations could be calculated by: $Q_e = \frac{V(C_i - C_e)}{W}$

Where V is the volume of the solution, C_i is the initial concentration of the adsorbate, C_e is the equilibrium concentration of adsorbate and W is the weight of the applied adsorbent (Crini, G et al., 2008).

Some experiments have been done to investigate the adsorption isotherm of paraquat on various adsorbents (Table 4).

Table 4 Freundlich isotherm parameters of pesticide adsorption on sorbents

Sorbents	K_F	1/n	Reference
Alginate	15.47	N = 0.381	Cocenza et al. (2012)
Activated bleaching earth	36.02	0.0294	Tsai et al. (2004)
Activated clay	55.108	0.0276	Tsai et al. (2003)
Muck	1416	1.01	Cheah et al. (1998)
Sandy soil	28.7	0.6	Cheah et al. (1998)
Ayou (Triplochiton schleroxylon) sawdust	2.973	0.388	Nanseu-Njiki. (2010)

Kinetic study

There are many models which have been developed and used to study basic adsorption mechanisms of pesticides onto biochar. For this study, there are three kinetic models: pseudo-first-order, pseudo-second-order and intrapaticle diffusion used to study the basic adsorption process of paraquat onto biochar (Nanseu – Njiki et al., 2010). The pseudo-first-order model was expressed as (Ho, & Mc Kay, 1998):

$$Log\ (Q_e - Q_t) = Log\ Q_e - K_1 t$$

The pseudo-second-order model was proposed by Ho and Mc Kay (1998) and used for the study as described in the Equation:

$$\frac{t}{Q_t} = \frac{1}{K_2 Q_e} + \frac{1}{Q_e} t$$

The intra-particle model is to plot the amount of paraquat adsorbed versus the square root of time, $t^{0.5}$ as follows (Nanseu – Njiki et al., 2010):

$$Q_t = K_{ip} t^{0.5}$$

Where Q_t and Q_e are the amount of pesticide adsorbed per gram of biochar (mg/g) at time t and at equilibrium, respectively and K_1 (1/hour), K_2 constant (g/ (mg hour) and K_{ip} are sorption rate constants of the pseudo-first-order, pseudo-second-

order and intra-particle models, respectively. All the model constants and the correlation coefficient (R^2) were determined.

Adsorption mechanisms between pesticide and biochar

Understanding the adsorption mechanism is useful to optimize adsorptive pesticides. Ordinarily, the pore filling, diffusion and partitioning, hydrophobic interaction, aromatic-π and cation-π interaction, electrostatic interaction and hydrogen bonding may be contribute to the main adsorption mechanism of pesticides onto biochar in Figure 9 below.

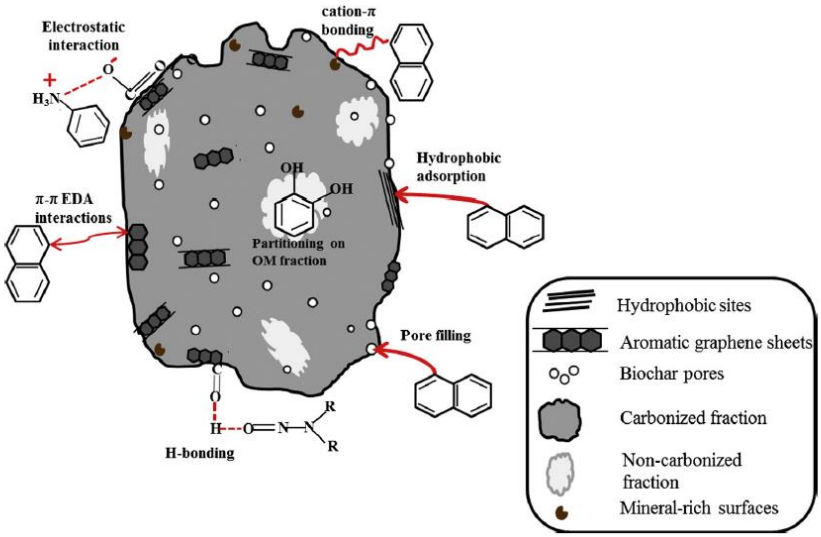

Figure 9 Adsorption mechanisms of pesticides on biochar

Source: Inyang. M., & Dickenson. E., 2015

The first mechanism is pore filling. There are 3 main types of structural pore for biochar. The first type is the micro-pore with the size of the pore less than 2 nm. The second type is the meso-pore with the size pore between 2-50 nm. The final type is the macro-pore with the size of the pore above 200 nm (Gul et al., 2015). The study of Pignatello et al., 2006 indicated that the micro-pores and meso-pores contribute to the majority of the surface area of the biochar and have a more important impact on the sorption of organic pollutants by the biochar. Moreover, the studies of Nguyen et

al., 2007 and Hao et al., 2006 confirmed that the mechanism of the sorption of the organic pollutants onto biochar is pore-filling as a function of the total micro-pore and meso-pore volumes. Besides, Kasozi et al., 2010 studied the sorption of organic sorbates on biochar by the pore-filling mechanism at relatively low solute concentrations or at low volatile matter content of the biochar. The characteristic of the pore filling mechanism is a fast occurrence of kinetic adsorption and often by non-linear, Langmuir adsorption isotherm. A previous study by Nguyen et al. (2007), indicated that the maximum adsorption is enhanced with decreasing molecular diameter such as phenanthrene, naphthalence, 1, 2-dichlorobenzene/ 1, 2, 4-trichlorobenzene, 14-dichlorobenzene onto a natural wood char (pitch pine biochar) by the adsorptive pore-filling mechanism.

The second mechanism is diffusion and partitioning. In general, the diffusion of pesticides into biochar is a process by which pollutants diffuse in to the pore network of the non-carbonized fraction of biochar (organic matter of biochar).

The third mechanism is hydrophobic interaction. The sorption of pesticides by the hydrophobic interaction mechanism means that the hydrophobic pesticide can interact with the hydrophobic surface of the biochar or the hydrophobic functional groups of biochar.

The fourth mechanism is π-π EDA (electron-donor–acceptor). Strong, non-covalent π-electron donor–acceptor (EDA) interactions have been invoked for the sorption of planar aromatic compounds on graphene-like biochar surfaces. Research by Zhu (2005) demonstrated that the total graphitization of biochar can increase, or reduce its electron density, creating π-electron-rich or deficient systems. The sorption affinity of atrazine to biochar for example, was attributed to π–π EDA interactions between the electron-withdrawing chlorine substituent in atrazine and the aromatic carbon on each biochar's surface (Zhang et al., 2013). Besides, the interaction between the aromatic-π of pollutant and cation-π of biochar such as Fe, Mg, Si, K or Ca can occur (Inyang, & Dickenson, 2015).

The fifth mechanism is electrostatic interaction. Electrostatic interactions are the principal mechanisms for the sorption of ionic and ionizable pesticides. Since, ionic sorbates are attracted to the sorbents with oppositely charged surfaces; cationic

pesticides will tend to adsorb on biochar surfaces which are typically negatively charged, while, anionic sorbates will bind on positively charged sites.

The sixth mechanism is hydrogen bonding. Hydrogen bonding (H-bonding) is a plausible mechanism for the sorption of polar pesticides on biochars. The abundant polar groups on biochars facilitate water sorption and promote H-bonding between biochars and organic sorbates containing electronegative elements (Sun et al., 2012). For example, the sorption of dibutyl phthalate (DBT) by rice straw and swine manure biochars, for instance, was attributed to H-bonding between H-donor groups or water molecules on biochar and O-atoms on DBT's ester group (Jin et al., 2014). The study of Liu reported that the enhancement of phenol adsorption by biochar was a major attraction between the oxygen of functional groups of biochar such as –OH and C=O and phenol molecules based on the hydrogen bond.

Biodegradation

Biodegradation of pesticides by *Pseudomonas putida*

Pseudomonas putida is extensively applied in environmental biotechnology based on its strong capacities in degradation and biotransformation of xenobiotic contaminants and aromatic pollutants (Loh, & Cao, 2008). It belongs to the family of Pseudomonadacease, genus of *Pseudomonas* spp and is a Gram-negative, mesophilic, aerobic bacterium. *Pseudomonas putida* commonly present throughout the environment for its abilities to degrade toxic compounds (Vizma Nikolajeva et al., 2012). Its cell size from 0.5 to 0.6 μm in diameter and from 1.4 to 1.7 μm in length (Hwang et al. 2008). A study by Mendoza et al. (2011), the strain of *Pseudomonas putida* and *Pseudomonas mendocina* has a good capacity for biodegrading insecticides and efficiency biodegradation up to 90% with the period of 15 days.

Biodegradation of paraquat (Intermediate products of paraquat)

Biodegradation is the microbial degradation which are the results of microorganism activity that causes the transformation or breakdown of paraquat. According to Amondham et al. (2006) reported that the biodegradation of paraquat is also an important process. There are several groups of microorganisms (bacteria, fungi (actinomyces), and yeast) that degrade paraquat as a nitrogen source. In the culture extract, biodegradation of paraquat is rapid, disappearing within 2–3 weeks.

However, degradation in mixed soil may be slower due to adsorption. Giardiana et al. (1978) stated that 50% of paraquat was transformed after 20 days at a 100–400 ppm application rate. Burn and Audus (1970) reported that microbial degradation of paraquat in soil can be limited by rapid soil adsorption. Adsorption on clay is slower than that on organic matter. Microbial degradation also slows when paraquat is fixed into a clay lattice.

The biodegradation of paraquat can occur during reactions, possible products which proposed that paraquat is strongly adsorbed and only gradually degraded. Some microorganisms, such as *Lipomyces starkeyi*, isolated from soils can degrade free paraquat completely. According to Smith et al. (1976) *Mucor hiemalis, Zygorhycchus hetrogamous, Aspergillus niger* and *Penicillium freuentans* are able to degrade paraquat and diquat, and have correspondingly low intracellular levels of the herbicides, and are able to tolerate high concentrations in the media. Degradation involves oxidation of one pyridine ring, which leads to bridge cleavage and then ring cleavage of the remaining ring. Cleavage of the second ring results in the formation of methylamine and CO_2 by both microbial and photolytic routes. This process is obviously illustrated in Figure 10 below:

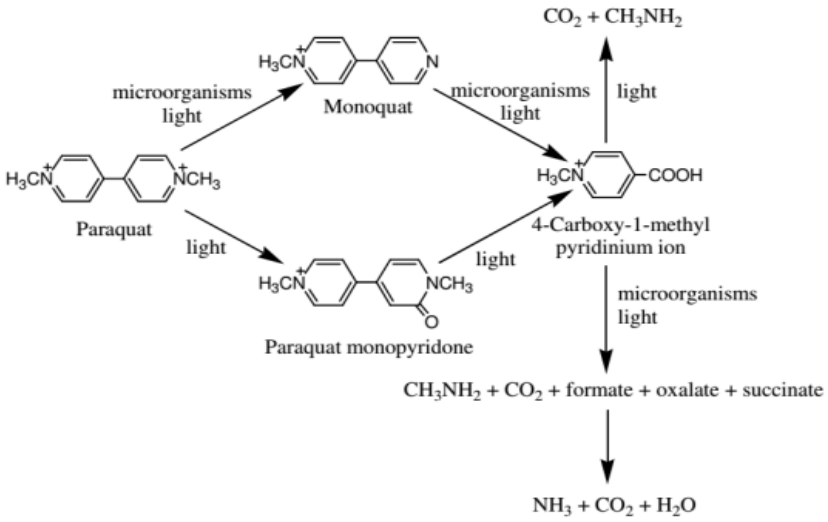

Figure 10 Pathways of Paraquat degradation

Source: Yamada, 2004

Cytoplasmic Membrane of bacteria

The cytoplasmic membrane has a dynamic structure with two main components which are phospholipids and proteins. The mass ratio of phospholipids to proteins ranges from1:4 to 4:1 (Weer J, M., 2000). The role of phospholipid components of the membrane create a permeable barrier to the transport of molecules and the role of protein components form transport structures of pumps and channels that allow selected molecules to transport into and out of the cell (Barak I and Muchova K., 2013). Therefore, the most important function of cytoplasmic membrane of bacteria can regulate the passage of solutes between the cell and the outer environment, prevent the entry of toxic compounds present in the environment (Dowhan et al., 2008) and is of special importance for the energy transduction of the cell (Sikkema et al., 1995).

Table 5 Components of cytoplasmic membrane of bacteria

Cytoplasmic membranes of bacterial strains	Percentage (%)
Phosphatidyl Ethanolamine (PE)	75
Phosphatidyl Glycerol (PG)	15–20
Cardio Lipin (CL)	5–10

Source: Sikkema et al., 1995

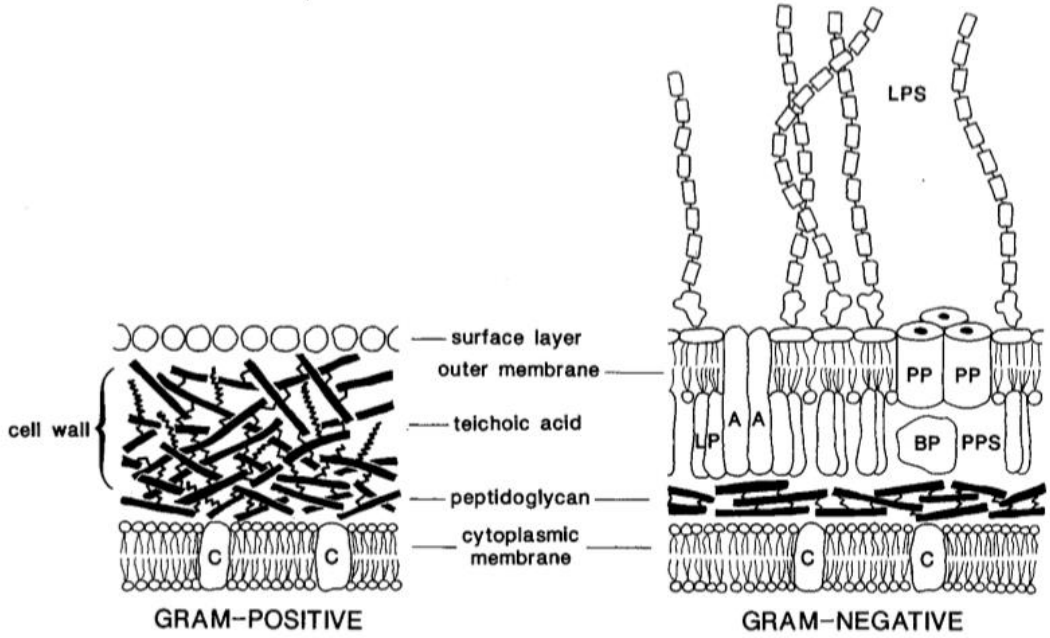

Figure 11 Schematic presentation of the cell envelope of gram positive and gram negative bacteria (PP, porin, C, cytoplasmic membrane embedded protein (e.g., carrier); BP, binding protein; PPS, perisplasmic space; A, outer membrane protein; LP, lipoprotein)

Source: Sikkema et al., 1995

Tolerance mechansims of bacteria to toxic compound

The major function of cytoplasmic membrane of bacteria is the protection of the bacterial cell from the entry of environmental contaminants. Hence, some organic toxicants are able to penetrate into cytoplasmic membrane resulting in cracking of the membrane and increase of membrane fluidity (Murinova, S., & Dercova, K., 2014).

In previous studies, microorganisms that developed a resistance to pesticides are frequent capability of biodegradation process (Kumar et al., 1996; Ortiz-Hernández, & Sánchez Salinas, 2010). The study of Bellinaso et al. (2003) indicated that temporary resistance against pesticides in general is involved to physiological changes that induce microbial metabolism to form a new metabolic pathway to bypass a biochemical reaction inhibited by a specific pesticide (Bellinaso et al., 2003). On the

other hand, permanent resistance depends on the operation of the genes inherited by subsequent generations of microbes (Johnsen et al. 2001; Herman et al. 2005). Thus, herbicide tolerance is a complex process which includes both physiological and genetic processes of the microorganism.

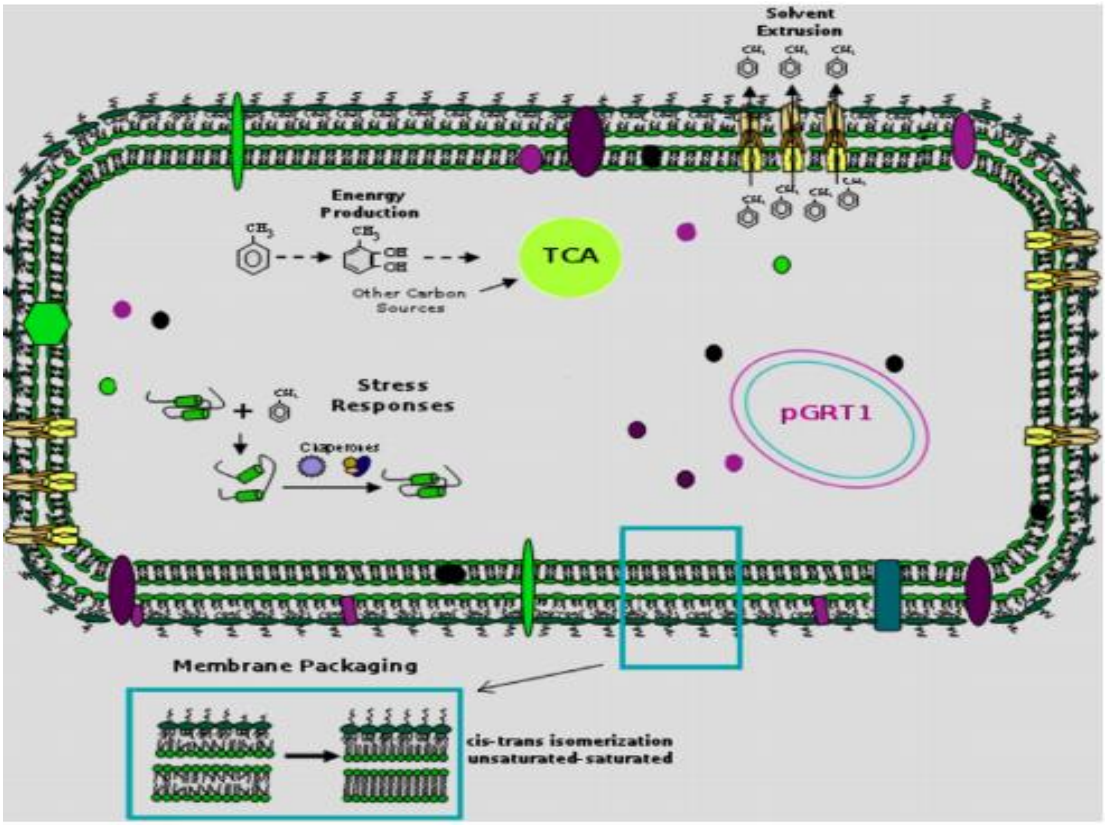

Figure 12 Schematic representation of the main mechanisms involved in the multifactorial solvent tolerance process in *P.putida* strains microorganisms

Source: Udaondo et al., 2012

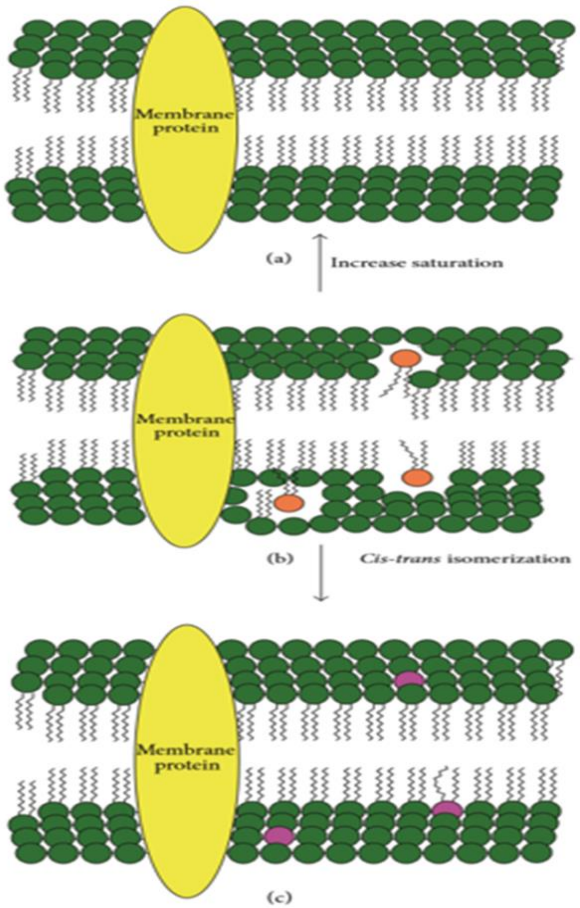

The first one (direction from (b) to (a)) describes the increase of the synthesis of saturated fatty acids (green circles) instead of *cis* unsaturated fatty acids (orange circles)

The second one (from (b) to (c) shows the isomerization of *cis* unsaturated fatty acids into corresponding *trans* isomers (purple circles)

Figure 13 Two mechanisms increasing bacterial membrane saturation and decreasing membrane fluidity. The first one (direction from (b) to (a)) describes the increase of the synthesis of saturated fatty acids (green circles) instead of *cis* unsaturated fatty acids (orange circles); the second one (from (b) to (c) shows the isomerization of *cis* unsaturated fatty acids into corresponding *trans* isomers (purple circles)

Source: Murinova, S., & Dercova, K., 2014

Immobilization of bacterial cells

Introduction

Immobilization can be defined as the containment/confinement of enzymes or whole cells within or on support materials. The methods for the immobilization of enzymes and cells are basically the same in most cases. Nevertheless, maintaining a

living cell is more complex than supporting an enzyme in an immobilized system. According to Dervakos and Webb (1991), the advantages of immobilized cells over free cells are such as: enhanced biological stability, high biomass concentration, improved mass transfer, advantageous partition effects, increased product yields, enhanced product stability, integration with downstream processing, advantages due to cell proximity, increased reaction selectivity, versatility in the selection of the reactor.

According to research by Hoskeri et al. (2014), the biodegradation of chloroaromatic pollutants such as 2-chlorobenzoic acid, 4-chlorobenzoic acid, 1,2-dichlorobenzene and 1,4-dichlorobenzene by bacterial consortium immobilized in polyurethane foam, possessed a higher tolerance to pH and temperature changes than free cells. A study by Yañez-Ocampo et al. (2009) indicated that the immobilized cells in alginate and the tezontle material gained higher removal percentage of methyl-parathion than free cells. This study showed that the time store is expanded up to 11 and 13 days as to the consortium immobilized using alginate beads and the biofilm on tezontle. More seriously, Leung et al., (1995) indicated that the κ-carrageenan-encapsulated *Pseudomonas aeruginosa* UG2Lr cells showed clearly excellent survival in an acidic forest soil and the bead structure of κ-carrageenan matrix protected the cells from environmental stresses caused by extreme temperature fluctuations such as freeze-thaw treatment.

Types of immobilization method

According to a review by Dzionek et al. (2016), immobilization methods include five major techniques which are adsorption, binding on a surface, flocculation, entrapment and encapsulation. However, immobilization methods by flocculation does not need a porous material and by encapsulation is almost similar to immobilization by entrapment. Therefore, immobilization methods by adsorption, binding on a surface (electrostatic and covalent) and entrapment presented below.

Adsorption method

Definition

According to Yea-Ling Ong et al., 1999, the adsorption method is the simple method of reversible immobilization that involves the cells are attached on the porous material/carrier (e.g., ceramics, porous glass, nylon web, diatomaceous earth, etc.) by

physical interaction. In this method, the cells transport from the bulk phase to the surface of the carrier/adsorbent, then adhere/attach and finally colonize on the carrier/adsorbent surface (Kilonzo and Bergougnou, 2012). Therefore, there is a direct contact between nutrients and the immobilized cells. The advantage of this method is high diffusion between cells and porous material. Moreover, the functional groups on the surface of the cell and support causes minimal cell damage. Nevertheless, the weak point of this method is weak attachment between cells and carrier. Because, physical bonding is not strong to keep the cell anchored to the carrier, thus it leads to cell leakage.

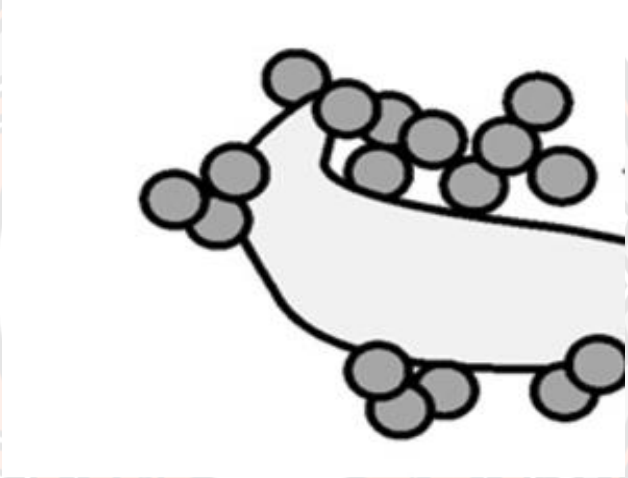

Figure 14 Adsorption method

Source: Dzionek et al., 2016

Mechanism of bacterial adsorption on biochar

A study by Samonin, & Elikova. (2004) indicated that a good porous material for bacterial cells must have a pore size greater than 2 – 5 times that of the cells in order to get maximum adsorption of dividing cells and pore diameter bigger than 4 times of cell size to have maximum adsorption of budding cells. The characterization of the surface of an adsorbent is a significant factor in influencing the process of cell immobilization. Hence, the specific surface area of a porous material should be more than 0.01 m^2/g. More specific, Figure 15 illustrates a schematic illustration of the immobilization of two kinds of microbial cells on porous materials

with different pore sizes. The adsorption of bacterial cells is good with the comparable size of adsorbent pores to the cell flagella (Figure 15a) or the cells themselves (Figure 15c). In contrast, the pore size of porous materials differs from the sizes of the cells and flagella, the cell immobilization on adsorbents is not good in Figure 15b and Figure 15d.

According to Quilliam et al. (2013), biochar macropores with an average pore diameter greater than 0.256 µm seems as a habitat due to the right size to accommodate bacteria. Micropores and mesopores could keep water and nutrients that are supplied for microbial metabolism. Moreover, Rong et al. (2008) showed that the forces of bacterial adsorption on adsorbent surfaces have two types of forces such as electrostatic and non-electrostatic interactions. They reported that the electrostatic force generates from the Coulombic interaction between the two charged entities and the non-electrostatic force includes hydrogen bonding, van der Waals force and hydrophobic interactions.

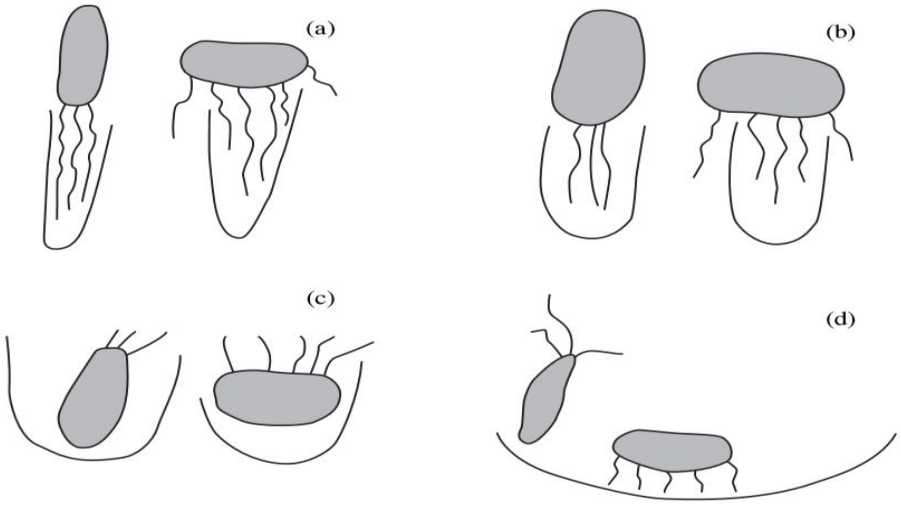

Figure 15 Schematic representation of the attachment of microbial cells to the spore surface: (a) the flagella of cells are firmly attached to the pore surface; (b) the flagella of cells are loosely attached to the surface pores; (c) cells are firmly attached to the adsorbent pores due to comparable sizes; (d) cells are loosely attached to the surface of a large pore because of its small curvature

Source: Samonin. V. V., & Elikova. E. E., 2004

Covalent binding method

Definition

A study by Najafpour (1990) indicated that the covalent binding method creates covalent bonds between functional groups present on the surface of the microorganism and the porous materials in the presence of a binding agent such as glutaraldehyde.

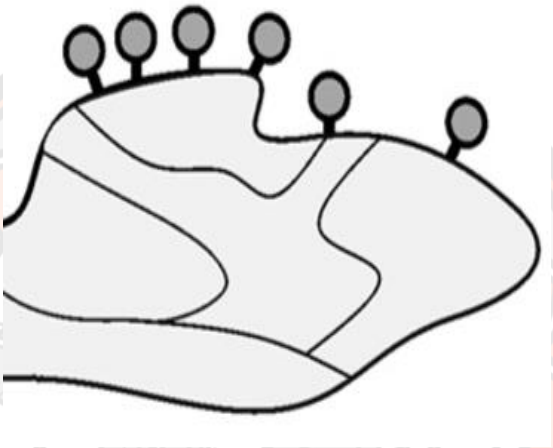

Figure 16 Covalent binding method

Source: Dzionek et al., 2016

The nature of the covalent binding method

The benefit of covalent binding method is eliminating the leakage cell phenomenon due to forming the stable bonding between cells and carrier. Besides, a study by Ramakrishna, & Prakasham, (1999), indicated the negative effect of linking reagents on the viability of microbial cells. Therefore, this leads to the low cell loading which is achieved by comparison to entrapment methods. Where viable cells can be covalently bound, any cell division is likely to result in cell leakage from the support, because the dividing cells will probably be less strongly attached (Tampion, 1989).

A study by Tampion (1989), there are some functional groups of cell membrane such as hydroxyl, aldehyde, keton, carboxyl, amino which is potential for formation of covalent binding with suitable porous material. Normally, there are two steps in the covalent binding of microorganisms to support materials. Firstly, a specific reagent is used to modify the functional group on surface of the porous material. Finally, the microbial cell is added to form a covalent bond with the porous material. According to Meyer et al. (2010), the reagent used for the activated surface of support materials such as N-(2-aminoethyl)-3-aminopropyltrimethoxy-silane (EDS), Polyethyleneimine (PEI) and Glutaraldehyde (GA) for chemical group (amine), Polyacrylic acid (PAA) for chemical group (COOH)

Entrapment method

Definition

A review by Cassidy et al. (1996), indicates that the entrapment method can be understood by the use of carrier materials for microorganisms such as both natural and synthetic polymers can overcome some of the problems associated with microbial survival in soil after inoculation. Some carriers such as biopolymer beads can enhance the ease of inoculant storage and reduce the chance of bio-aerosol formation.

Moreover, according to John et al. (2011), the entrapment method is an irreversible method, in which cells were entrapped in a carrier material to form beads. Those beads are permeable allowing transfer of nutrients, gases and metabolites for retaining cell viability within the beads.

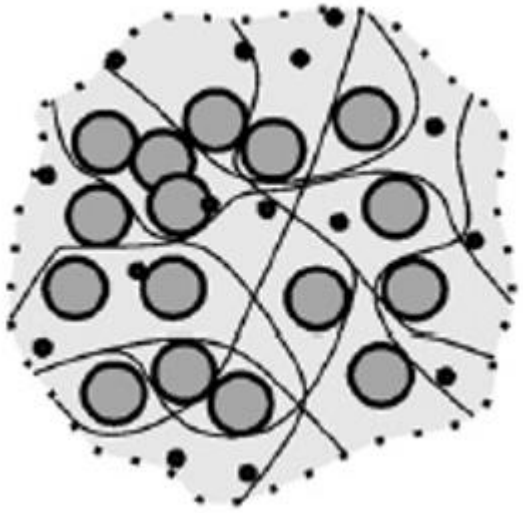

Figure 17 Entrapment method

Source: Dzionek et al., 2016

Nature of entrapment method

In 1989, the characteristics of algal polysaccharides used for cell immobilization were reviewed by Guiseley. He showed that the physical and chemical properties of algal polysaccharide are variable. In particular, alginate is synthesized by brown algae such as *Macrocystis pyrifera, Laminaria digitate and Eklonia cava.* Alginate is a linear polymer of β (1,4)-D –mannuronic acid and α(1,4)-L-gulu-ronic acid monomers. Various algae synthesize alginates that vary in monomer composition, arrangement and chain length. When exposed to Ca^{+2} ions, a cross-linking network is formed by the bonding of Ca^{+2} ions with polyguluronic portions of the polymer strands, a process known as ionic gelation. The guluronic acid units that bind Ca^{2+} lead to better and stronger gel formers.

Figure 18 The ionic gelation process by the bonding of Ca^{+2} ions with polyguluronic portions of the polymer strands

Source: Guiseley, 1989

To form beads, the alginate concentrations could use from 1 to 8% (w/v) of sodium alginate in water. The carrier/cell suspension is extruded dropwise into a 0.05-2.0% CaCl2 solution. The ionic bonding between interacting strands of polymers and Ca^{+2} ions occurs immediately on contact with the solution, and the resulting polymer network which is formed and the cells are trapped. After gelation, the beads can be used in a nutrient solution to encourage additional cell growth inside the gel-matrix. This method is suitable for various types of microorganisms. However, Mattiasson, B (1982) reported that the different methods of immobilization affect the performance of the bacteria; for example entrapment in a polymeric matrix introduces a diffusion barrier through which nutrients and (waste) products need to be transported. The fixed cells can survive and maintain their metabolic activity and adaptation to the surrounding environmental conditions (Cassidy et al., 1996).

CHAPTER III

METHODOLOGY

This chapter described the materials and methods of this study, the details of each part is introduced below.

General framework of the study

This study includes three main parts to achieve the objectives as mentioned in Chapter One. The first part was the synthesis of biochar from different biomasses in order to explore the fundamental properties of each type biochar and to evaluate the adsorption ability for PQ removal. Effect of pH on Paraquat adsorption onto the biochars was investigated. Then, adsorption studies were explored isotherm adsorption to identify the PQ adsorption capacity of different biochars. Moreover, kinetic adsorption was determined the movement of paraquat into the biochar and discussed about mechanism adsorption of paraquat and biochar.

The second part was to study the free cells of *Pseudomonas putida* on the removal of PQ. The specific objectives of the experimental design for free cells were designed for assessing the growth of bacteria under different environmental conditions such as pH and various initial concentrations to get the optimal condition. Then, adsorption studies were explored to identify the PQ adsorption capacity of free cells which include living cells and dying cells. Moreover, PQ tolerance of *Pseudomonas putida* and EPS synthesis in response to oxidative stress were determined and discussed.

The third part was to study the fixed cells of *Pseudomonas putida* on different biochars with different immobilization methods for the removal of PQ. The specific objectives of the experimental design for fixed cells were designed to determine isotherm and kinetic adsorption of each type of fixed method on specific biochar. Then, the comparisons of different fixed cells of *Pseudomonas putida* on different biochars to achieve the PQ removal efficiencies were studied.

Figure 19 illustrates the framework of this study.

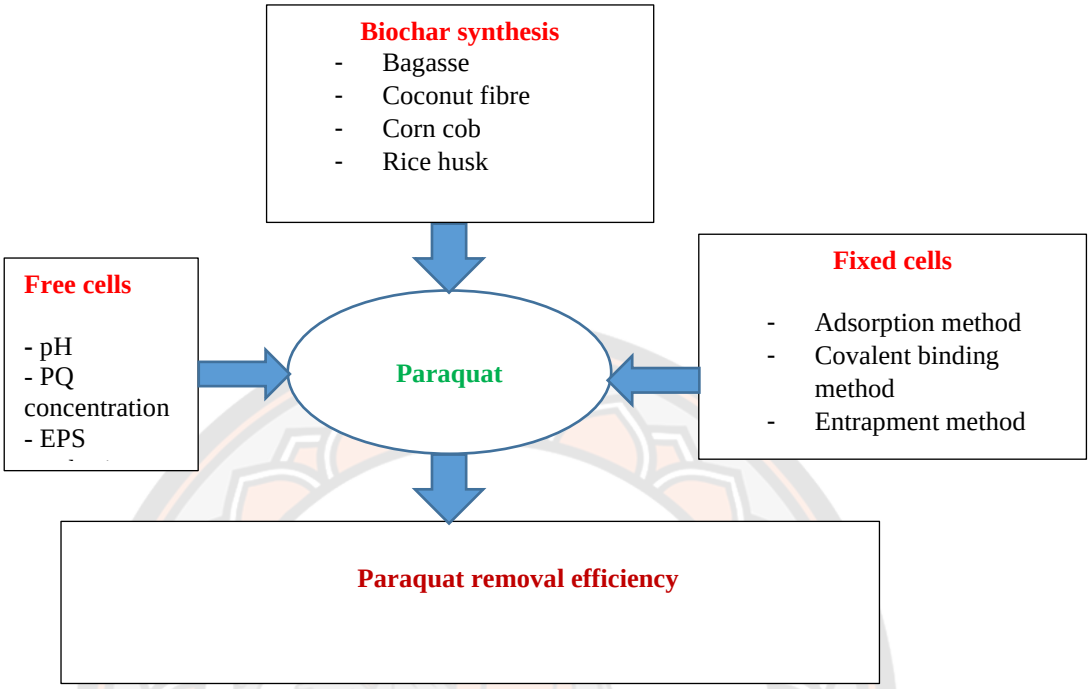

Figure 19 Framework of work study

PART 1 ADSORPTION

In the first part, the experiments include the following:

Synthesis of biochar and characteristics of different biochars

Characterization of biochar

Batch adsorption experiments

Adsorption isotherm

Kinetic study

Synthesis of biochar and characteristics of different biochars

The biochar feedstocks were collected from around Naresuan University in Phitsanulok.

The collected samples were dried at 105^0C in an oven for 4 hours to remove most of the moisture. After that, they were pyrolyzed in a furnace (Nabertherm, Germany) under oxygen-limited conditions (Figure 20) for 4 - 6 hours. The selection of the pyrolysis period was based on the efficiency of the adsorption

capacity (Liu et al 2015). The increasing temperature increased at 3^0C per minute (Krzesin´ska, & Zachariasz, 2007). Biochar production at each temperature under the same conditions were replicated at least two times (twice). The quantity of the feedstock used for the pyrolysis was in the range of 30 g. The feedstocks were added in ceramic pots fitted with a lid and then the pot were placed in a furnace at optimum temperatures and time. Finally, the biochar were milled to produce the suitable particle size and stored at room temperature in sealed glass bottles.

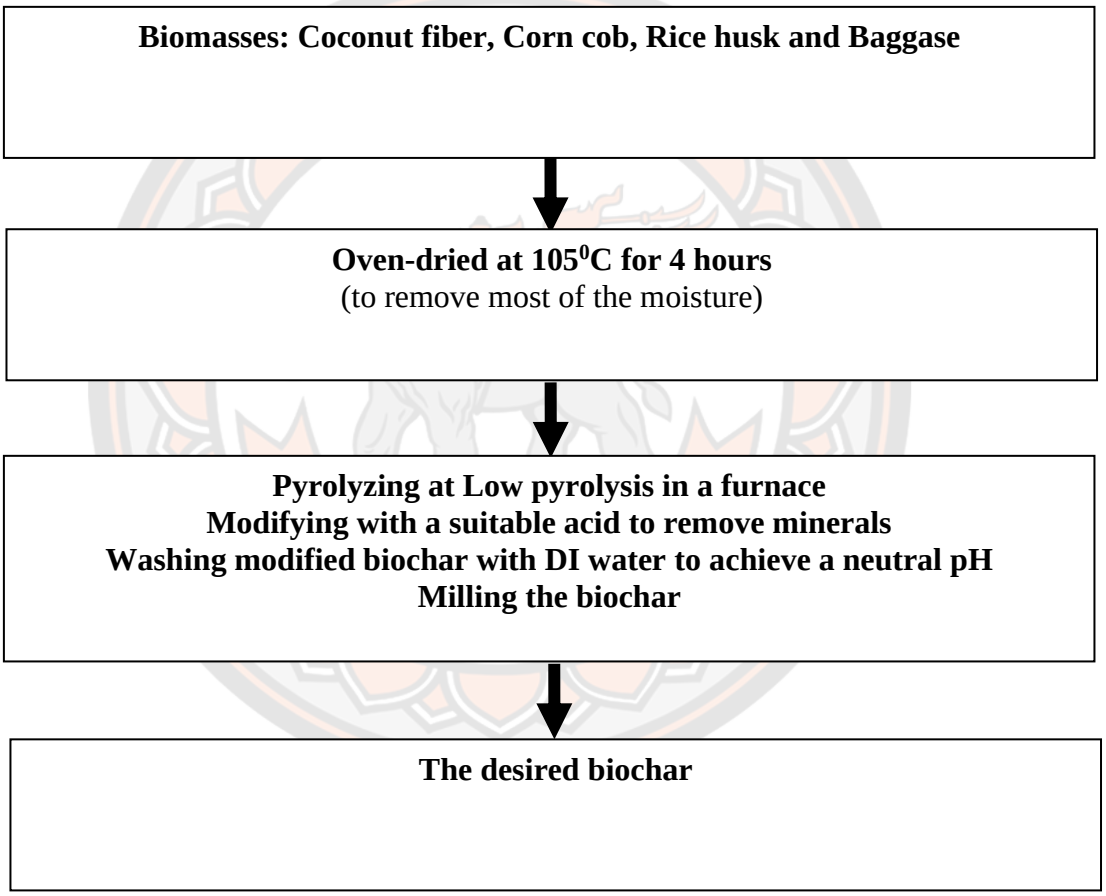

Figure 20 Preparation of biochar

Characterization of biochar

Characterization of biochar was analyzed in this study (Table 6). The surface morphology of the different biochar were analysed by scanning electron microscope (SEM) (LEO 1455 VP model, Carl Zeiss Microscopy GmbH, England), the biochar samples were loaded on tape coated with gold before analysing. The

specific surface area and total pore volume of the biochar were measured by BET (Brunauer–Emmett–Teller) method (TriStar II 3020, Micromeritics Instrument Corporation, USA), the functional groups of biochar were analysed according to the FT-IR method (Frontier, PerkinElmer, Germany).

Table 6 Characterization of biochar

Characteristics of Biochar	Method of Study	References
Physical properties		
Surface area	Adsorption of N_2 or CO_2	Liu et al. (2015)
Pore size, size distribution	Extended N_2 and CO_2 adsorptions	Liu et al. (2015)
Chemical properties		
Chemical state	FTIR	Liu et al. (2015)
Surface morphology	SEM	Liu et al. (2015)
Charged value	pHzpc	Srivastava et al. (2011)

Batch adsorption experiments

Adsorption study was implemented by batch adsorption experiment as in Figure 21. The effect of pH of solutions was investigated in the adsorption process. The pH of solution was prepared in the range of 1.0 to 12.0. H_2SO_4 and NaOH solution were used to adjust the pH of paraquat solutions.

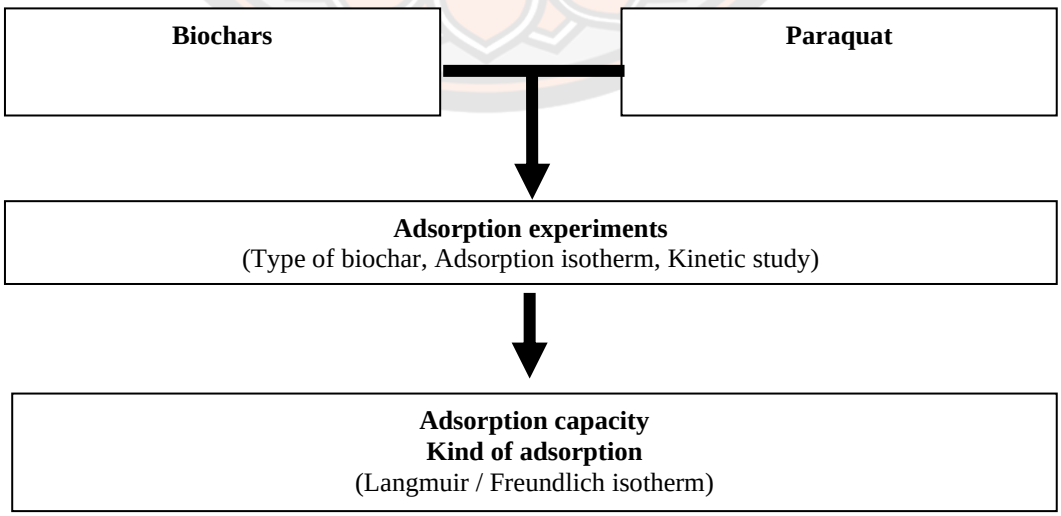

Figure 21 Paraquat adsorption onto Biochar experiments

Adsorption Isotherm

Based on the previous experiment, the best synthesis condition of biochar was chosen. The dosage of biochar (1.5 g/L) mixed with different initial concentration of paraquat (5-50 mg/L) as in Figure 22 below:

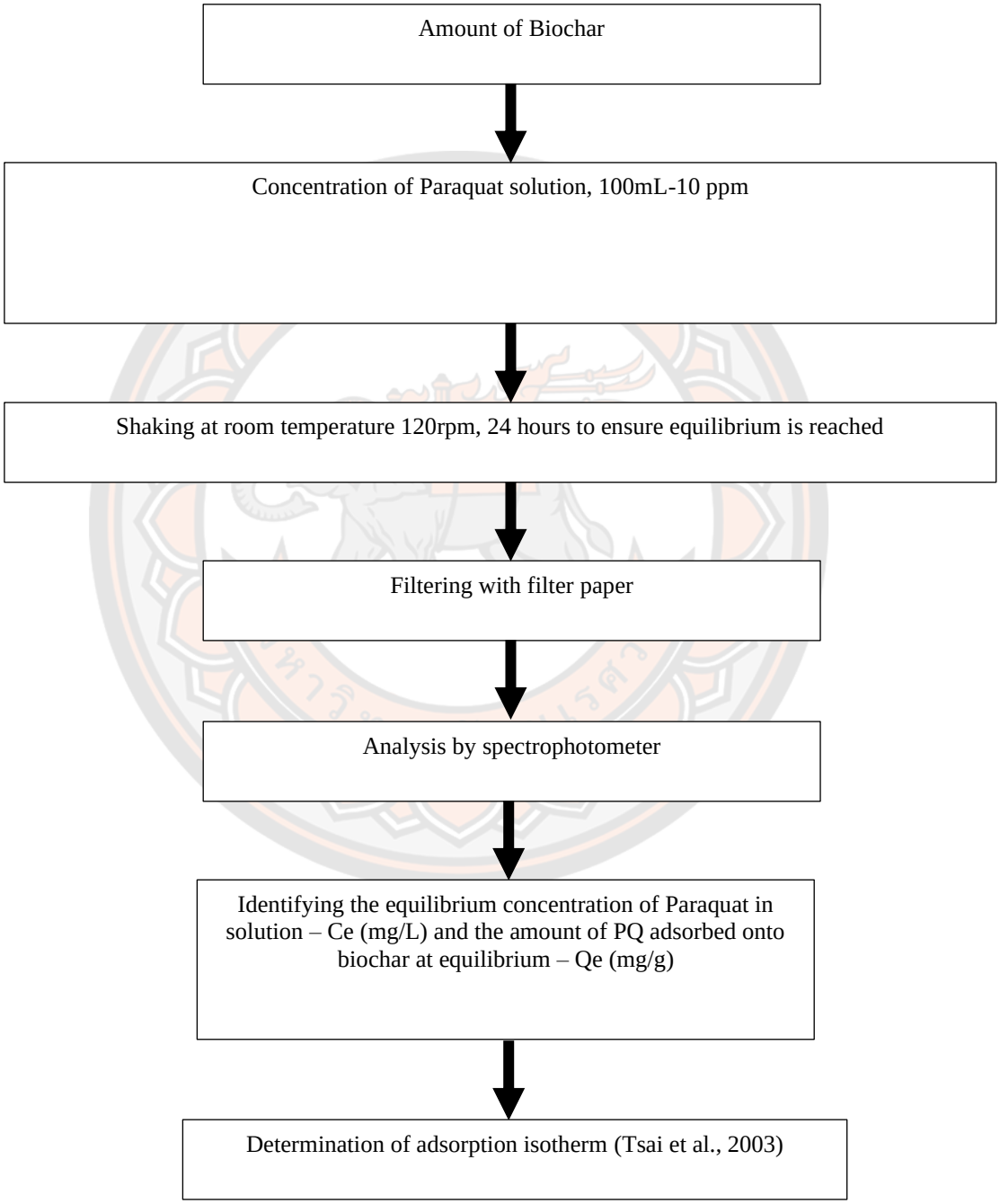

Figure 22 Identification of adsorption isotherm

Kinetic study

The suitable dose of biochar of isotherm experiment was tested with an initial concentration 5, 10,15, 20, 25, 30 mg/L of paraquat with varying time (Figure 23). The varying time was from 0 to 24 hours.

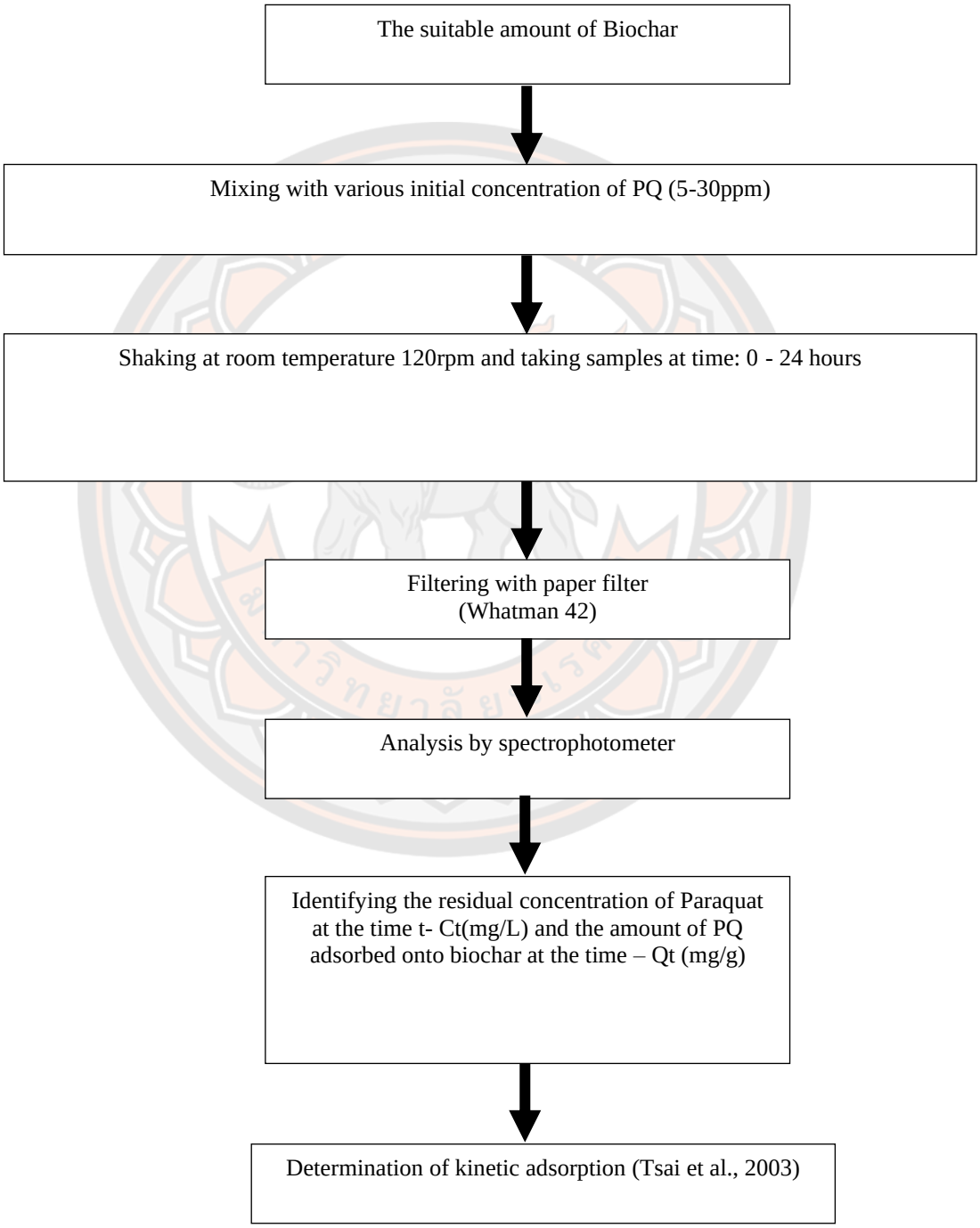

Figure 23 Identification of kinetic adsorption

PART 2 FREE CELLS

In the second part, the experiments include the following:

Chemicals and culture medium

Preparation of free cell suspension

Experimental design for free cells

Chemicals and culture medium

PQ was purchased from Agro-chemical Company (Thailand). All reagents used in this study were AR grade supplied by Himedia Laboratories. The nutrient medium for the growth of *P. putida* was 20% Luria-Bertani (LB) medium contained (g/L): tryptone 10 g; yeast extract 5 g; NaCl 10 g and 80% Minimal salt medium (MSM) contained (g/L): NH_4Cl 0.057g; K_2HPO_4 0.017g; $MgSO_4.7H_2O$ 0.43g; NaCl 0.43 g, yeast extract 0.2 g. The agar plates were prepared by adding agar with 15g/L ratio. The medium for biodegradation was DI water and PQ at desired concentration. The medium was sterilized at 121^oC for 15 minutes.

Preparation of free cell suspension

P. putida was purchased from Thailand Institute of Scientific and Technological Research. A single colony of *P. putida* was initially inoculated into 10 mL of medium, shaken at 150 rpm in 30°C for 8 hours. Then, 4 mL of the pre-culture were then transferred to 100 mL of the same medium and cultivated for 24 hours. The viable cell density was aseptically enumerated by the dilution and plating on medium agar. The cells were harvested by centrifugation at 6,000 rpm for 20 min. The cells were washed with sterilized DI water twice, and re-suspended in DI to obtain above 10^9 CFU/mL. The bacterial suspension was used further for cell immobilization experiments.

Experimental design for free cells

All experiments were implemented using the batch method in 500 mL Erlenmeyer flasks and incubated at room temperature under shaking conditions of 120 rpm.

The objectives of the experimental design for free cells were aimed at assessing the growth of bacteria under different environmental conditions such as pH and various initial concentrations. The experiments were contained in 100 mL bacteria suspension and 400 mL of PQ solution with various initial concentrations.

The pH optimization to assess the influence of pH on PQ removal by free cells of *Pseudomonas putida* was studied in the pH range of 3.0, 5.0, 7.0, 9.0, 11.0. Samples were taken at different times to count the cells, and the residual PQ concentrations were measured.

For isotherm experiments, 5 mL of suspended bacteria (living cells) or dying cells were mixed with 20 mL of paraquat solution in 50 mL Erlenmeyer flask with initial concentrations. The flask was incubated at room temperature under shaking conditions at 120 rpm for 24 hours.

PART 3 FIXED CELLS

In the third part, the experiments include the following:

Materials for immobilization process

Preparation of immobilized cells by adsorption method

Preparation of immobilized cells by covalent binding method

Preparation of immobilized cells by entrapment method

Experimental design for fixed cells

Materials for immobilization process

The biomass materials were collected from the Faculty of Agriculture, Natural Resources and Environment, Naresuan University, Phitsanulok, Thailand. The agricultural waste, corncob was pyrolysed to obtain biochar. The quantity of feedstock was 30 (g) and placed in a ceramic pot fitted with a lid. The pots were placed in a furnace (Nabertherm, Germany) at optimum temperatures. Finally, the biochar was milled to produce a suitable particle size and stored at room temperature in sealed glass bottles. Biochar samples were produced from different pyrolysis temperatures and times such as Bagasse Biochar (BGB) BGB 600^{0}C - 6 h with HF-H_2SO_4 modification, Coconut Fiber Biochar (CFB) CFB 600 ^{0}C-4 h with HCl modification, Corn Cob Biochar (CCB): CCB600 ^{0}C-4 h with HF modification, and Rice Husk Biochar (RHB): RHB500 ^{0}C-6 h with HF modification. All chemicals were of analytical grade quality. The biochar was ground and sieved through a 0.5 mm mesh. To remove excess ash, the biochar was washed with acid 0.1 M with stirring at room temperature for 1 h and then repeatedly washed with distilled-deionized (DDI) water until the pH reached neutral. Finally, the dried biochar was autoclaved at 121°C for 15 min.

Table 7 The conditions of each immobilization method

Immobilization method	Adsorption method		Covalent binding method		Entrapment method	
	Biochar dosage (g/L)	Ionic strength (mM)	GA conc. (%v/v)	Ionic strength (mM)	SA conc. (%w/v)	SA:BA ratio (w/w)
CFB	5	0	0.3	0	2	1:1
CCB	10	20	0.3	5	2	1:1.5
BGB	10	50	0.5	5	2	1:1.5
RHB	15	50	0.3	5	2	1:1.5

Source: Adapted from Nguyen Thi Hai Ha, 2018

Preparation of immobilized cells by adsorption method

CFB, CCB, BGB, RHB and bacteria suspension were mixed with ratio in table 7 and shaken at 120 rpm for 2 hours. The combination of bacteria and biochar adsorpsion was obtained by filter paper (Whatman No. 41,) and rinsed three times with phosphate buffered saline solution (PBS 0.1 M, pH 7.4). Finally, they were dried overnight at 37^{o}C. Bacteria adsorption on biochar was improved by ionic strengths at suitable concentration of $MgSO_4$ in Table 7.

Preparation of immobilized cells by covalent binding method

CFB, CCB, BGB, RHB and glutaraldehyde solution were uniformly mixed with a ratio in table 7 and shaken at 80 rpm for 8 hours. After that, the modified biochar was rinsed three times with PBS solution to remove excess glutaraldehyde. The cell immobilization procedure was carried out in similar steps to cell immobilization using the above adsorption method. But the improvement by ionic strength at suitable concentration of $MgSO_4$ in Table 7.

Preparation of immobilized cells by entrapment method

CFB, CCB, BGB, RHB and bacteria suspension were uniformly mixed with ratio of 10 g/L in a shaker at 120 rpm for 2 hours. The sterilized sodium alginate (SA) was added into the biochar mixture and bacteria suspension. The different weight ratios of SA: Biochar were also determined with a suitable ratio in Table 7.

The mixture was extruded through a 20 mL syringe to 2% (w/v) $CaCl_2$ solution to form spherical beads. After 12 hours, the immobilized beads were harvested from the $CaCl_2$ solution with gauze and rinsed with sterilized DI water. The beads were stored at 4°C in the refrigerator for subsequent experiments.

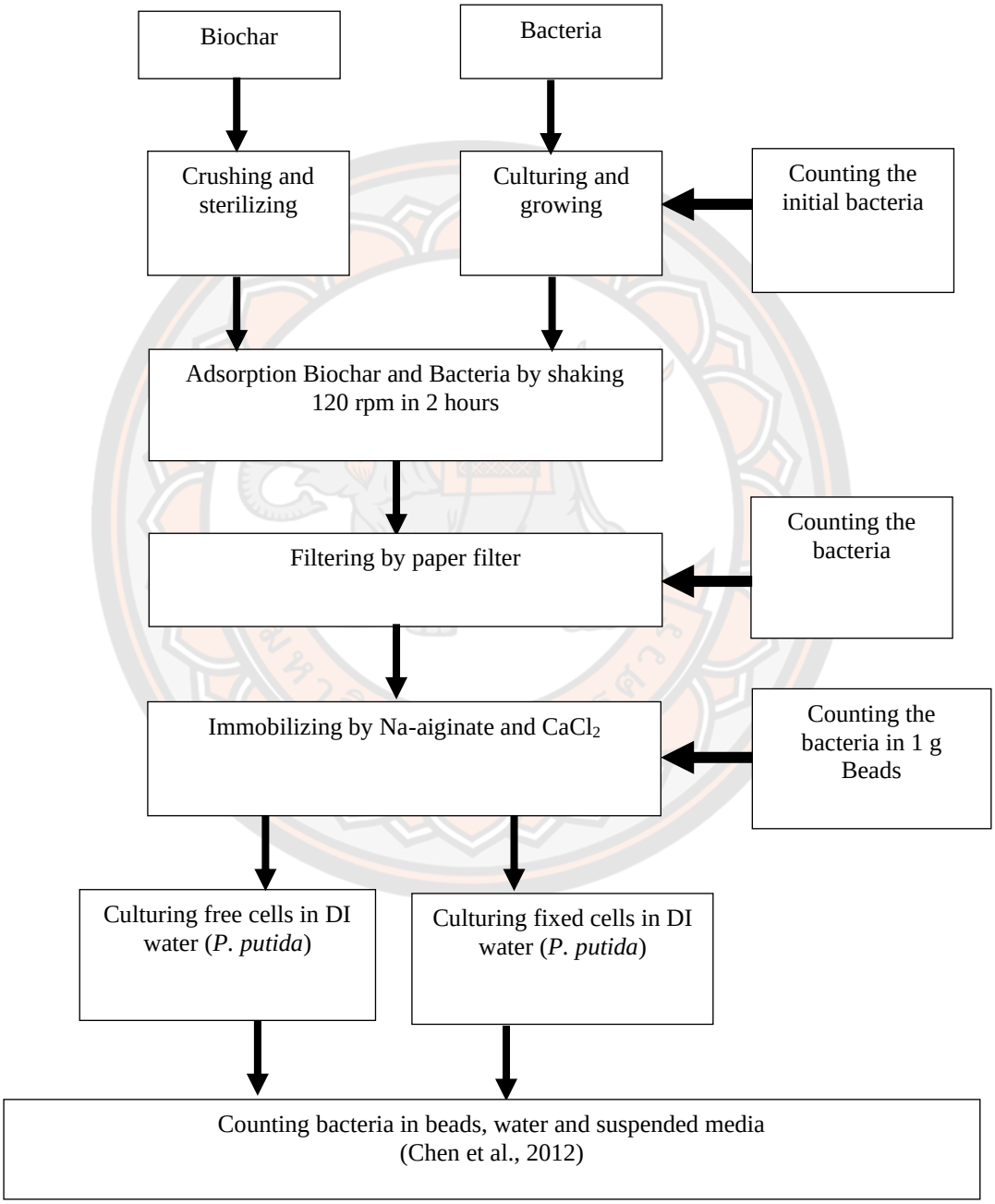

Figure 24 Immobilization and biodegradation of bacteria onto biochar

Experimental design for fixed cells

Isotherm

50 mg of cells fixed on the biochars by different methods was mixed with 25 mL of the desired paraquat solution (concentration between 5 – 50 mg/L in 50 mL conical flasks and agitated in an orbital shaker at 120 rpm

Analysis

Take 3-5 mL samples periodically to measure residual PQ. The PQ concentration was measured according to the colorimetric method using UV-Vis spectrophotometer (Shimadzu UV-Vis) (AOAC, 2000). After it had been filtered through filter paper (Whatman No. 41), the sample was gently mixed with 0.1% sodium dithionite in 0.1 M sodium hydroxide and detected within 1 min at 600 nm wavelength. All experiments were implemented in duplicate and under the same set of conditions. For the estimation of EPS, the samples were analysed for their extra-cellular polysaccharide content by determining the quantity of hexoses in biomass extracts (Dubois et al. 1956).

Kinetic models

The Pseudo First-order model, and the Pseudo-Second order model were employed as described below (Kundu et al., 2016; Felshia et al., 2017).

Eps analysis

The samples were analyzed for their extra-cellular polysaccharide content by determining the quantity of hexoses in biomass extracts (Dubois et al. 1956). Taking 2 mL sample of fixed and free cell samples was homogeneous which contains a total hexose of between 0.0010 - 0.0100 mg were mixed with 1 mL of 5% phenol in test tube digestion reagent vial 5 mL sulphuric acid was then added quickly to the tube and mixed thoroughly. The mixtures were left at room temperature for 10 minutes and then incubated at 30^0C for 20 minutes.

Enumeration of viable cells

The amount of bacterial adsorption was identified using the dilution and spread plate technique. One gram of beads was re-suspended in 9 mL of 0.1M PBS (phosphate buffer solution) at pH 7.3 as the Figure 25 below. After the suspension was spun for 3 min to recover the immobilized bacteria on the biochar, serial dilution and spread plate were conducted afterward. The colonies were counted after the

incubation of plates for 24 hours at 30°C. All counts were performed in duplicate. The results are expressed as CFU/g dry immobilized cells on biochar (adsorption method and covalent binding method) or CFU/g bead (entrapment method).

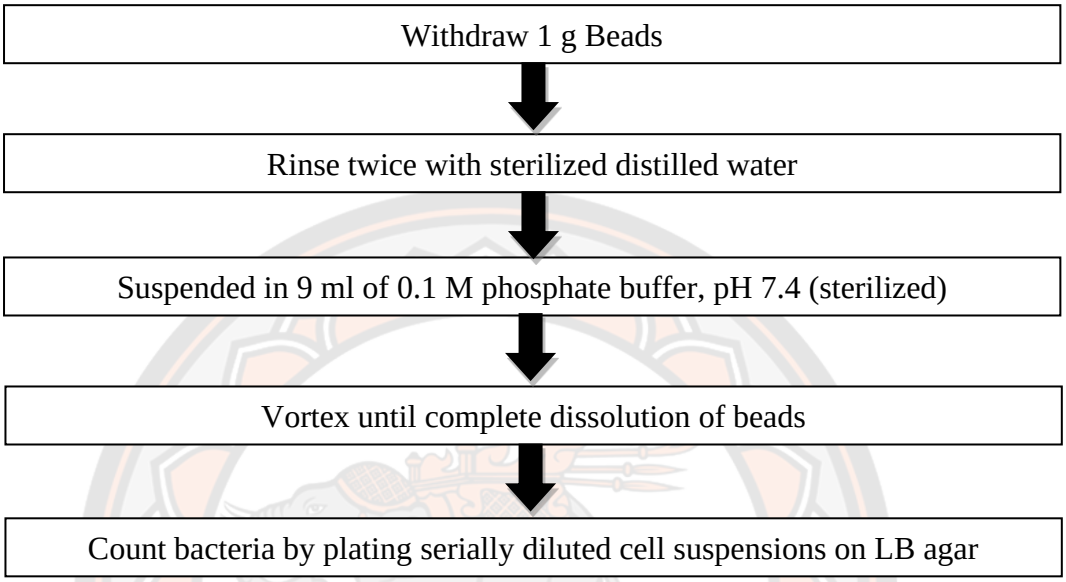

Figure 25 Counting bacteria in bead

CHAPTER IV

RESULTS AND DISCUSSION

Part 1- A. Adsorption studies of corn cob biochar produced from different pyrolysis conditions

This work studied the isotherm, kinetic and mechanism of Paraquat adsorption in aqueous solution by using corn cob biochar produced from different pyrolysis temperatures and times. The kinetic and isotherm data was fitted by the Pseudo-second-order and Langmuir models. These results showed that the adsorption capacity decreased with increasing pyrolysis temperatures during 6 hours in the order 200, 300, 400, 500, 600^{o}C and decreasing pyrolysis time in the order 2, 3, 4, 5, 6 hours, respectively at 200^{o}C. The mechanisms possibly contributed to hydrogen bonding and pore filling while π-π interaction was minor contributor in the adsorption process. Therefore, the corn cob biochar can become an alternative and promising adsorbent for Paraquat removal from an aqueous solution.

1. Surface morphology

The SEM images of biochar are shown the surface morphologies of the corn cob biochars synthesized at different pyrolytic temperatures (200, 400, and 600^{o}C) in Fig.26. From this work, the morphologies of biochar have some characteristics as follows: (i) All biochar have porous physical structure; (ii) The pore size of biochar reduced with the increasing of pyrolysis temperature (in images (A), (C) and (E)); (iii) From the image (B), the structure of BC200-6 has no small hole inside the pore; (iv) The structures of BC400-6 in image (D) and BC600-6 in image (F) appeared clearly the small longitudinal holes and became broken.

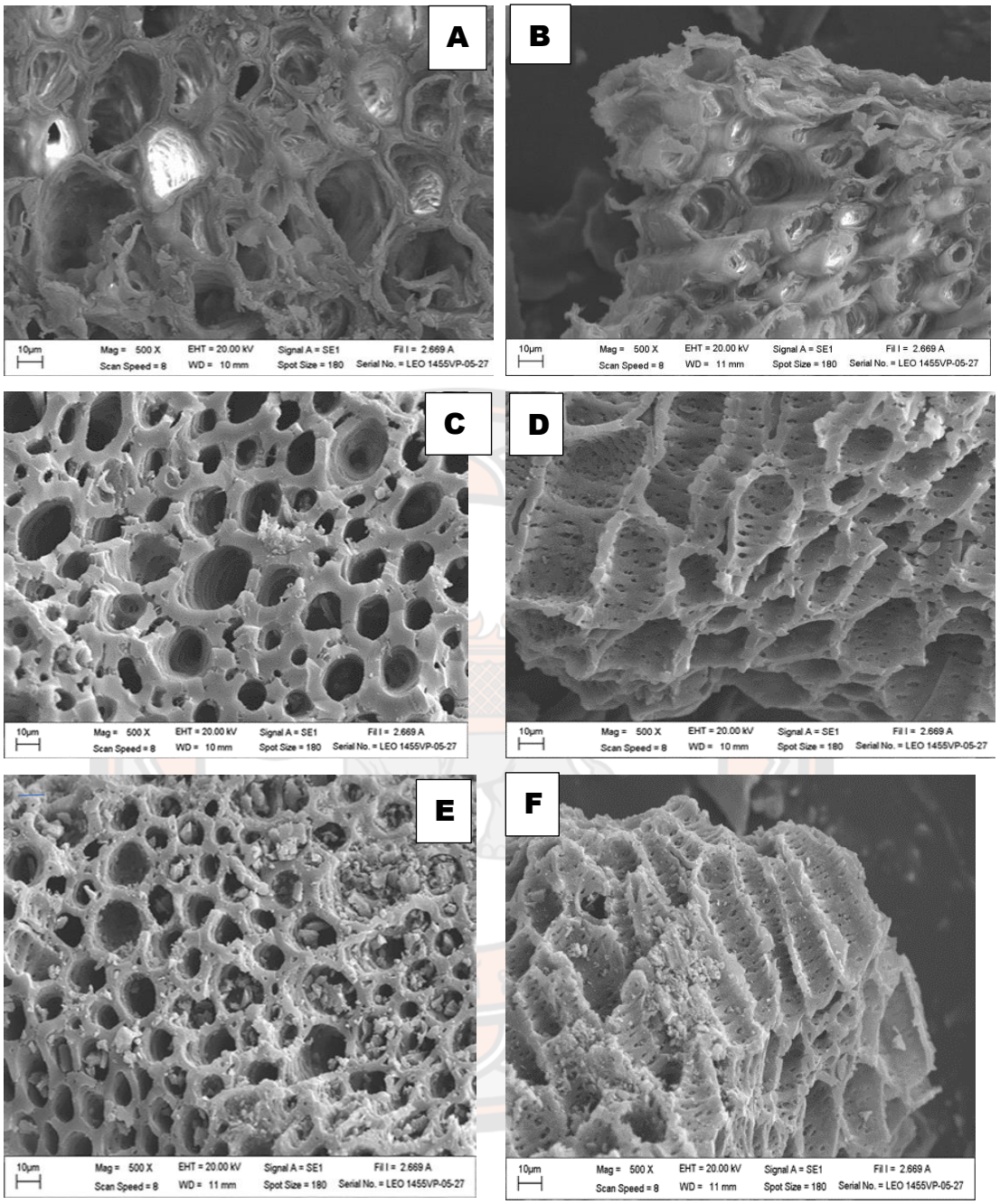

Figure 26 Scanning electron microscopy (SEM) images of corn cob biochars synthesized by slow pyrolysis at 200^{o}C (A, B), 400^{0}C (C, D) and 600^{o}C (E, F) during 6h

2. FTIR analysis

Chemical analysis of biochars produced at different pyrolysis temperatures and pyrolysis periods by FTIR was used to determine the functional groups as shown in **Figure 27**. FTIR spectra of the biochars displayed clearly peaks indicating the presence of typical functional groups. In specific, the broad peak at 3292.06 cm^{-1} was observed in **Figure 27** of BC200-6 represented to the O-H stretching vibration (Zhang et al. 2011). Then, this broad band dramatically decreased when increasing pyrolytic temperature to 400^0C, indicating the dehydration of cellulose and lignin at 300^0C (Keiluweit et al., 2010). Furthermore, the absence of bands at 1513.90 displaying for aromatic C=C ring stretching of lignin for both BC400-6 and BC600-6; 1426.95 cm^{-1} corresponding to the CH_2 unit for BC600-6 (Chen et al. 2008) occurred. This suggests a decrease of polar aliphatic fractions such as –O-H, especially, these bands were disappeared when the pyrolysis temperature enhanced.

Besides, the presence of bands at 2311.18 cm^{-1} for BC600-6 account for a concentration of carbon dioxide (CO_2) greater than atmospheric, similar to adsorbe within micro pores (Liu et al., 2011; Herbert, 2012). The appearance of bands at 2119.63 cm^{-1}, and for BC600-6, which represented C≡C (Coates, 2000), demonstrated that increasing pyrolysis temperature had the effect on functional groups of biochar.

The possession of band at 1709.83 cm^{-1} for BC200-6 exhibited carbonyl groups (C=O) corresponding to various acids, aldehydes and ketones which are mostly formed by dissociation of cellulose and hemicellulose (Liu et al., 2011; Yang et al., 2007). The presence of bands at 1581.89 cm^{-1} for BC400-6 and 1557.68 cm^{-1} for BC600-6, which displayed stretching of aromatic C=C (Cheng et al., 2006; Sharma et al., 2004). The bands at 1236.03 cm^{-1}, 1226.93 cm^{-1} and 1229 cm^{-1} which can be clearly observed for BC200-6, BC400-6 and BC600-6 respectively, regarding to the presence of OH− groups present in phenols and carboxylic acids (Kalinke et al. 2016).

Moreover, the intensities of bands from 1440 to 700 cm^{-1} regarding to aliphatic C-H aromatic C-H groups, respectively (Liu et al., 2015) appeared and gradually enhanced with increasing pyrolytic temperature. According to Zhang et al.

(2011) and Zhou et al. (2016), it indicates the enhancement the quantities of aromaticity and the carbonization degree of biochar structure.

FTIR spectrum of the biochars produced at different burning time (2, 4 and 6h) are also compared in Fig 3b. However, there is very slight difference from spectra of each biochar. According to Yavari et al. (2015), the burning time is also a production variable impacting biochar sorption potential. This factor permits the carbonization process to be optimal completion and to get the maximum surface area. In this case, there is no remarkable change at different holding time for biochar produced at 200^0 C.

In summary, the functional groups in corn cob biochar are polarity in BC200-6, aromaticity in BC400-6 and BC600-6. The surface of corn cob biochar BC200-6 was hydrophilic and based on the principle of “like dissolves like”.

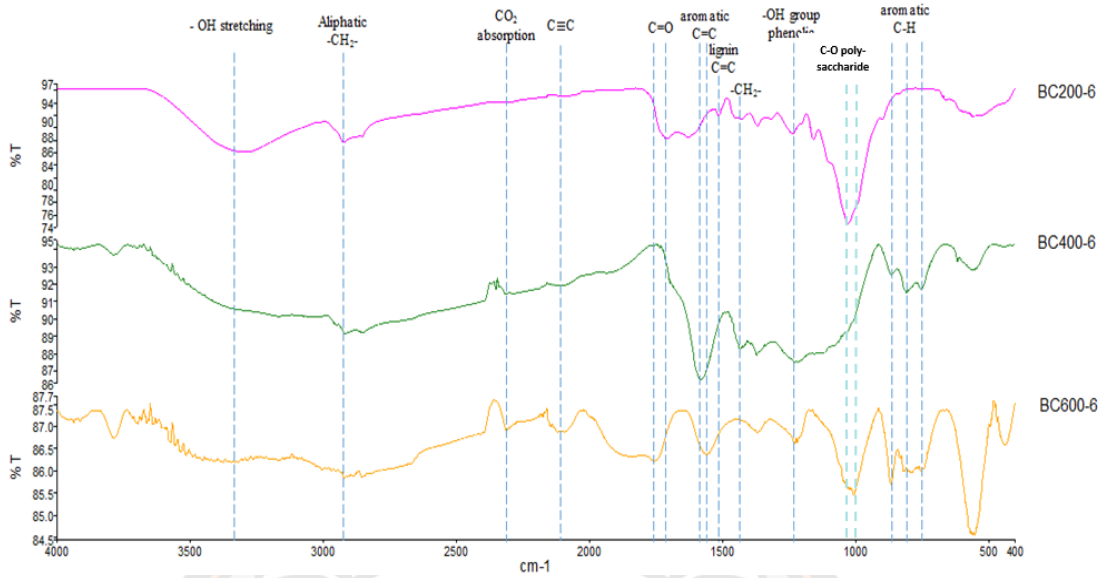

(a) Comparison of FTIR Spectra from corn cob biochars produced at 200, 400 and 600°C for 6h

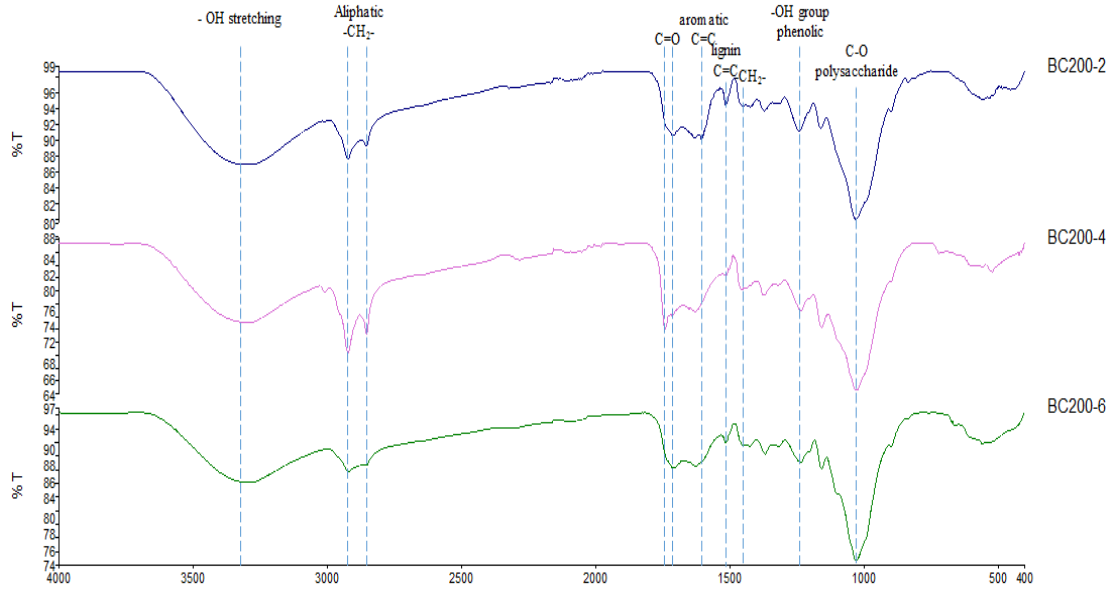

(b) Comparison of FTIR Spectra from corn cob biochars produced at 200°C for 2, 4 and 6h

Figure 27 Comparison of FTIR Spectra from corn cob biochars produced by different pyrolysis temperatures and burning periods

3. Carbonization process, surface charge, surface area and yield of biochars

The carbonization process of corn cob biochar is highly complex phenomenon. In the carbonization process, coal, as a result of thermal effect in an inert atmosphere and slow heating rate, undergoes structural modifications that produce a raw gas and a molecular rearrangement of the carbon cluster, the result of which is a highly carbonaceous. The heating rate of the carbonization process was varied at the temperature of 200, 400 and 600^{o}C. The carbonization temperature that gave the highest biochar yield at 200 ℃. When the carbonization temperature was further increased to 600 ℃, the yield of biochar was reduced. As temperature increases, the volatile matter in the sample released faster resulting in the increasing of gaseous products. These gaseous products can be either condensable or non-condensable gas and they could be recovered for additional value.

The solution pH plays a crucial role in the optimization of adsorption process. Therefore, the pH of point of zero charge (pHpzc) of biochar was determined to understand the ability and conditions in which biochar sorb contaminant. Fiol, & Villaescusa (2009) defined that a pH value at which the total surface charge is a zero value. For examples, when pH of solution is lower than pHpzc, the surface of biochar is positively charged. When pH of solution is greater than pHpzc, the surface of biochar is negatively charged. In this case, the results show that all of biochar produced at different pyrolysis conditions were positive in the very low pH and the pHpzc was between 0.73 and 2.03 for all of biochars (Table 8).

Table 7 presented the pH of point of zero charge of biochar produced from different pyrolysis conditions. The results show that all of biochars were positive in the very low pH and the pHpzc was between 0.73 and 2.03. In specific, pyrolytic temperature does not affect much on point zero charge of surface of biochar due to loss a fixed quantities of functional groups such as –OH groups. On the other hand, pyrolysis time affected on point zero charge of surface of biochar because of the loss amount of –OH groups. At 200^{0}C, biochar produced from pyrolysis time during 2h can loss amount of –OH groups less than biochar during 6h. This can explain the pHpzc of BC200-2 which possesses highest pH of point of zero charge at 2.03.

Table 8 Surface charge, surface area and yield of biochars

Code	Temperature (°C)	Pyrolysis time (hour)	Biochar yield (%)	pH pzc	Specific surface area (m^2/g)	BET surface area (m^2/g)	Total volume in pores (A°)
BC200-2	200	2	80.08	2.03	0.68	1.45	58.80
BC200-4	200	4	72.04	0.73	1.22	3.01	86.32
BC200-6	200	6	71.53	0.98	0.99	1.87	172.10
BC400-6	400	6	34.40	1.1	2.07	7.52	147.61
BC600-6	600	6	13.04	0.93	3.10	4.10	147.61

The morphologies of the corn cob biochars synthesized at different pyrolysis conditions were presented in Table 8 with pore properties such as Specific surface are (SSA), BJH adsorption average pore width, BET surface area and total volume in pore. The SSA of biochar enhanced with increasing pyrolysis temperature, from 0.99 m^2/g at 200^0C to 3.10 m^2/g at 600^0 during 6h due to decomposition of original material to form pore network in biochar. Similarly, Chen et al. (2008) and Zhao et al. (2013) found that the effect of temperature was the main parameter in determining and increasing the surface area of biochar.

Results of yield of biochar produced from different conditions are shown in Table 8. The biochar yield increased with decreasing pyrolysis temperature from 600^0C (13.04%) to 200^0C (71.53%) during 6 hours and pyrolysis time from 6 hours (71.53%) to 2 hours at 200^0C (80.08%).

The rate of weight loss was the fastest from 400^0C to 600^0C, losing approximately 66-87 % of the corn cob biomass. Due to the rapid weight loss, the pyrolysis decomposition of corn cob which mainly included cellulose, hemicelluloses and lignin happened from 250-500^0C (de. Wild et al., 2009). The components of biomass such as cellulose, hemicelluloses and lignin have an important role on physicochemical properties of biochar (Lian and Xing, 2017; Luo et al., 2022).

Moreover, the more cellulose/hemicellulose contents in biomass have tendency to form more microporous structures, while the higher lignin contents usually bring about more mesoporous structures, larger SSA, and higher aromaticity (Luo et al., 2022, Solanki and Boyer, 2017, Zhang et al., 2017). Interestingly, Vyavahare (2019) indicated that higher total organic carbon contents in biochar could promote the adsorption of organic contaminants.The more lignin exists in biomass, the higher production yield and the fixed carbon content of biochar will become.

In addition, the composition of corn cob was contained approximately 48% of cellulose, 37% of hemicellulose and 15% of lignin (Vassilev et al., 2012)**.** On the other hand, the rate of weight loss was low pyrolysis time from 2 hours to 6 hours at 200^{o}C, similarly losing about 20-28% of original biomass because of hydrolysis/dehydration processes at low temperature around 200^{o}C which broken down from high-molecular weight compound to low-molecular weight compounds of corn cob such as oligosaccharides, glucose, amino acid (de. Wild et al., 2009; Funke and Ziegler., 2010).

4. Effect of initial pH solution on Paraquat adsorption onto biochar

The effect of initial solution pH on the efficiency of paraquat removal by biochar was indicated in Figure 28. In this case, the results showed that all of the biochar produced from different materials had an enhanced percentage of paraquat removal in the pH ranges of 5-7, 9-11, and got the highest PQ removal at pH 11. However, the pH level of the solution in this study was from 1 to 11 and greater than the pH point of zero charge (Table 8), leading to the charge of the biochar being negative. According to a report by Tantrirantna et al. (2011), the pKa of cationic paraquat was about 9-9.5. This can explain why, when the pH of the solution is lower than pKa about 9-9.5, the paraquat molecular structure is negatively charged. When the pH of the solution is greater than pKa of paraquat, the molecular structure is positively charged. At pH 11, PQ became positively charged, therefore, PQ can interact efficiently with biochar with a negative charge on the surface based on electrostatic interactions during the adsorption process. This finding is in agreement with the study of Tsai et al., (2003), who similarly noted that the cationic paraquat adsorbed quantitatively onto the negatively charged sites of the adsorbent when the pH values increased due to the loss of H^{+} from surface.

Point zero charges of biochars are very low (less than 2). Therefore, the surface charge of almost biochar is negative charge at solution pH higher than 2, favoring the adsorption of positive charge of pollutants. The biochars that presented the lower Point zero charge (PZC) values are compatible with cationic paraquat, because the pH of the solution can be easily adjusted to be higher than the pH at the PZC. When the solution pH of paraquat higher than pH_{PZC} of biochar, the biochar's surface is negatively charged, favoring the adsorption of cations.

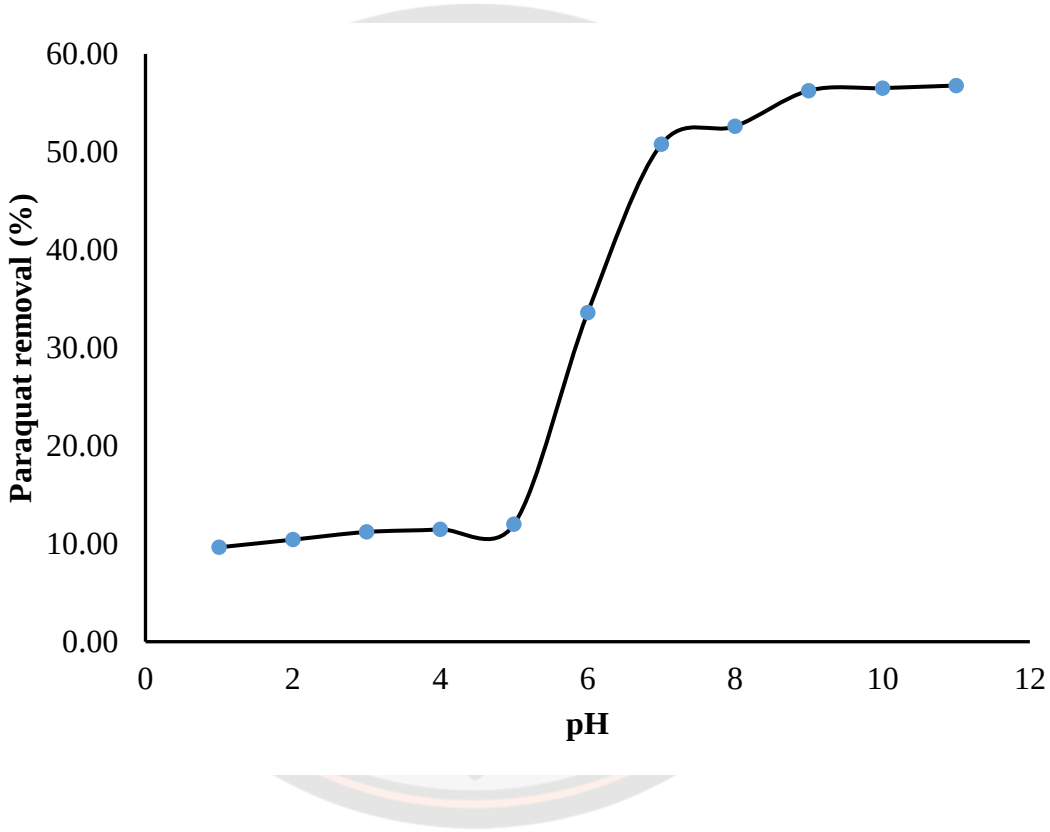

Figure 28 The effect of pH on Paraquat removal by Corn cob biochar (biochar dosage 1 g/L, [PQ]: 5 mg/L

Adsorption Isotherms

Tables 8 shows the isotherm parameters of paraquat removal using corn cob biochars produced from different pyrolysis temperatures. There are two most common adsorption isotherm models, Langmuir and Freundlich isotherms. Because these isotherms can test/explain paraquat adsorption by adsorbents such as activated bleaching earth, activated carbon, clay (Tsai et al., 2003, 2004, 2005, 2006; Hamadi et

al. 2004). Table 8 illustrated that the adsorption of paraquat on biochar can be described using both Langmuir and Freundlich isotherm models because both models have the suitable correlation coefficient. Considering R^2, the values of R^2 of Langmuir model (0.944 – 0.984) were higher than the values of correlation coefficients of Freundlich model (0.859 – 0.984). Hence, the adsorption characteristics of paraquat on biochar were obviously described by the Langmuir model. More interestingly, Figure 29 shows the effect of different pyrolysis temperatures on the adsorption of paraquat onto corn cob biochar. When temperature increased from 200^0C to 600^0C the corresponding adsorption capacitiy (Qo) values decreased from 71.83 to 33.90 mg/g. The maximum adsorption capacity of paraquat onto biochar obtained at 200^0C. These results implied that the paraquat adsorbed capacity was dependent on pyrolysis temperature and decreased in the order BC200-6 > BC300-6 > BC400-6 > BC500-6 > BC 600-6, respectively. In conclusion, the adsorption capacity of paraquat on biochar is affect by pyrolysis temperature. Likely, Yavari et al. (2015) reviewed that the temperature was one of the main factors determining the characteristics of biochar.

For this reason, the pyrolysis temperature is a main effect on biochar structure in Fig. 27. The structures of biochar have pore size reducing in the order BC200-6 > BC400-6 > BC600-6 (Figure 2) and the total volume in pores decrease in the order BC200-6 (172.10 A^o) > BC400-6 (147.61 A^o) > BC600-6 (147A^o). Furthermore, the molecular sizes of paraquat are approximately 13.4 A^o x 3.6 A^o (Draoui et al. 1999). Thus, these pollutants can fill into the pores of biochar depending on the total volume in pores of each type of biochar. Hence, this thing can explain why the adsorption capacity of paraquat on biochar reduced when increasing pyrolysis temperature, similar to pore-filling mechanism suggested by Nguyen et al. (2007). She indicated that the decreasing sorption of contaminants (1,4-dichlorobenzene and 1,2,4-trichlorobenzene) onto pitch pine biochar was caused by the small molecular diameters which proposed mainly to pore-filling mechanism.

Nowadays, farmers can make biochar at their farm in industrial scale. Therefore, we can apply biochar for removal pesticides, especially paraquat from field. As our results show that the adsorption of paraquat on biochar mainly base on pore-filling mechanism more than chemical properties such as surface function groups. When we apply biochar removal paraquat in field, the adsorption rate also

depend on environmental conditions. Environmental conditions such as temperature, pH and moisture can effect on the rate of biochar adsorption. However, as our best knowledge, the biochar adsorption of paraquat also follows Langmuir or Freundlich isotherm models, when it is applied in the field.

Table 9 Isotherm parameters of paraquat adsorption onto corn cob biochars produced from different pyrolysis temperatures

Types of biochar	Langmuir parameters			Freundlich parameters		
	Qo (mg/g)	B (L/mg)	R^2	Kf $(mg/g)(L/mg)^{1/n}$	1/n	R^2
BC200-6	71.83	1.53	0.983	41.78	0.23	0.984
BC300-6	51.81	0.53	0.949	8.74	0.52	0.859
BC400-6	39.22	0.31	0.955	10.94	0.42	0.887
BC500-6	34.84	0.31	0.984	4.25	0.52	0.907
BC600-6	33.90	0.19	0.944	8.67	0.39	0.938

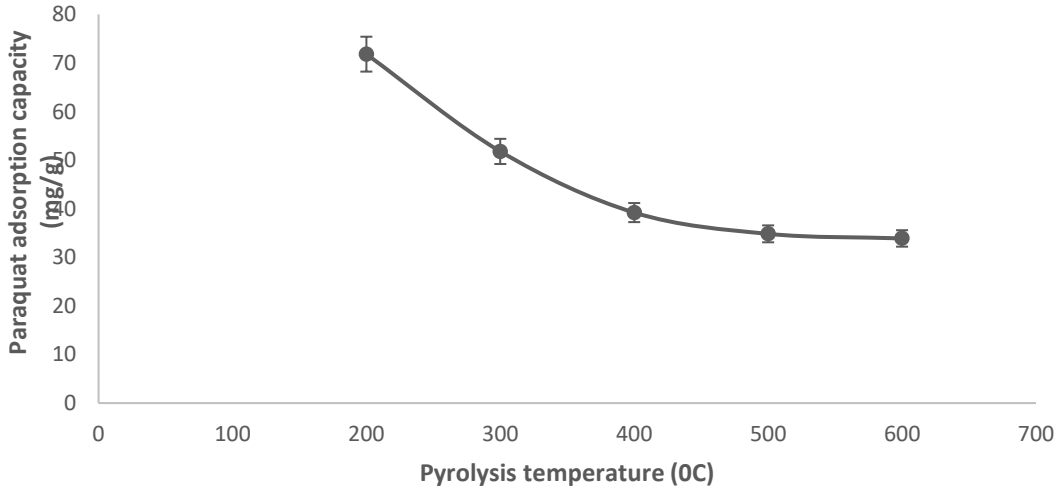

Figure 29 Paraquat adsorption capacity of corn cob biochars produced from different temperatures during 6h (Initial paraquat concentrations 5 mg/L (, adsorbent dosage = 30 mg/135 mL, Initial pH =11)

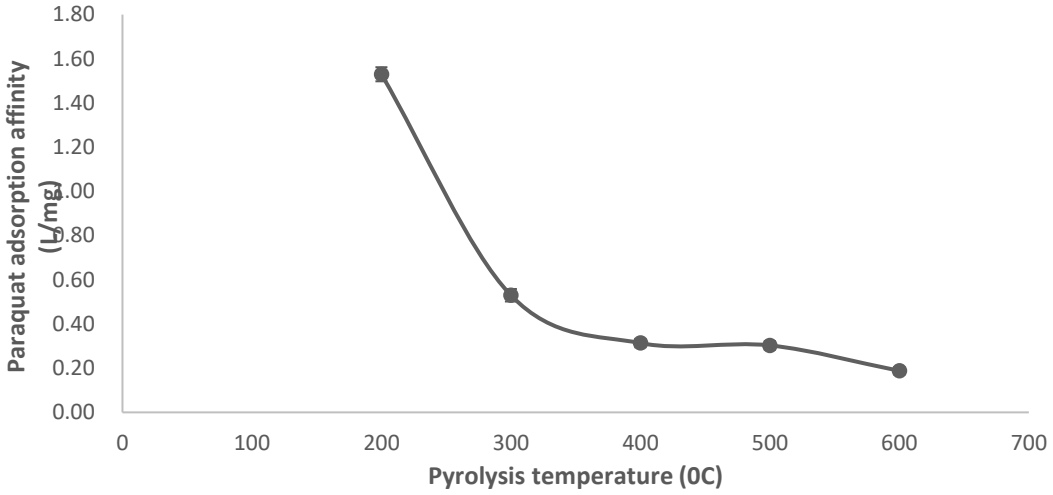

Figure 30 Adsorption affinity between paraquat and biochar produced different pyrolysis temperatures during 6h (Initial paraquat concentrations 5 mg/L, adsorbent dosage = 30 mg/135 mL, Initial pH =11)

Figure 30 illustrates the affinity between paraquat and biochar produced different pyrolysis temperatures. The temperature increases from 200^{o}C to 600^{o}C corresponding to the affinity/attraction of adsorbent and adsorbate values decrease from 1.34 to 0.19 L/mg. The highest affinity of paraquat and biochar obtained at 200^{o}C. These results shows that the increase pyrolytic temperature leads to decrease the attraction of paraquat on biochar. Thus, the attraction of paraquat on biochar is affected by pyrolysis temperature. This study is agreement with the study of Sun et al.,2016. At low pyrolysis temperature (300^{o}C) increasing pollution adsorption to compare with high temperature at 400 and 500^{o}C. For explaining this, the increasing pyrolysis temperature (from 200 to 600^{o}C) leads to loss some functional groups such as O-H, nonpolar aliphatic (C=C rings, CH_2) groups in Figure 27a. From this loss, the paraquat adsorption affinity of biochar may reduce. Moreover, BC400-6 and BC600-6 have some C=C aromatic groups which can be cause steric effect to limit the diffusion of paraquat inside their pore network. Xiao and Pignatello (2015) demonstrated that steric effects caused negatively efficiencies of molecular volume of pollutant by adsorption process. Besides, BC200-6 has the functional groups such as –OH groups, -OH phenolic groups, -CH2- groups, carbonyl groups (C=O) corresponding to various

acids, aldehydes and ketones,-CH2- groups and C-O polysaccharide. These significant functional group can form hydrogen bonding which will discuss in detail in next section. Based on this bonding, it can enhance the paraquat adsorption attraction of biochar. These are basic reasons to explain the order in reducing affinity of paraquat and biochar responding to the enhancing the pyrolysis temperature in sequencing BC200-6, BC300-6, BC400-6, BC500-6, BC 600-6, respectively.

The effect of pyrolysis time on the adsorption capacity of paraquat onto corn cob biochar was illustrated in Figure 30. From the Figure 31, it can be seen that as the pyrolysis periods increases from 2 hours to 6 hours the corresponding adsorption capacitiy (Qo) values increase. This indicates that the maximum adsorption capacity of paraquat onto biochar reached at pyrolysis period for 6 hours. These results implied that the paraquat adsorbed capacity is dependent on pyrolysis period and increases in the order 2, 3, 4, 5 and 6 hours with approximately 50.76, 55.86, 63.79, 64.13 and 71.83 mg/g, respectively. On the other hand, Figure 32 shows the affinity between paraquat and biochar produced different pyrolysis time. The pyrolysis time from 2h to 6h corresponding to the attraction of biochar and paraquat values increase from 1.15 to 1.53 L/mg. The highest affinity of paraquat and biochar obtained at 6h. These results means that the attraction of paraquat on biochar is denpendent on pyrolysis time and increases in the order BC200-2 > BC200-3 > BC200-4 > BC200-5 > BC200-6, respectively. In conclusion, the adsorption capacity and affinity of biochar and paraquat were increased with increasing pyrolytic time. To explain for this, the total volume in pores increased with increasing pyrolysis time in order BC200-2 (58.80 A^o) < BC200-4 (86.32 A^o) < BC200-6 (172.10A^o). This indicates that the increasing of pyrolysis time can generate more volume in pores. Therefore, the paraquat with smaller sizer (approximately 13.4 A^o x 3.6 A^o) can fill into the pores or the pores network of biochar. Similar to the increasing pyrolysis temperature, this leads to enhance the paraquat adsorption capacity of biochar as increasing pyrolysis time. From the higher quantity paraquat adsorption of biochar, it is sure to enhance the interaction between the significant functional groups of biochar and paraquat molecular and increase the paraquat adsorption affinity of biochar.

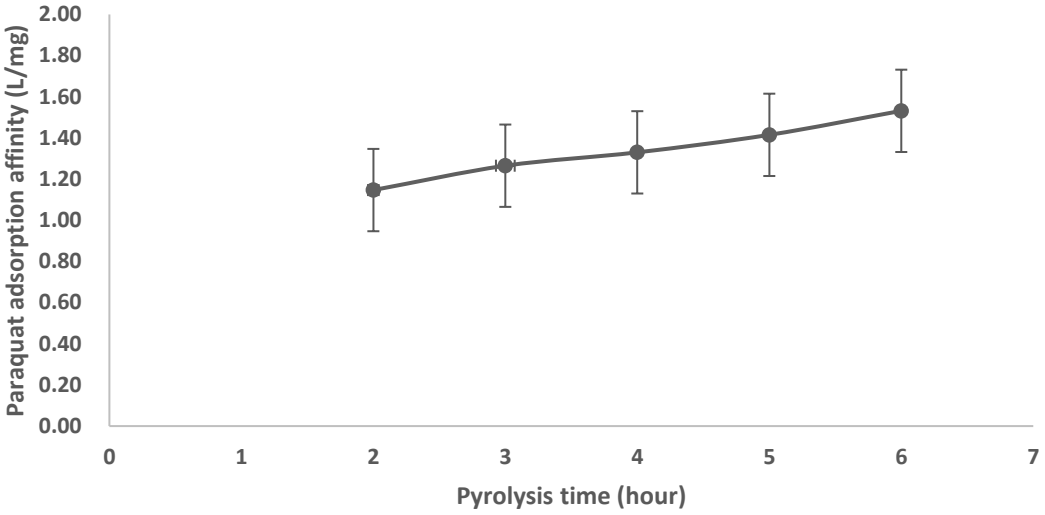

Figure 31 Paraquat adsorption capacity of corn cob biochars produced from different pyrolysis time at 200ºC (Initial paraquat concentrations 5 mg/L, adsorbent dosage = 30 mg/135 mL, Initial pH =11)

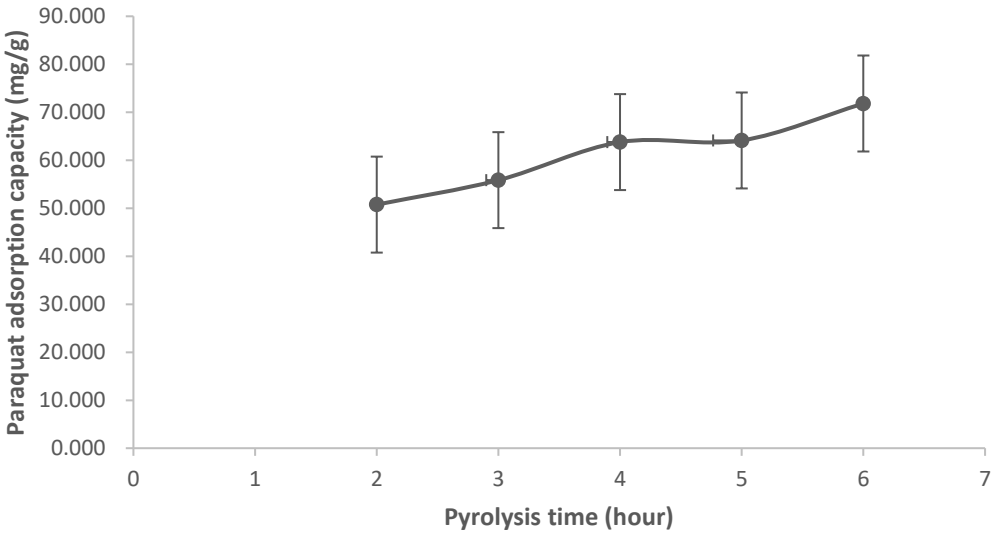

Figure 32 Adsorption affinity between paraquat and corn cob biochar produced from different pyrolysis time at 200ºC (Initial paraquat concentrations : 5 mg/L, adsorbent dosage = 30 mg/135 mL, Initial pH =11)

Adsorption Kinetics

Figure 33 illustrates kinetic adsorption of paraquat with the initial concentration of 5 mg/L by biochars produced from different pyrolysis temperature and time. This can be observed that the adsorption process of paraquat and biochar occurs quickly within the 5 minutes. For biochars produced from different pyrolysis temperature, the removal efficiencies of paraquat by BC200-6, BC600-6, BC400-6, BC500-6 and BC300-6 were 92.86%, 52.94%, 45.09%, 30.92%, and 29.16%. For biochars produced from different pyrolysis period, the removal efficiencies of paraquat by, BC200-5, BC200-4, BC200-3, BC200-2, and BC200-6 were, 98.64%, 98.10%, 97.41%, and 96.80%, and 92.86% after 5 minutes.

The comparison the adsorption kinetic of biochar making from corn cob (our study) with the biochar making from swine-manure (Tsai and Chen., 2013), the result show that highest adsorption kinetic of our study is 1.305 g/mg min, where the highest adsorption kinetic is 0,015 g/mg min.

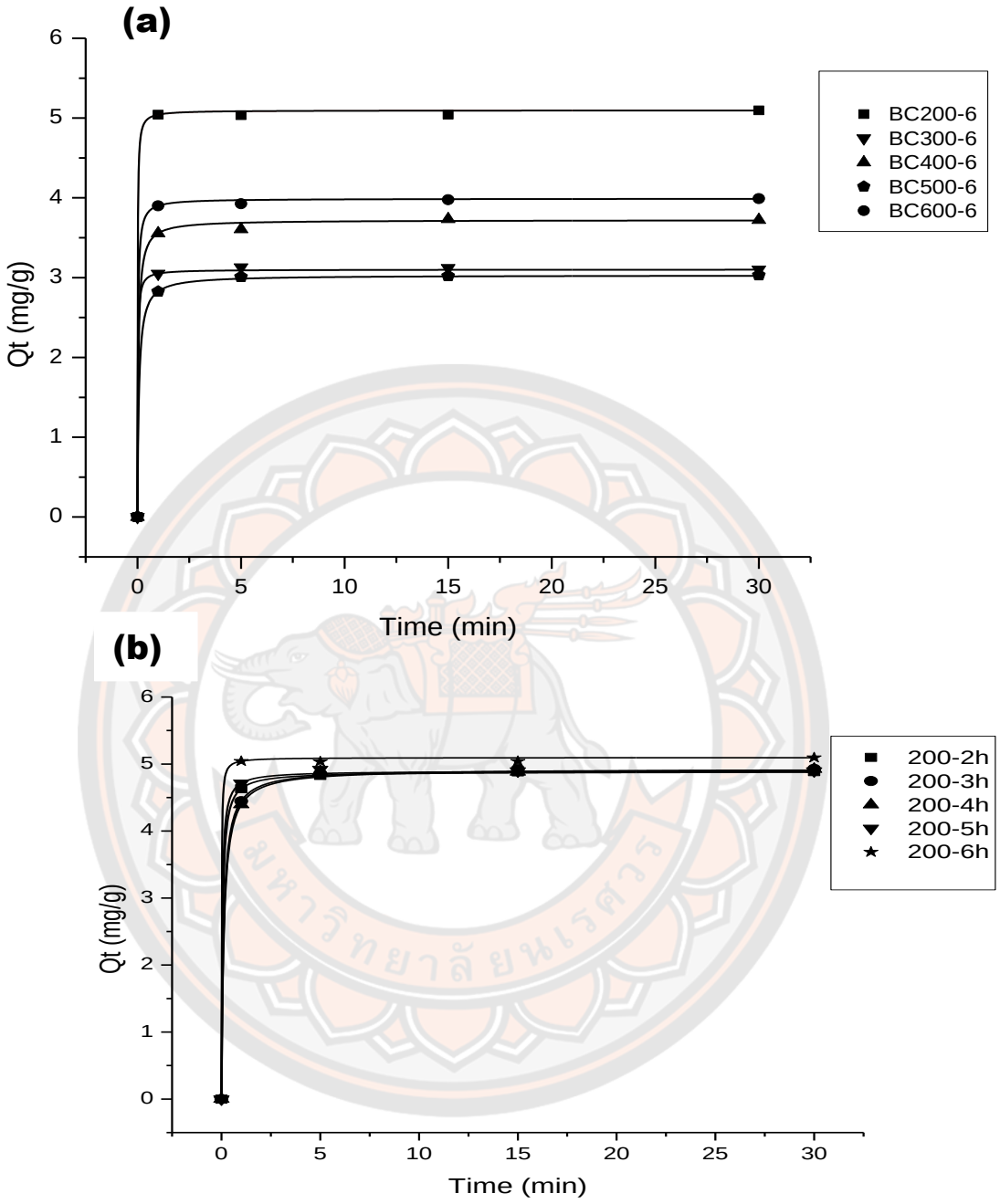

Figure 33 Adsorption kinetics of paraquat onto biochar – (a) different pyrolysis temperatures and (b) different pyrolysis time (Initial paraquat concentrations = 5 mg/L, adsorbent dosage = 0.8 g/L, and room temperature)

Table 10 Values of kinetic parameters in paraquat removal by adsorption process using biochar

Biochar	Kinetic models								
	Pseudo-first order			Pseudo-second order			Intra-particle diffusion		
	qe (mg/g)	K1 (1/min)	R^2	qe (mg/g)	K2 (g/mg min)	R^2	Ci (mg/g)	Kip (mg/g)	R^2
BC200-6	0.059	-0.007	0.1705	5.045	1.070	1.0000	3.780	0.099	0.1408
BC300-6	0.004	0.354	0.0112	1.910	0.990	0.9985	0.999	0.132	0.4114
BC400-6	0.495	0.020	0.2209	3.020	0.790	0.9987	1.759	0.184	0.3068
BC500-6	0.661	0.010	0.0737	1.984	0.620	0.9879	1.272	0.122	0.2673
BC600-6	0.284	0.016	0.1155	3.577	1.305	0.9998	1.982	0.236	0.3684
BC200-5	0.185	0.008	0.7852	4.990	0.407	1.0000	3.689	0.089	0.1478
BC200-4	0.280	0.017	0.2735	4.990	0.361	1.0000	3.611	0.094	0.1660
BC200-3	0.127	0.001	0.0002	4.946	2.284	1.0000	2.782	0.326	0.3602
BC200-2	0.090	-0.003	0.0023	4.897	3.258	1.0000	2.838	0.312	0.3325

The kinetic parameters of paraquat removal using corn cob biochar produced from different pyrolysis conditions were obtained from the experiments and are illustrated in Table 10**.** Experimental data were fitted by the Pseudo-second order, Pseudo-first order and Intra-particle diffusion models. The values of correlation coefficients (R^2 = 0.9879-1.0000) of the Pseudo-second order model were higher than the value of R^2 (0.0002-0.7852) of the Pseudo-first order model and R^2 (0.1408-0.4114) of the Intra-particle diffusion models. Thus, the Pseudo-second order model could adequately describe the kinetic of paraquat removal by adsorption process using corn cob biochar, similar to kinetic model with rapid adsorption suggested by Tsai et al. 2013 and Kumar et al. 2012.

Mechanisms in adsorption process

According to review of Inyang and Dickenson in 2015**,** adsorption mechanisms in organic contaminant by biochar can include pore filling, diffusion and partitioning, electrostatic interaction, hydrophobic interaction, π-π interaction and hydrogen bonding. In this study, the paraquat adsorption mechanism of the corn cob biochar was discussed as follows:

Hydrophobic interaction, diffusion and partitioning

First of all, the property of paraquat is polar compound, high solubility in water with 700 g/L (Rodea-Palomares et al. 2015) and not hydrophobic compound due to its low log Kow. Thus, the hydrophobic and partition interactions do not considerate as contributing to adsorption mechanism of paraquat on corn cob biochar. Based on the above kinetic results, the Intra-particle diffusion model does not use to describe adsorption process. These results suggested that diffusion and partitioning mechanisms do not involve to contribution of adsorption mechanism in paraquat removal by corn cob biochar.

Electrostatic interaction

Principal of electrostatic interaction is interaction between a cationic sorbate and an anionic sorbent. It is known that the pKa of cationic paraquat was 9 (Rodea-Palomares et al. 2015). Therefore, the paraquat is negatively charged at pH 11 and obviously adsorbed on a positively-charge surface of sorbent. On the other hand, the values of point zero charge (pzc) for biochar were determined as presented in Table 1. The pzc of BC200-6, BC400-6 and BC600-6 were identified in the same range 1.0. When pH solution is greater than pHpzc, the surface of all biochars are negatively charged. Hence, the surface of biochar is negatively charged at pH 11.

Thus, this indicates that the mechanism of paraquat adsorption on corn cob biochar does not involve electrostatic interaction.

π-π interaction (π-π electron donor–acceptor (EDA) interaction)

In considering the π-π interaction between paraquat and biochar, paraquat molecule has two pyridine rings which possesses electron-rich moieties. Thus, these rings can act as π-electron of donor and aromatic rings of biochar. Hao et al. (2013) suggested that the π-π interaction can happen between π-electron of pesticide as donor and π-electron acceptor in aromatic rings of biochar. Therefore, the possible π-π interaction between paraquat and biochar can occur (Figure 34C)**.** However, the enhancement of pyrolytic temperature leads to more aromatic formation of biochar at 400 and 600^{o}C such as aromatic -CH - and aromatic C=C groups. Moreover, the results of adsorption capacity of paraquat onto biochar reported that the adsorption capacity of BC400-6 and BC600-6 lower than the adsorption capacity of BC200-6.

Hence, π-π interaction was minor adsorption mechanism in paraquat removal by corn cob biochar.

Pore filling

In this study, the previous results of the total volume in pores in Table 8 and the reducing of paraquat adsorption capacity of biochar by increasing pyrolysis indicated that the pore filling may contribute to adsorption mechanism of this phenomenon. However, the specific surface area and BET surface area of biochar also increased from 200^{o}C to 600^{o}C and could lead to enhance the adsorption capacity, but the experimental results of highest adsorption capacity was the BC200-6. To explain this thing, the above affinities results indicated that the quantity of important functional group decided the paraquat adsorption capacity of biochar. Therefore, pore filling can involve to adsorption mechanism of biochar.

Hydrogen bonding

Regarding to hydrogen bonding formation, the results of the FTIR indicated that the BC200-6 possessed –OH groups, -OH phenolic groups, -CH2- groups, carbonyl groups (C=O) corresponding to various acids, aldehydes and ketones,-CH2- groups and C-O polysaccharide which formed hydrogen bonding with hydrogens of paraquat (Figure 34). Hydrogen bonding mechanism is able to occur in 2 cases. The first case, the negatively charged oxygens of –OH, C-O polysaccharide, C=O of biochar interact with positively charged atoms such as hydrogens of paraquat (Figure 34A), similar to adsorption mechanism of phenol on biochar suggested by Liu et al (2011). This study reported that the enhancement of phenol adsorption by biochar was major attraction between the oxygen of functional groups of biochar such as –OH, C-O polysaccharide and C=O and phenol molecules based on hydrogen bond.

The second case, the attraction between hydroxyl groups (–OH groups, -OH phenolic groups, -CH2- groups) of biochar and the aromatic rings of paraquat (Figure 34B). This phenomenon is known as Yoshida hydogen bonding. More agreeably, Blackburn pointed out interactions between –OH groups of polysaccharide and aromatic ring residues of dye molecule (Yoshida hydrogen bonding interaction) in 2004. With results of adsorption capacitiy of paraquat onto biochar, BC200-6 is the highest adsorption capacity. More importantly, Zhu et al. 2009 studied that the pseudo-second order model shows the kind of adsorption may be chemical adsorption.

Therefore, hydrogen bonding plays an important adsorption mechanism in paraquat removal by corn cob biochar.

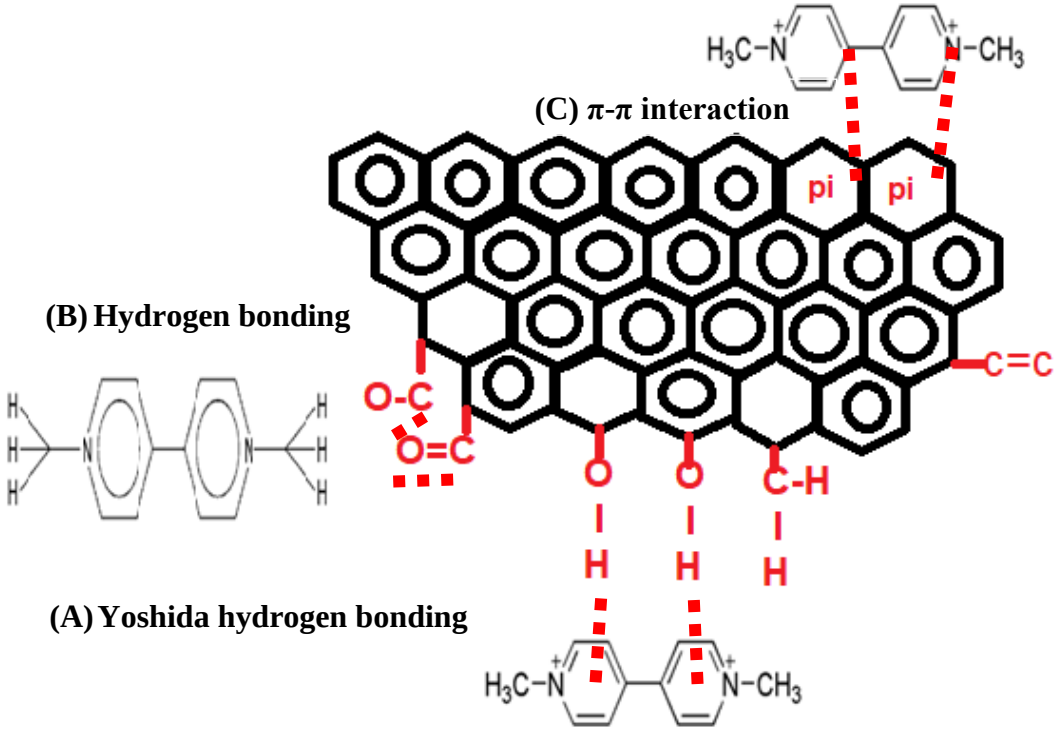

Figure 34 Possible adsorption mechanisms in removal of paraquat by corn cob biochar

Practical application

Some previous studies reported that activated carbon is well known as typical and oldest adsorbent (Hassler., 19630), but it requires a huge energy and high cost with physical activation process (600-1200^{o}C) and chemical activation process from 450^{o}C to 900^{o}C with acid or base (Carrott., 2007). Furthermore, Ahmad et al., 2014 estimated that the price of activated carbon is approximately US $1476 per ton, while the price of biochar is US $246 per ton. Therefore, application of biochar can feasibly apply in developing countries. According to these experimental results given in Table 8, the yield of best biochar produced from 200^{o}C for 6 hours was found

71.13%. It means that this biochar can manufacture at low temperature and used as alternative and economic absorbent for pollutant compound in rural areas.

Biochar with pore system can provide a habitat for soil microorganisms such as mycorrhizal fungi, actinomycetes bacteria based on Compant et al., 2012. Moreover, farmers can make biochar at their farm in industrial scale. Therefore, we can apply biochar for removal pesticides, especially paraquat from field. Specifically, *Pseudomonas putida* achieved 95% degradation of initial paraquat dose at 69.76 mg/L in the presence of 15 g/L activated charcoal after 3 days of treatment (Zauscher et al., 2002) and four types of microorganisms such as *Roseateles terrae, Bacillus sp., Escherichia coli,* and P. *fluorescens* degraded paraquat up 97% (100 mg/L) in a mixed culture for paraquat over 7 days. Thus, corn cob biochar can help immobilize bacteria to enhancing paraquat removal from contaiminated water (Nguyen et al., 2021).

As our results show that the adsorption of paraquat on biochar mainly base on pore-filling mechanism more than chemical properties such as surface function groups. When we apply biochar removal paraquat in field, the adsorption rate also depend on environmental conditions. Environmental conditions such as temperature, pH and moisture can effect on the rate of biochar adsorption. However, as our best knowledge, the biochar adsorption of paraquat also follows Langmuir or Freundlich isotherm models, when it is applied in the field. Furthermore, amendment of biochar to soil reduced soil acidity and increased the content of nitrogen and organic carbon (Mierzwa-Hersztek et al., 2016).

Summary

The corn cob biochar obtained from optimal pyrolysis conditions at 200oC during 6 hours could have adequate characteristics with suitable surface morphology, suitable functional groups for paraquat adsorption with maximum capacity 71.83 (mg/g). The kinetic and isotherm data was fitted and well explained by the Pseudo-second-order and Langmuir models, which indicated that the adsorption capacity decreased with increasing pyrolysis temperatures and decreasing pyrolysis time. The dominant adsorption mechanisms of paraquat on biochar possibly contributed to hydrogen bonding and pore filling. Therefore, this biochar can become an alternative and economic adsorbent for Pesticide removal in agricultural water treatment.

Part 1 - B. Kinetic, Isotherm and Mechanism in Paraquat Removal by Adsorption Process Using Biochars

This part aimed to explore the isotherm, kinetic and mechanism of paraquat adsorption in aqueous solution by coconut fiber (CFB), corn cob (CCB), bagasse (BGB) and rice husk (RHB) biochars. The biochar characteristics were identified using SEM, BET, and FTIR. Kinetic and isotherm data were followed the Pseudo-second-order and Langmuir models. The biochars were arranged according to their capacity: CFB (12, 72 mg/g), CCB (10.27 mg/g), RHB (9.72 mg/g), BGB (7.79 mg/g) where specific surface area and pore volume determined the adsorption capacity. The intraparticle diffusion model was used to assess the kinetic rate of the adsorption process, which indicates the rate constant of the external diffusion phase where Kip1 was higher than the Kip2 and Kip3 phases. Film diffusion played a major role in the adsorption process. Pore filling, diffusion, hydrogen bonding, π-π and electrostatic interactions contributed to the mechanism of adsorption. CFB has the highest adsorption capacity (12.72 mg/g), and can be an alternative adsorbent

1. Characteristics of different biochars

1.1 Surface morphology

The SEM images of biochar show the surface morphologies of four types of biochar produced from different biomasses with different porous structures in Figure 36. From this work, it can be seen that the morphologies of biochar types have similar characteristics which have porous structures. Thus, the porosity of each type of biochar may be a significant factor of the efficiency of paraquat removal in the adsorption process. The pores have a variety of different sizes and shapes, such as: (i) The pore size of coconut fiber biochar refers to CFB in Figure 36 (A) from 100 to 270 µm. (ii) The pore size of corn cob biochar refers to CCB in Figure 36 (B) from 80 to 400 µm. (iii) The pore size of rice husk biochar refers to RHB in Figure 36 (C) from 60 to 270 µm. (iv) The pore size of bagasse biochar refers to BGB in Figure 36 (D) from 50 to 240 µm. This characteristic can affect the physical adsorption properties of each biochar.

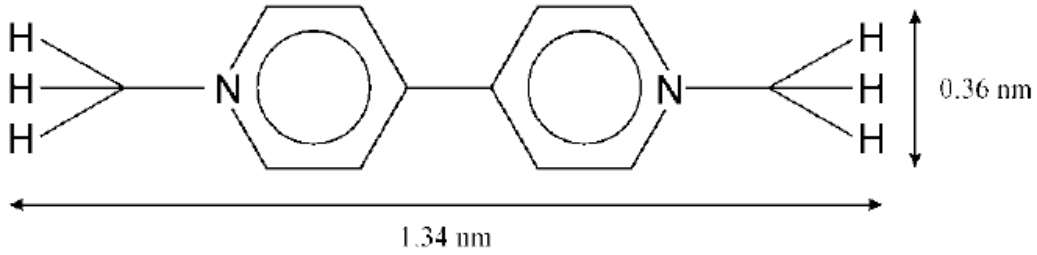

Figure 35 Size of paraquat molecular

Source: Draoui et al. 1999

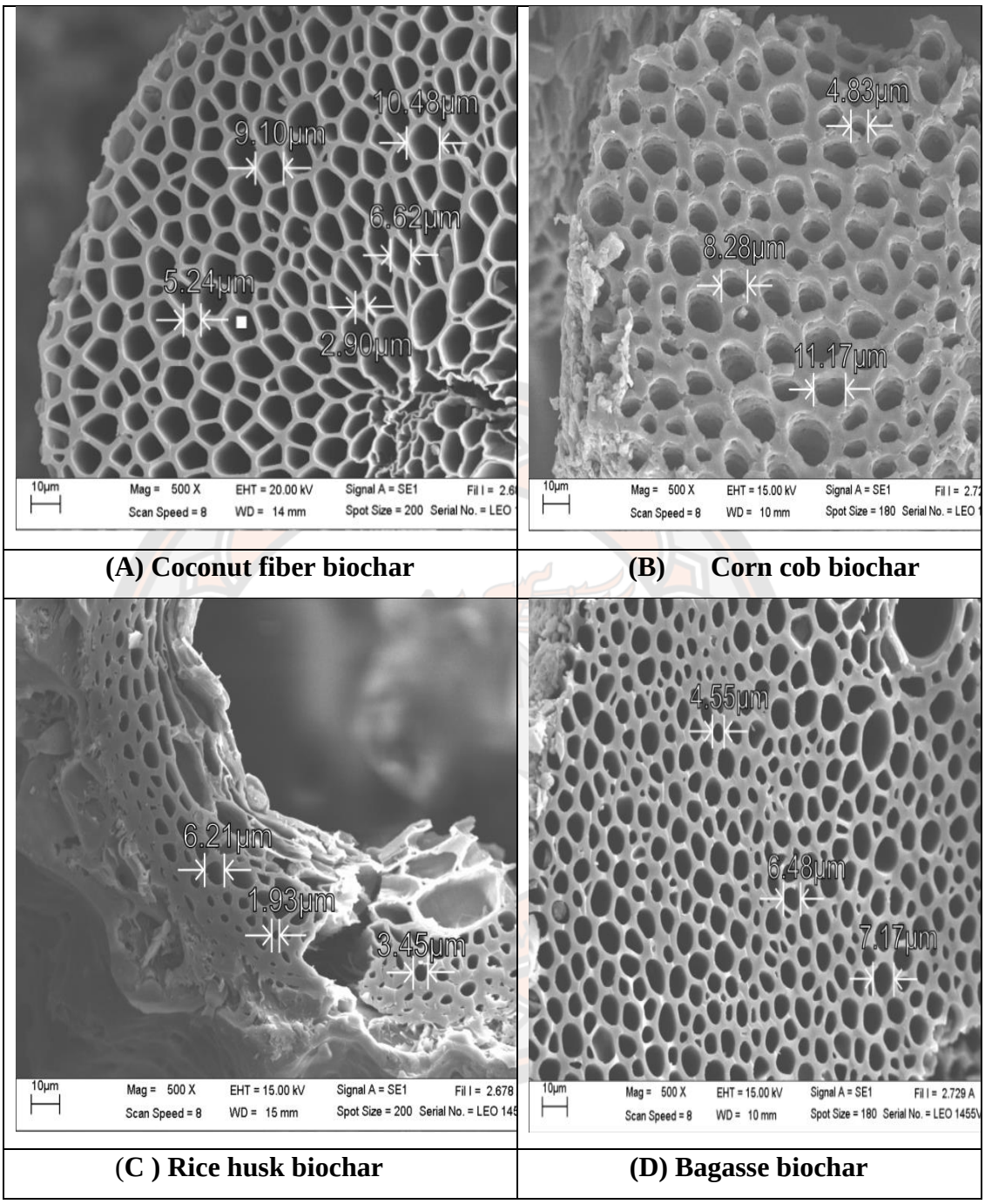

(A) Coconut fiber biochar | **(B) Corn cob biochar**

(C) Rice husk biochar | **(D) Bagasse biochar**

Figure 36 Scanning electron microscopy (SEM) images of four different biochar types produced from corn cob biochar, rice husk biochar, coconut fiber biochar and bagasse biochar

1.2 Surface charge, surface area of biochar

The solution pH plays a crucial role in the optimization of the adsorption process. Therefore, the pH of point of zero charge (pHpzc) of the biochar was determined to understand the ability and conditions in which biochar adsorps paraquat. Fiol and Villaescusa, (2009) stated that the pH value is the total (net) surface charge of biochar is a zero value. At this point value, the biochar is neutral. When the pH of solution is lower than pHpzc, the surface of biochar is positively charged. When the pH of solution is greater than pHpzc, the surface of the biochar is negatively charged. In this study, the results show that all of the biochars produced from four types of biomass were positively charged when under a very low pH condition (less than between 0.70 and 0.75 in Table 11) and have negative charges when in solution pH greater than 1.

The morphologies of the four types of biochar produced from different biomasses are presented in Table 8 with pore properties such as Specific Surface Area (SSA), Total Pore Volume (TPV), and pore size distribution. The SSA and TPV of four types of biochar enhanced in consequent as BGB < RHB < CCB < CFB. These pore properties may create good characteristics of the biochar for pollutant adsorption.

Table 11 Physical and chemical properties of biochars

Biochar	SSA	TPV	pHpzc	The pore size distributions (%)			
				Micropores	Narrow mesopores	Mesopores	Macropores
	m^2/g	cm^3/g		< 2 nm	2-20 nm	20-50 nm	> 50 nm
CFB	402.43	0.151	0.7	17.40	69.22	6.10	7.28
CCB	292.92	0.117	0.75	21.24	56.57	10.39	11.81
RHB	153.27	0.055	0.72	7.90	59.26	13.97	18.87
BGB	67.42	0.029	0.7	16.88	59.29	15.75	8.07

1.3 FTIR analysis

The functional groups of the four types of biochar produced from different biomasses, were analyzed using FTIR which clearly displays the peaks indicating the presence of typically functional groups. Specifically, the broad peak near 3789.21 cm^{-1}, 3789.74 cm^{-1} and 3725.38 cm^{-1} , of CFB, CCB and BGB were observed in Fig. 37, and these peaks represented the hydroxyl group (O-H stretching vibration) (Zhang et al. 2011). Some previous studies suggested this group is related to hydrogen-bonding interactions (Zhang et al. 2011 and Chen et al., 2011). A report by Kinney et al., 2012, sugested that the peaks at 2970.09 cm^{-1}, 2915.56 cm^{-1}, 2916.64 cm^{-1}, 2911.14cm^{-1} of CFB, CCB, RHB and BGB respectively, were refered to as the alkyl group or aliphatic group (C-H stretching vibration) and possessed characteristic of chemical hydrophobicity. Moreover, the peaks at 2299.83 cm^{-1}, 2383.01 cm^{-1} , 2299.59 cm^{-1}, 2298.66- $cm^{1}$of CFB, CCB, RHB and BGB respectively, were indicated to the ketone group C=O with stretching vibrations (Nuithitikul et al., 2010). Besides, the possession of bands at 1715.94 cm^{-1}, 1734.47 cm^{-1}, 1716.20 cm^{-1}, 1736.00 $cm^{-1}$of CFB, CCB, RHB and BGB respectively, exhibited for carbonyl groups (C=O) corresponding to various acids, aldehydes, ester and ketones which are mostly formed by dissociation of cellulose and hemicellulose (Liu et al., 2011; Yang et al., 2007 and Liu et al., 2015). The peaks at 1571.84 cm^{-1}, 1568.03 cm^{-1} , 1601.57 cm^{-1}, 1563.24 cm^{-1} of CFB, CCB, RHB and BGB respectively displayed the stretching of aromatic C=C (Cheng et al., 2006; Sharma et al., 2004 and Ahmad et al., 2007). The peaks at 1216.70 cm^{-1}, 1216.86 cm^{-1}, 1216.65 $cm^{-1}$of CFB, CCB, and BGB respectively were related to the aromatic C-O stretching of phenolic hydroxyl (Chun et al., 2004). On the other hand, the peaks at 1047.05 cm^{-1}, 1045.82 cm^{-1}, 1063.19 cm^{-1}, 1099.12cm^{-1} of CFB, CCB, RHB and BGB respectively, were indicated to the aromatic C-O stretching of alcohol (Saffari et al., 2015). The peaks at 878.86 cm^{-1}, 871.80 cm^{-1}, 791.71 cm^{-1}, 874.50$cm^{-1}$of CFB, CCB, RHB and BGB respectively, indicated the aromatic C-H (Tran et al., 2017).

In summary, the FTIR analysis indicated that there are 8 major functional groups on the surfaces of biochar. These can be classified into 2 functional characters, polar groups (hydrophilic characters): Hydroxyl groups (O-H), Ketone groups (C=O), Carbonyl groups (C=O), Aromatic C-O phenolic hydroxyl groups,

Aromatic C-O alcohol groups, Aromatic C-H groups and non-polar groups (hydrophobic characters) such as Alkyl groups and Aromatic (C=C) groups. Therefore, the hydrophilic groups account for the main functional groups. This characteristic can indicate that biochar behavior was hydrophilic and agreed with the study by Nanseu-Njiki et al. 2010.

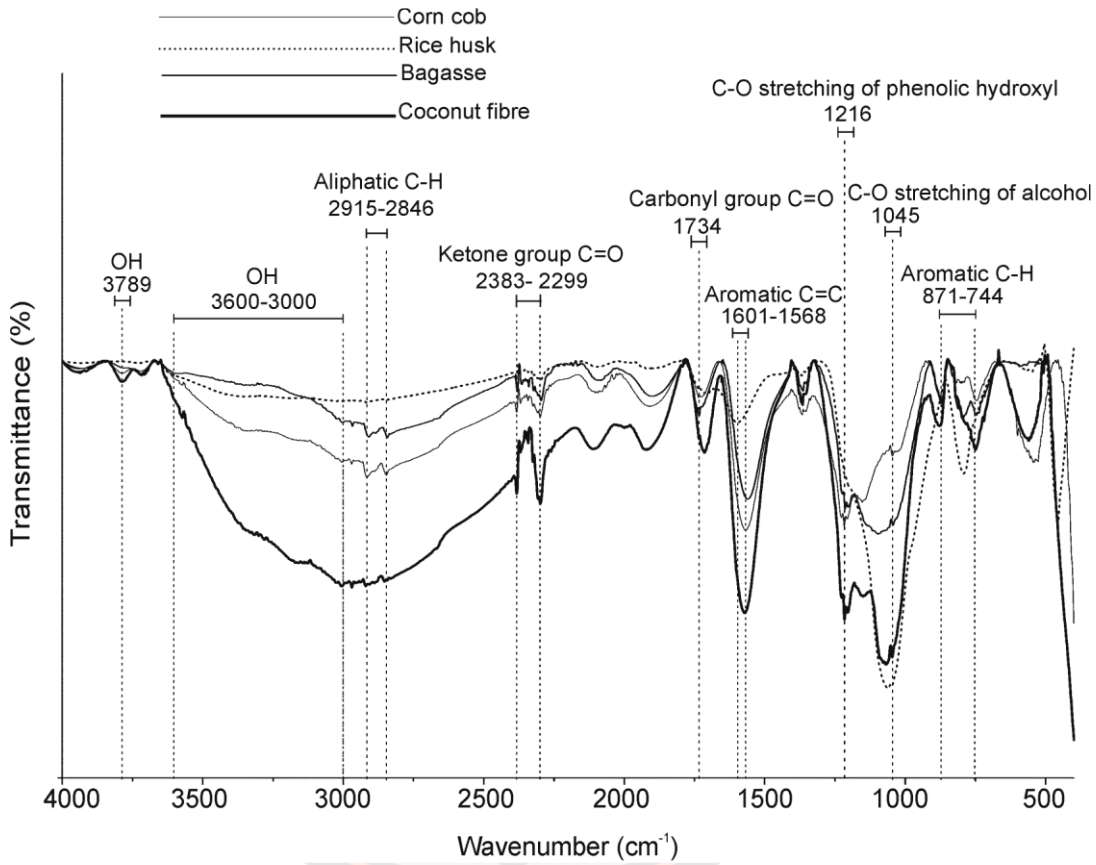

Figure 37 FT-IR spectra analysis of the different biochars

2. Effect of pH on Paraquat adsorption onto the biochar

The effect of pH on the efficiency of paraquat removal by four types of biochar was indicated in Fig. 38. In this case, the results showed that all of the biochar produced from different materials had an enhanced percentage of paraquat removal in pH ranges of 5-7, 9-11 and got the highest at pH 11. However, the pH level of the solution in this study was from 1 to 11 and greater than the pH point of zero charge in Table 11 leading to the charge of the biochar being negative.

According to the report of Tantrirantna et al. 2011 the pKa of cationic paraquat was about 9-9.5. This can explain why when the pH of the solution is lower than pKa about 9-9.5, the paraquat molecular structure is negatively charged. When the pH of the solution is greater than pKa of paraquat, then the paraquat molecular structure is positively charged. At pH 11, PQ became positively charged. Therefore, PQ can interact efficiently with biochar with a negative charge on the surface based on electrostatic interactions during the adsorption process. This finding is in agreement with the study of Tsai et al. (2003) who similarly noted that the cationic paraquat adsorbed quantitatively onto the negatively charged sites of adsorbent when pH values increased due to the loss H^+ from surface.

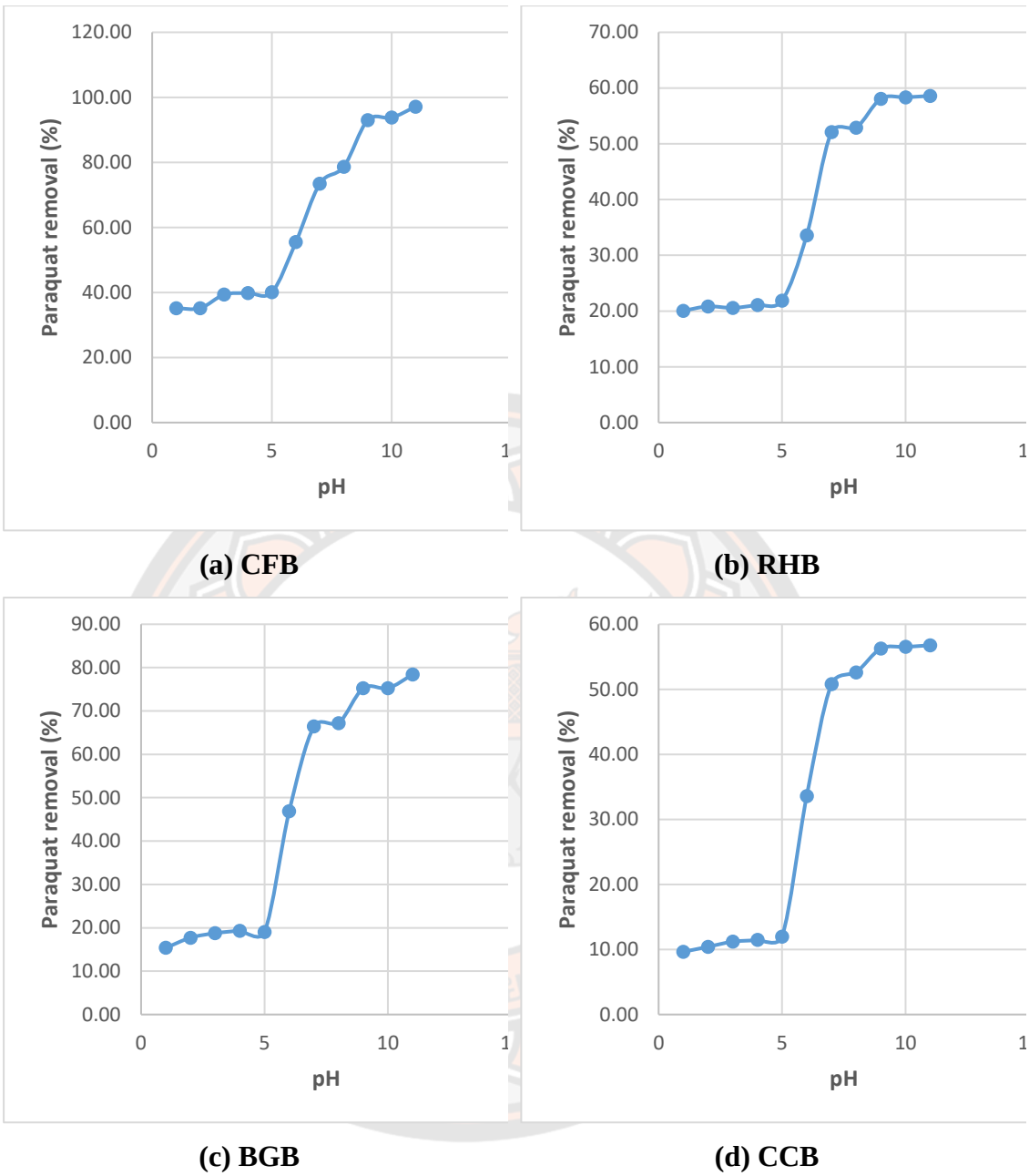

Figure 38 The effect of pH on Paraquat removal by biochars: (a) Coconut fiber biochar, (b) Rice husk biochar, (c) Bagasse biochar, (d) Corn cob biochar (biochar dosage 1 g/L, [PQ] = 3.1 mg/L

Adsorption Isotherms

Table 12 shows the isotherm parameters of paraquat removal using four types of biochar produced from different biomasses. There are two common adsorption isotherm models, Langmuir and Freundlich isotherm models. These

isotherms can explain paraquat adsorption by adsorbents such as activated bleaching earth, activated carbon, clay (Tsai et al. 2003, 2004, 2006; Hamadi et al. 2004). Table 12 illustrated that the adsorption of paraquat on biochar can be described using both Langmuir and Freundlich isotherm models because both models have a suitable correlation coefficient. Considering R^2, the values of R^2 of the Langmuir model (0.868 – 0.998) were higher than the values of correlation coefficients of the Freundlich model (0.554 – 0.931). Hence, the adsorption characteristics of paraquat on biochar are obviously described by the Langmuir model.

Table 12 Isotherm parameters of paraquat adsorption onto the different biochars

Types of biochar	Langmuir parameters				Freundlich parameters		
	Qo (mg/g)	b (L/mg)	R^2	RL	Kf $(mg/g)(L/mg)^{1/n}$	1/n	R^2
CFB	12.74	13.08	0.998	$2.31x10^{-3}$	11.39	0.04	0.931
CCB	11.03	0.77	0.868	$3.92x10^{-3}$	6.35	0.18	0.584
RHB	9.90	1.81	0.988	$16.5x10^{-3}$	7.46	0.09	0.554
BGB	7.94	1.24	0.992	$23.78x10^{-3}$	5.11	0.15	0.625

According to study of Hamdaoui, O.,(2006), the favorable nature of adsorption process can be defined in terms of dimensionless separation factor of equilibrium parameter as follow:

$$\mathbf{R}\mathrm{L} = \frac{1}{1 + \mathrm{bCo}}$$

Where b is the Langmuir constant and Co is the initial concentration of Paraquat in solution. The value of RL indicates the type of isotherm to be irreversible (RL=0), favorable (0<RL<1), linear (RL=1) or unfavorable (RL>1). RL values for paraquat adsorption onto the four types of biochar from $2.31x10^{-3}$ to $23.78x10^{-3}$ were less than 1 and greater than 0 suggesting favorable adsorption. All the above suggests that the Langmuir model fits well for four types of biochar produced from different

biomasses. This means that Paraquat adsorption onto the biochars implements by a monolayer surface.

Comparison of Paraquat adsorption capacity by the biochars

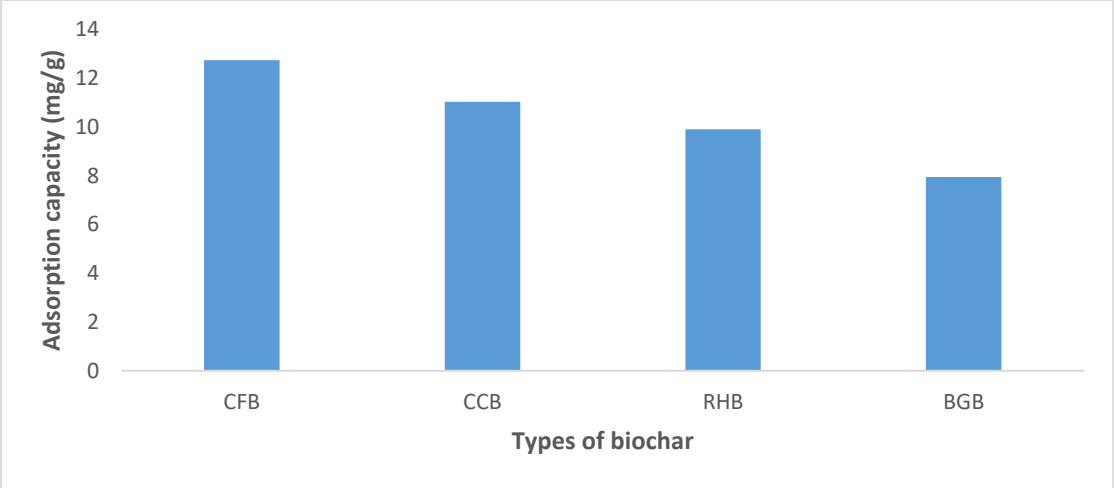

Figure 39 Paraquat adsorption capacity of four types of biochar produced from different biomasses (Initial paraquat concentrations = 10 - 33 mg/L, adsorbent dosage = 1.5 g/L, Initial pH =11)

More interestingly, Figure 39 shows the comparison of Paraquat adsorption by four types of biochar with different paraquat adsorption capacities. The following biochars are arranged according to their order of capacity: CFB (12, 74 mg/g), CCB (11.03 mg/g), RHB (9.90 mg/g), BGB (7.94 mg/g), respectively. The maximum paraquat adsorption capacity of biochar is coconut fiber biochar with 12.74 (mg/g). For this reason, the structure of four types of biochar in Figure 33 and Table 11 with fundamental pore properties. The first one could be the Specific Surface Area (SSA) of different biochars increased as the consequence in order BGB (67.42 m^2/g) < RHB (153.27 m^2/g) < CCB (292.92 m^2/g) < CFB (402.43 m^2/g). Similarly, the second one can be caused by the Total Pore Volume (TPV) of four types of biochar enhanced in consequence as BGB (0.029 cm^3/g) < RHB (0.055 cm^3/g) < CCB (0.117 cm^3/g) < CFB (0.151 cm^3/g). Therefore, the SSA and TPC can form the nature of the structures of four types of biochar and is the reason why the different paraquat adsorption

capacities of biochars as CFB (12, 74 mg/g) > CCB (11.03 mg/g) > RHB (9.90 mg/g) > BGB (7.94 mg/g).

Furthermore, the molecular sizes of paraquat are approximately 13.4 A^0 x 3.6 A^0 or 1.34 nm x 0.36 nm in Figure 35 (Draoui et al. 1999). Thus, these pollutants can fill the pores or the pore network of the four types of biochar which had a larger pore size than the molecular size of paraquat. Besides, the biochars have a pore size distribution with a variety of shapes and are distributed on different sizes. These factors have a strong effect on enhancing the adsorptive capacity of biochar. Hence, this finding can present more evidence for the different adsorption capacity of paraquat on different types of biochar by pore-filling mechanism. A similar study was conducted by Nguyen et al. (2007) where she indicated that the maximum sorption of contaminants on a natural wood char reduced with increasing the number of small molecular diameters of aromatic hydrocarbons such as phenanthrene, naphthalene, 1,2-dichlorobenzene, 1,2,4-trichlorobenzene, 1, 4-dichlorobenzene was caused mainly to pore-filling mechanism.

Kinetic adsorption

Figure 40 illustrates kinetic adsorption of paraquat with an initial concentrations of 10 mg/L, 15 mg/l, 27 mg/L by biochars produced from different biomasses. The experiment carries determines the time necessary for the adsorption process to reach equilibrium after 8 hours. However, the kinetic studies of Nanseu-Njiki, et. al., (2010) found that it could take only 10 min to complete the adsorption process.

Furthermore, it can be observed that the adsorption process of paraquat occurs more quickly with CCB and BGB which have lower PQ adsorption capacities than the others. This finding is seen in the reaction half time $t^{1/2}$(hour) of CCB and BGB with 0.23 hour around 13.41 – 14.11 minutes in table 13 was calculated using the following equation:

$$t^{1/2} = \frac{1}{K2qe}$$

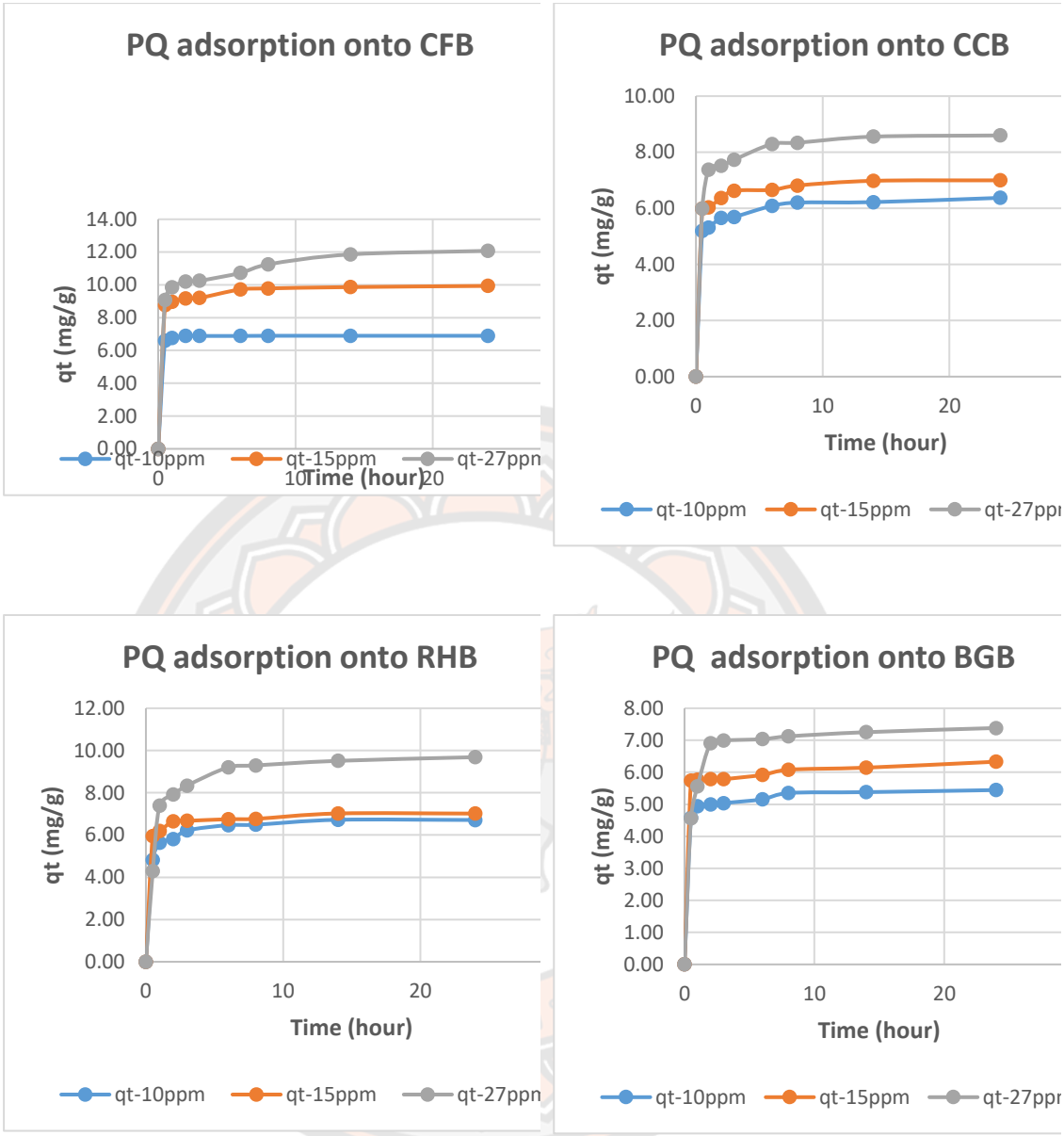

Figure 40 Adsorption kinetics of paraquat onto the biochars (Initial paraquat concentrations: 10 mg/L, 15 mg/L, 27 mg/L, adsorbent dosage = 1.5 g/L, and room temperature)

Table 13 Values of kinetic parameters in paraquat removal by adsorption process using biochars

Biochar	PQ Conc (mg/L)	Pseudo-first order model				Pseudo-second order model			
		qe exp (mg/g)	Qe,cal (mg/g)	K1 (1/hour)	R^2	Qe, cal (mg/g)	K2 (g/mg hour)	$T^{1/2}$ (hour)	R^2
CFB	27	12.07	4.27	0.19	0.828	12.15	0.23	0.37	0.999
CCB	27	8.60	2.88	0.30	0.896	8.67	0.52	0.23	1.000
RHB	27	9.69	4.09	0.25	0.856	9.82	0.25	0.41	0.999
BGB	27	7.38	2.03	0.23	0.683	7.42	0.58	0.23	1.000

The kinetic parameters of paraquat removal using four types of biochar produced from different biomasses and obtained from the experiments are illustrated in Table 13. Experimental data were fitted by the Pseudo-second order and Pseudo-first order models. The values of correlation coefficients (R^2 = 0.9995-0.9998) of the Pseudo-second order model were higher than the value of R^2 (0.683-0.896) of the Pseudo-first order model. Thus, the Pseudo-second order model could adequately describe the kinetic of paraquat removal by adsorption process using the biochars, similar to kinetic model with rapid adsorption suggested by Tsai et al. 2013 and Kumar et al. 2012.

Moreover, the qe, exp value (12.07 mg/g) is the experimental equilibrium amount of paraquat adsorption onto biochar, agreed very well with the qe, cal (12.15 mg/g) which is calculated from the second-order kinetic model. More importantly, Zhu et al. 2009 studied the pseudo-second order model which shows that the kind of adsorption could be chemical adsorption. Therefore, this implies that limiting the step of paraquat adsorption on the biochar is by chemisorption.

Table 14 Kinetic parameters in paraquat adsorption onto biochar using Intra – particle diffusion model (Initial paraquat concentrations = 27 mg/L, adsorbent dosage = 1.5 g/L, and room temperature)

Biochar	Intra-particle diffusion model								
	Fast adsorption stage			Slow adsorption stage			Equilibrium adsorption stage		
	Cf (mg/g)	Kip1 (mg/g.$h^{1/2}$)	R^2	Cs (mg/g)	Kip2 (mg/g.$h^{1/2}$)	R^2	Ce (mg/g)	Kip3 (mg/g.$h^{1/2}$)	R^2
CFB	0.39	10.41	0.953	9.35	0.55	0.885	8.82	0.82	0.984
CCB	0.14	7.59	0.988	6.43	0.76	0.999	8.03	0.12	0.822
RHB	0.17	7.14	0.981	5.44	1.56	0.959	8.72	0.19	0.983
BGB	0.12	5.72	0.986	6.76	0.11	0.842	6.77	0.13	0.995

According to the study of Tantrirantna et al. 2011, the Intra-particle diffusion model was used to assess the contribution of the diffusion of paraquat in the entire adsorption process in Table 14. The contribution of this diffusion can tend to be divided into three phases:

(1) rapid external diffusion – fast phase refers to paraquat moving easily into macro pores of the biochar (Tantrirantna et al. 2011) with intra-particle diffusion constants (Kip1) of 5.72-10.41mg/g. $h^{1/2}$, (2) slow adsorption phase due to the blocking of micro and meso pores (Liu et al.,2015) with Kip2 of 0.11-1.56 mg/g. $h^{1/2}$, (3) the equilibrium phase with Kip3 of 0.13 – 0.82 mg/g. $h^{1/2}$. Therefore, particle diffusion has a role in the adsorption process.

Moreover, it is seen from Figure 40 that the linear of the curve of the Intra-particle diffusion model does not pass through origin, indicating that the process of paraquat adsorption onto biochar is a complex process (Crini, G et al. 2008). This adsorption process includes both surface adsorption and internal diffusion.

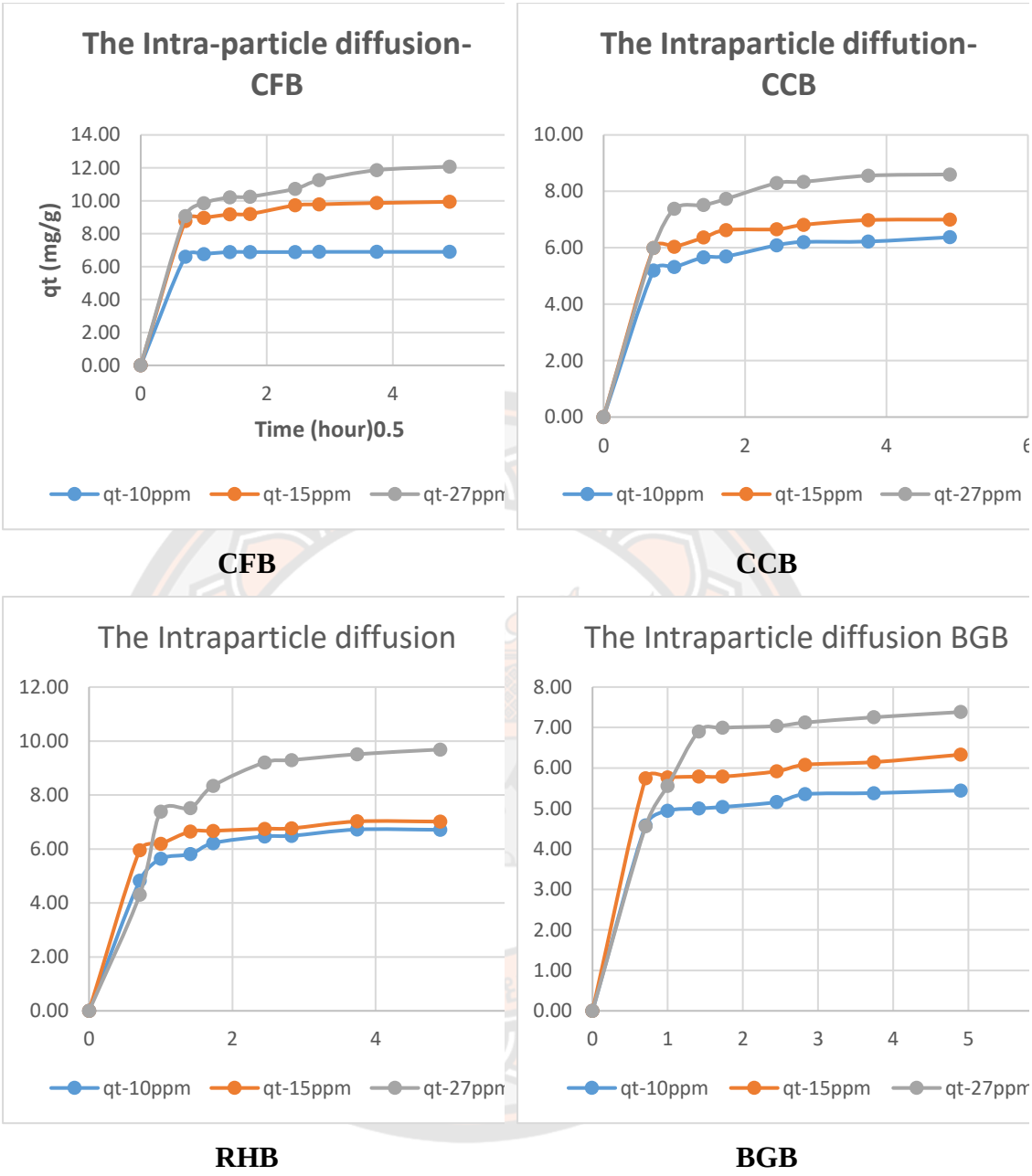

Figure 41 Figure 41 Adsorption kinetics of paraquat onto the biochars using the Intra-particle diffusion model (Initial paraquat concentrations: 10 mg/L, 15 mg/L, 27 mg/L, adsorbent dosage = 1.5 g/L, and room temperature)

Mechanisms in adsorption process

In this study, the paraquat adsorption mechanism of the biochars was discussed as follows:

1. Hydrophobic interaction

First of all, the property of paraquat is polar compound, high solubility in water with 700 g/L (Rodea-Palomares et al. 2015) and not hydrophobic compound due to its low log Kow.Thus, this pollutant was hydrophilic character. Moreover, the results of FTIR analysis indicated that all biochars possess hydrophilic characteristic. Besides, four types of biochar have the alkyl groups which have chemical hydrophobicity. Therefore, the hydrophobic interactions are not considered as contributing to the adsorption mechanism of paraquat on the biochars.

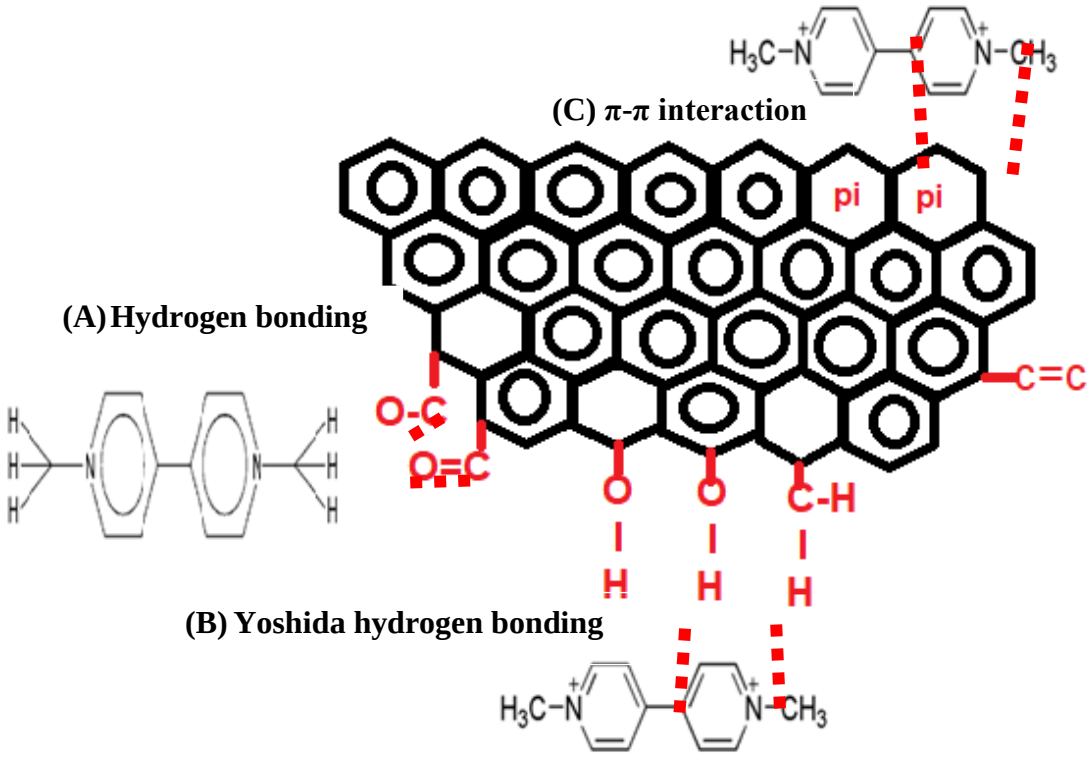

Figure 42 Possible chemical adsorption mechanisms in the removal of paraquat by biochar

2. Pore filling

In this study, the previous results of the values of SSA and TPV in Table 11 and the Paraquat adsorption capacity of biochar have the same sequential consequence CFB >CCB >RHB>BGB, respectively.Moreover, the molecular size of paraquat are smaller than the pore size of the biochar. Thus, these pollutants can fill the pores or the pore network of four types of biochar. These factors have a strong effect on enhancing the adsorptive capacity of the biochar. Hence, this findingis evidence ofenhancing the adsorption capacity of paraquat in enhancing the pore size such as SSA and TPV of biochar by pore-filling mechanism. A study by Nguyen et al. (2007) indicated that the maximum adsorption increased with decreasing the molecular diameter such as phenanthrene; naphthalence; 1,2-dichlorobenzene; 1, 2, 4-trichlorobenzene; 14-dichlorobenzene onto a pitch pine biochar by adsorptive pore-filling mechanism.

3. Diffusion

The film diffusion and the particle diffusion models are two models which can identify the rate-limiting step of paraquat adsorption onto the biochars.

The film diffusion model refers to the movement of paraquat to the external surface of the biochar. The particle diffusion model evaluates the diffusion of paraquat molecules into the pores of the biochar (Nanseu-Njiki et al. 2010; Liu et al. 2016).

The formula of the particle diffusion model is as follows (Liu et al. 2016):

$$-\ln\left(1-X^2(t)\right)=\frac{D_P\pi^2}{r_o^2}t=k_pt$$

Where X (t) = q_t/q_e, D_p is the particle diffusion coefficient, r_o is the biochars radius, k_p is used for calculating effective intra-particle diffusivity.

$$k_p=\frac{D_p\pi^2}{r_o^2}$$

The k_p value can be calculated from the slopes of the graph made by plotting –ln (1-X^2 (t)) against t.

The formula of the film diffusion model is as follows:

$$-\ln\left(1 - X(t)\right) = k_f . t$$

Where k_f can be calculated from the slopes of the graph that was made by plotting the –ln (1-X(t)) against t, D_f is the film diffusion coefficient.

$$D_f = \frac{k_f r_o \delta C_r}{3C_e}$$

C_e is the concentration of paraquat in the liquid, C_r is the concentration of paraquat as adsorbed by the biochars, δ is the thickness of the liquid film (10^{-5} m) (Liu et al. 2016).

The D_f and D_p values of the film and particle diffusion models for paraquat adsorption onto biochars from the different biomasses are shown in Table 14.

Table 15 Diffusion coefficients and constants for paraquat adsorption onto biochars (Paraquat concentration: 33 mg/L)

Biochar	Parameters of film diffusion model			Parameters of particles diffusion model		
	k_f (h^{-1})	D_f (m^2/s)	R^2	k_p (h^{-1})	D_p (m^2/s)	R^2
CFB	0.240	1.09×10^{-11}	0.974	0.229	2.21×10^{-13}	0.973
CCB	0.326	1.92×10^{-11}	0.923	0.277	4.50×10^{-13}	0.977
RHB	0.214	0.87×10^{-11}	0.910	0.197	1.51×10^{-13}	0.902
BGB	0.304	1.00×10^{-11}	0.985	0.286	1.70×10^{-13}	0.983
Michelsen et al. 1975	*10^{-10} - 10^{-12} m^2/s*			10^{-15} - 10^{-18} m^2/s		

k_f (h^{-1}): the liquid film diffusion constant, D_f (m^2/s): the film diffusion coefficient

k_p (h^{-1}): the effective intraparticle diffusivity, D_p (m^2/s): the particles diffusion coefficient

In comparing with D_p value of the particle diffusion model in the range of 10^{-15} - 10^{-18} m^2/s, and D_f value of the film diffusion model in rang of 10^{-10} - 10^{-12} m^2/s (Michelsen et al. 1975), the D_f values of the film diffusion were experienced in the range of 0.87 x 10^{-11} to 1.92 x 10^{-11} m^2/s fits suitable Df values of Michelsen et al. 1975. On the other hand, the D_p values of the particle diffusion were in the range of 1.51 x 10^{-13} to 4.5 x 10^{-13} m^2/s and different from the Dp values of Michelsen et al. 1975. Therefore, paraquat adsorption is the best described by the film diffusion mechanism than the particle diffusion mechanism. The obvious correlation coefficient was from 0.910 to 0.985. Based on the above kinetic results, it may be noted that the Intra-particle diffusion model is used to describe the adsorption process. These results suggest that the diffusion mechanisms contribute to the adsorption mechanism in paraquat removal by chemical adsorption.

4. Electrostatic interaction

The principal of electrostatic interaction is the interaction between a cationic sorbate and an anionic sorbent. It is known that the pKa of cationic paraquat was about 9-9.5 (Tantrirantna et al. 2011 and Rodea-Palomares et al. 2015). Therefore, the paraquat was positivey charged at pH 11. Moreover, the values of the point zero charge (pzc) for biochar were determined as presented in Table 8. The pzc of the biochars were identified in the range 0.70-0.75, lower than 1.0. When the pH solution is greater than pHpzc, the surface of all biochars are negatively charged. Hence, the surface of the biochar is negatively charged at pH 11.

Thus, this indicates that the mechanism of paraquat adsorption on the biochar closely involves electrostatic interaction**.**

5. Hydrogen bonding

Regarding hydrogen bonding formation, the results of the FTIR indicated that the biochars possessed –OH groups, -OH phenolic and alcohol groups, -CH2- groups, carbonyl groups (C=O) corresponding to various acids, aldehydes and ketones,-CH2- groups which formed hydrogen bonding with the hydrogens of paraquat (Figure 42). The hydrogen bonding mechanism is able to occur in 2 cases.

The first case is where the negatively charged oxygen of functional groups such as –OH, C=O of biochar interacts with positively charged atoms such as the hydrogens of paraquat (Figure 42A). A similar adsorption mechanism of phenol on

biochar was suggested by Liu et al (2011). The study of Liu reported that the enhancement of phenol adsorption by biochar was a major attraction between the oxygen of functional groups of biochar such as –OH and C=O and phenol molecules based on the hydrogen bond.

In the second case, the attraction between the hydroxyl groups (–OH groups, -OH phenolic groups, -CH2- groups) of biochar and the aromatic rings of paraquat (Figure 42B). This phenomenon is known as Yoshida hydrogen bonding. Blackburn pointed out that the interactions between –OH groups of polysaccharide and the aromatic ring residues of dye molecules (Yoshida hydrogen bonding interaction) in 2004. More importantly, Zhu et al. 2009 studied the pseudo-second order model, which shows that the kind of adsorption may be chemical adsorption. Therefore, hydrogen bonding plays an important adsorption mechanism in paraquat removal by biochar.

6. π-π interaction (π-πelectron donor–acceptor (EDA) interaction

In considering the π-π interaction between paraquat and biochar, the paraquat molecule has two pyridine rings which possess electron-rich moieties. Thus, these rings can act as π-electron donor and aromatic rings of biochar. Hao et al. (2013) suggested that the π-π interaction can happen between the π-electrons of the pesticide as a donor and the π-electron acceptor in the aromatic rings of the biochar. Therefore, the possible π-π interaction between paraquat and the biochar can occur (Figure 42C). Hence, the π-π interaction was a relevant adsorption mechanism in paraquat removal by biochar.

7. Practical application

Some previous studies reported that activated carbon is well known as a typical and as well as the oldest adsorbent (Hassler, 1963), but it requires huge energy and high costs with the physical activation process (600-1200^{0}C) and chemical activation processes from 450^{0}C to 900^0 C with acid or base (Carrot and Carrott, 2007). Furthermore, Ahmad et al., 2014 estimated that the price of activated carbon is approximately US $1476 per ton, while the price of biochar is US $246 per ton. Therefore, the application of biochar can feasibly apply in developing countries. According to these experimental results, given the four types of biochar produced

from different biomasses, these biochars can be applied and used as alternative economic absorbents for the removal of pollutant compounds in rural areas.

8. Summary

In this part, the isotherm data was explained by the Langmuir model. These results indicate the adsorption capacity of the different biochars investigated. The levels of paraquat adsorption were determined to determine their adsorption capacity. The capacities of the different biochars are indicated in order: coconut fiber, corncob, rice husk and bagasse. The adsorption capacity is determined according to the surface area and total pore volume.

The kinetic data was well fitted with the Pseudo-second-order model that can be indicated as a chemisorption process. The intra-particle diffusion model was clearly used to assess the kinetic rate of paraquat adsorption. This implies that the rate constant of the external diffusion phase (Kip1) move more rapidly than the rate constants of the slow (Kip2) and equilibrium (Kip3) phases. The film diffusion has a role in the adsorption process of paraquat and biochar. Therefore, the mechanisms of pore filling, hydrogen bonding, π-π and electrostatic interactions could contribute to the adsorption process. The adsorption ability of the four types of biochar produced from different biomasses indicated that the maximum paraquat adsorption capacity of biochar is coconut fiber biochar with 12.72 (mg/g). Thus, the coconut fiber biochar can become an alternative adsorbent for paraquat removal from an aqueous solution and wastewater treatment in agriculture.

PART 2 FREE CELLS

In the free cells part, the results included the following:

1. Characteristics of corn cob biochar, fee cells and fixed cells of *Pseudomonas putida*
2. Influence of pH on PQ removal by free cells of *Pseudomonas putida*
3. Influence of initial concentrations of PQ on the survival of *Pseudomonas putida*
4. Influence of contact time on PQ adsorption equilibrium
5. Paraquat tolerance – EPS synthesis in response to oxidative stress
6. Comparison of PQ removal by living and dying cells

Characterization of biochar, free and fixed cells of *Pseudomonas putida*

1. Free cells

The *Pseudomonas putida* is a bacterium of the family of *Pseudomonadacease*, genus of *Pseudomonas spp*. It is a gram-negative, mesophilic, aerobic bacterium commonly present throughout the environment which can degrade various natural and synthetic compounds (Vizma Nikolajeva et al., 2012). Its cell size is from 0.5 to 0.6 µm in diameter and from 1.4 to 1.7 µm in length (Hwang et al., 2008).

Table 16 Physical properties of corn cob biochar

No.	Parameter	Corn cob biochar
1	Surface area (BET), m^2/g	4.1
2	Total volume in pores, A^0	147.61
3	pHpzc	0.93

2. Structure and size of paraquat

The basic chemical properties of paraquat that are related to its fate and transport are solubility in water and its volatility. Based on a report of the National Institute for Occupational Safety and Health, authored by Husband (2001), the high solubility in water is 680 g/L at 200C and at pH 7.2; the vapor pressure is <10-7 mmHg (20^0 C). So Henry's Constant is H=VP/S = 5 x 10^{-17} atm-m^3/mole. From Henry's law constant << 10-7 atm-m3/mole, paraquat is nonvolatile. Moreover, paraquat with log Kow = -4.5 at 25^0C. In other words, this means Kow = $10^{-4.5}$ and less than 10. Therefore, it can be said that paraquat is hydrophilic or soluble (like water).

Immobilization/Fixation of microorganisms

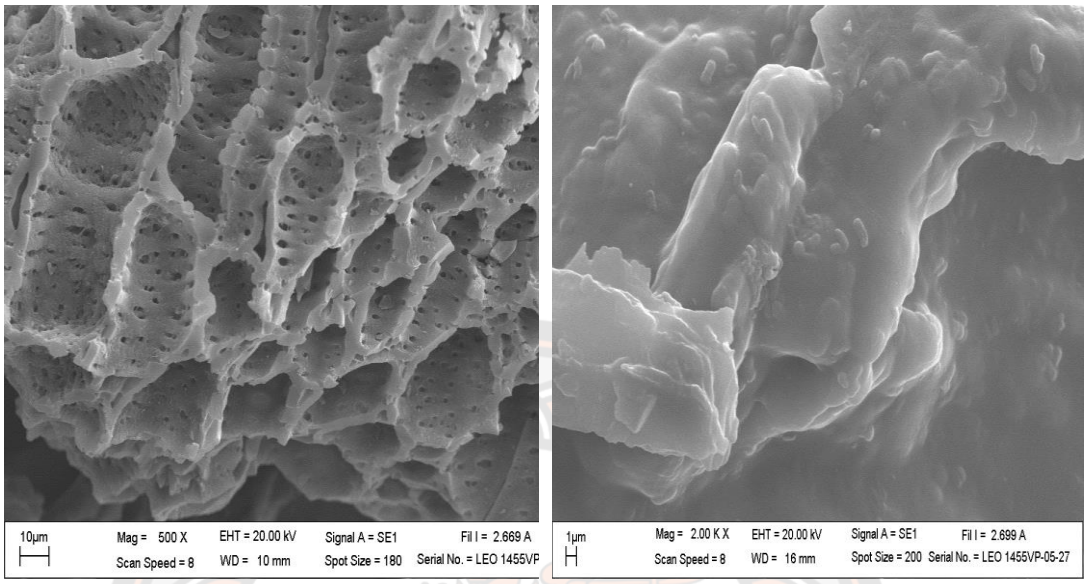

Biochar before immobilization *Pseudomonas putida* immobilized on biochar

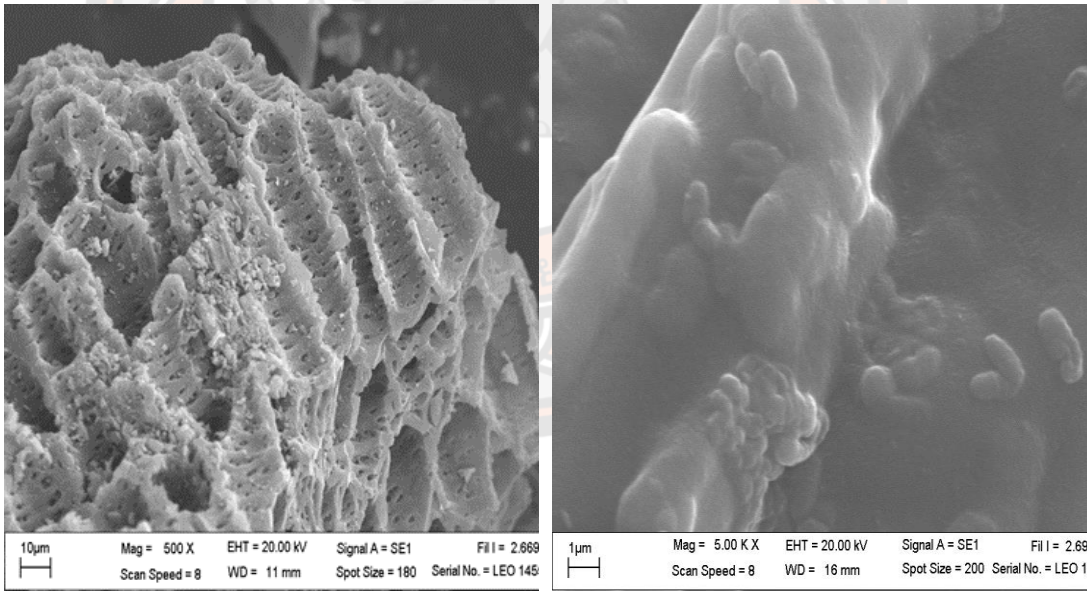

Figure 43 Scanning electron microscopy (SEM) images of *Pseudomonas putida* fixed on biochar in the present study

Figure 43 illustrates the SEM images of *Pseudomonas putida* immobilized on the biochar. The smooth surface indicates alginate coverage of the bacteria. From the SEM, it is evident that cells were entrapped and grew on the surface of the biochar.

Influence of pH on PQ removal by free cells of *Pseudomonas putida*

Figure 44 shows the survival of *Pseudomonas putida* in solution 15mg/l under different pH from 3 to 11. At pH 7, the survival of *Pseudomonas putida* was highest. At pH 3 and 11, the survival of *Pseudomonas putida* was lowest. The pH is the significant factor effecting the growth of bacteria based on the study of Karpouzas and Walker (2000). Therefore, the growth of bacteria impacts on PQ removal in the biodegradation process.

Figure 45 shows the PQ removal by *Pseudomonas putida* under different pH values from 3-11. The highest PQ concentration was removed by *Pseudomonas putida* at pH 7 and lowest PQ concentration was removed at pH 3. It can be observed in Figure 4 that PQ removal is enhanced in the pH ranges of 3-7. The PQ removal decreased in the pH ranges of 9-11. The highest PQ removal was at pH 7. Additionally, Figure 3 indicates the growth of *Pseudomonas putida* free cells was optimal at pH 7.0. It is popular for most bacteria to refer to neutral pH. This agrees with the results of Elsayed and El-Nady 2013 who isolated *Pseudomonas putida (E15)* from pendimethalin-contaminated soil. They found that maximum growth occurred at pH 7.0.

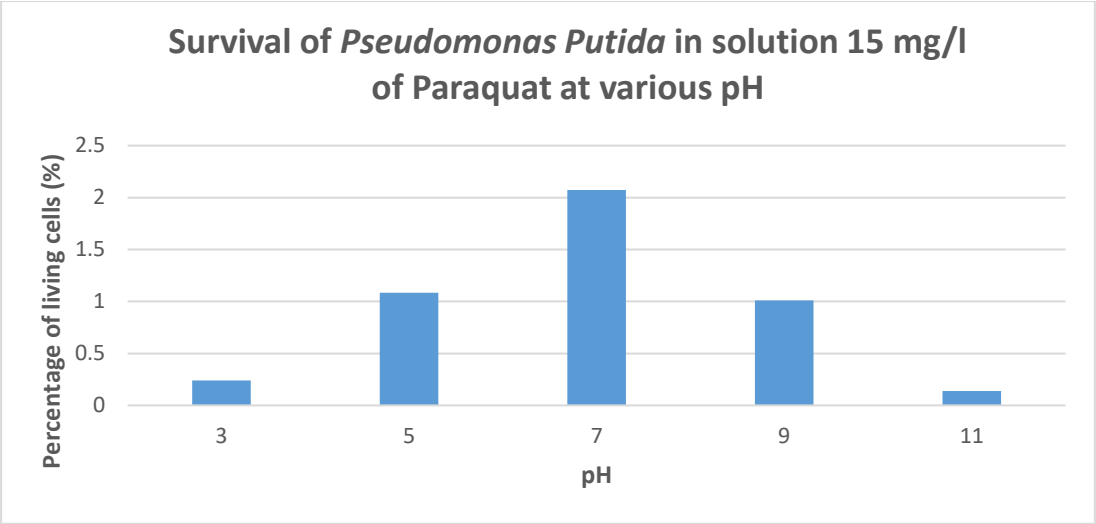

Figure 44 Survival of *Pseudomonas putida* at various pH (room temperature and the initial PQ concentration was 15 mg/L)

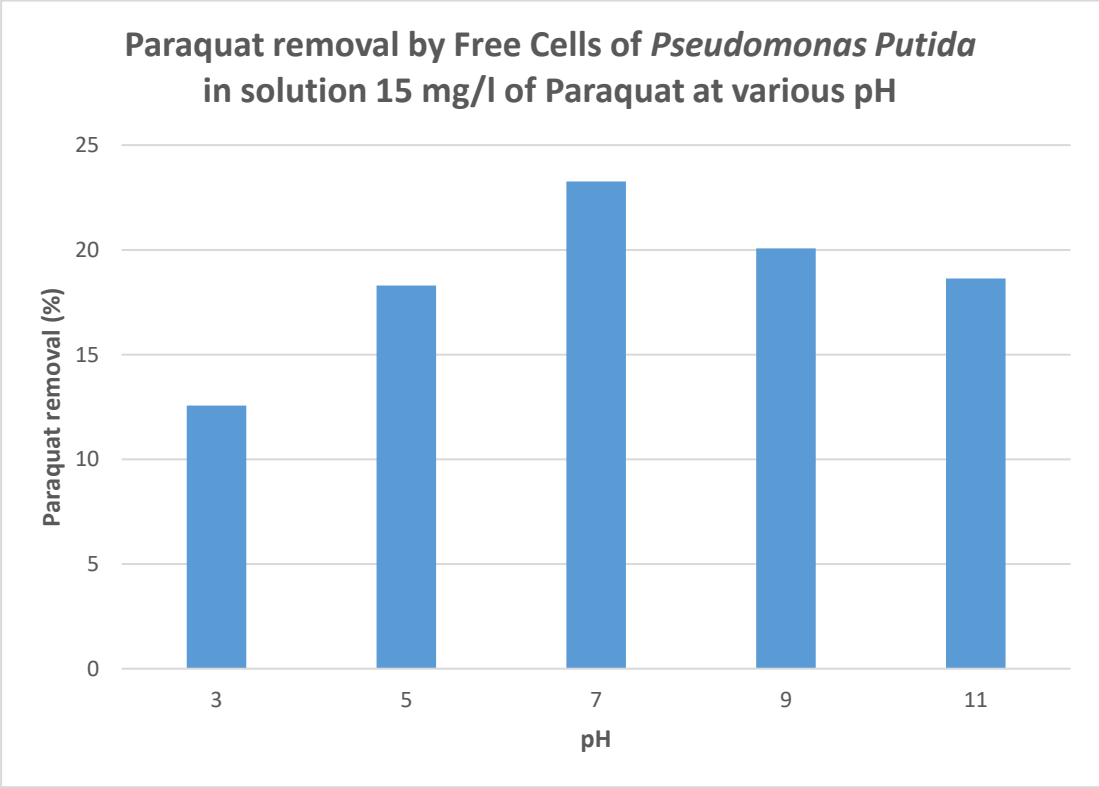

Figure 45 PQ removal by free cells of *Pseudomonas putida* at various pH (room temperature and the initial PQ concentration was 15 mg/L)

Influence of initial concentrations of PQ on the survival of *Pseudomonas putida*

Figure 46 shows the survival of *Pseudomonas putida* in solution of PQ at various concentrations. PQ concentration and incubation time affected the growth of *Pseudomonas putida*. The enhancement of the PQ concentration would be followed by a reduction in growth, based on the reduced of number of cells. With 24 hours incubation at paraquat 0 ppm, the number of bacteria decreased from 10^{11} to $6x10^{10}$ CFU/mL; but at paraquat 5 ppm the number of bacteria $27x10^{9}$ CFU/mL, 26 ppm and 58 ppm the number of bacteria were $44x10^{8}$ CFU/mL and $21x\ 10^{8}$ CFU/ml. The bacteria initially died after 1 hour for 5ppm, 26 ppm and 58ppm. After 6 hours, the number of bacteria that survived did not change much. Hence, there was an interaction between PQ concentrations and incubation time. The higher the PQ concentration and the longer the incubation time, influenced the reduction in the growth of the bacteria. This implies that high concentrations of PQ are toxic to *Pseudomonas putida*.

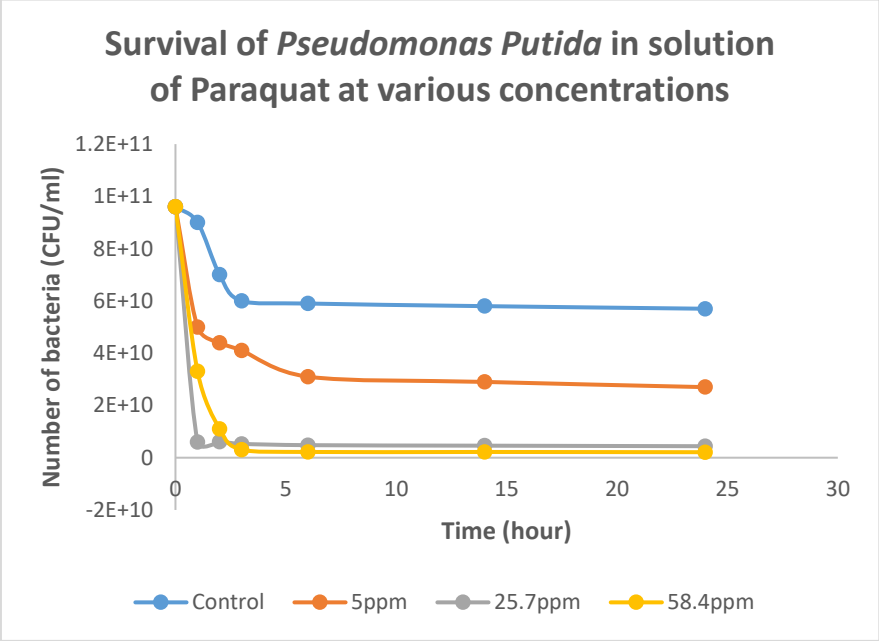

Figure 46 Effect of various initial concentrations (5 ppm, 25.7 ppm and 58.4 ppm) of PQ on the survival of free cells of *Pseudomonas putida* under room temperature and 120 rpm

On the other hand, Figure 47 shows PQ removal by free *Pseudomonas putida* cells at various concentrations. During the incubation time of 24 hours, there was a decrease in PQ concentrations, especially at the initial concentration; indicating that *Pseudomonas putida* removed PQ. The results were similar to studies of Carr [43] where a yeast *Lipomyces starkeyi*, was able to degrade PQ in minimal media and used this chemical as N source. He indicated that degradative activities of *Lipomyces starkeyi* toward PQ was related to cell membrane and cell wall. Moreover, if there was cell wall desruption caused by peroxidation reaction by free radicals, this yeast will lost its activity to degrade paraquat. Oxidation pressure in environmental stress will induce specific reaction of microbial cells in order to survive.

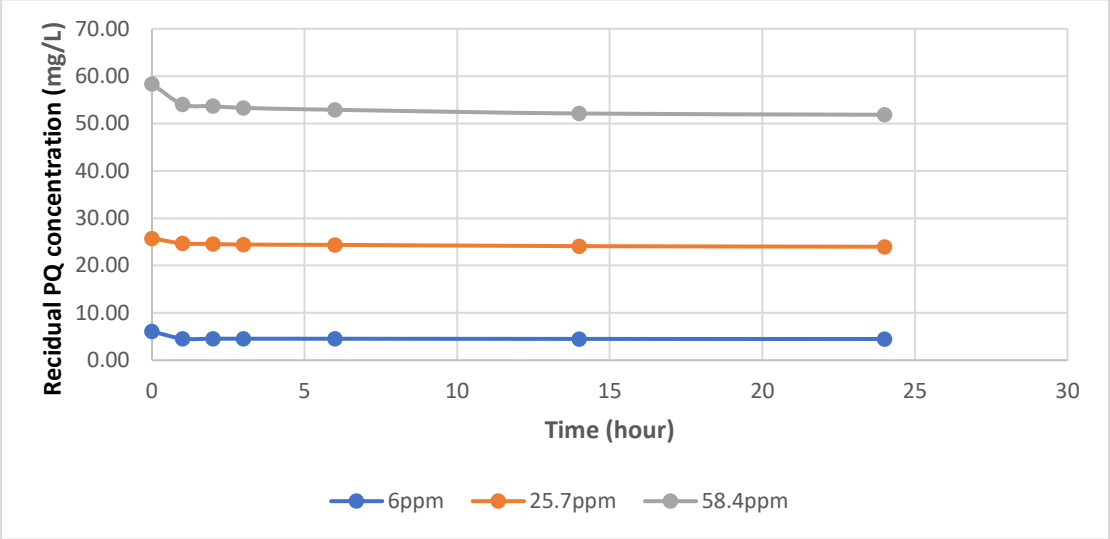

Figure 47 PQ removal by free cells of *Pseudomonas putida* at various concentrations under room temperature and 120rpm

Paraquat tolerance – EPS synthesis in response to oxidative stress

According to Ahemad, & Khan, (2012), the amount of Extra-Poly-Saccharide (EPS) generated by *P. putida strain PS9* increased with the increase in herbicide concentrations that were explained by the herbicides and might have acted as inducers of EPS secretion. Figure 48 shows PQ tolerance of *Pseudomonas putida* through EPS generation. It was shown that there is very low EPS at 0 ppm PQ (control). The EPS production by bacteria increased from 5 ppm to 26 ppm. Optimum

increase of the EPS was found at 26 ppm of PQ. However, the EPS production decreased from 26ppm to 58 ppm. In relation with PQ tolerance of microorganisms, oxidative stresses occur when PQ was diluted in water where it produced the free radicals superoxides in solution. The release of these free radicals will induce cell reaction to reduce through EPS secretion in limitation. This means that the limited EPS production produced with a limitation of the initial number of bacteria. When the high PQ concentrations means the high free radicals superoxide of PQ. If the free radicals superoxide of PQ was higher than the capacity of free cell which can generate. This leads to inactivated cells. Therefore, the EPS production was reduced at 58ppm. These findings agreed with the study of Ahemad and Khan, (2012).

In previous studies, microorganisms that developed resistance to pesticides are frequent capability of biodegradation process (Kumar et al. 1996; Ortiz-Hernández, & SánchezSalinas 2010). The study of Bellinaso et al. (2003) indicated that temporary resistance against pesticides in general is involved to physiological changes that induce microbial metabolism to form a new metabolic pathway to bypass a biochemical reaction inhibited by a specific pesticide (Bellinaso et al., 2003). On the other hand, permanent resistance depends on the operation of the genes inherited by subsequent generations of microbes (Johnsen et al., 2001; Herman et al., 2005). Thus, herbicide tolerance is a complex process which includes both physiological and genetic processes of the microorganism.

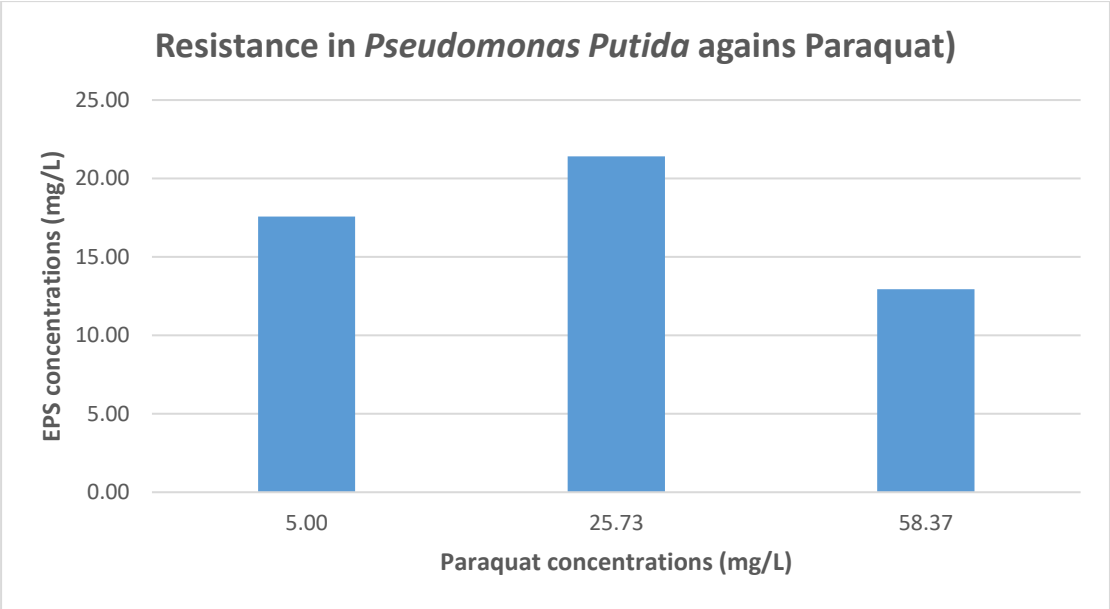

Figure 48 PQ tolerance of *Pseudomonas putida* at different PQ concentrations (under room temperature and 120rpm)

Comparison of PQ removal by living and dying cells

Table 17 Langmuir and Freundlich parameters for PQ removal by (free cells) living and dying cells of *Pseudomonas putida* at pH 7 and room temperature

Types of biochar	Langmuir parameters			Freundlich parameters		
	Qo (mg/g)	b (L/mg)	R^2	Kf $(mg/g)(L/mg)^{1/n}$	1/n	R^2
Living cells	3.15	0.56	0.9406	1.64	0.20	0.3443
Dying cells	2.41	1.76	0.9482	1.66	0.12	0.0933

Table shows the isotherm parameters of paraquat removal using living and dying cells of *Pseudomonas putida*. There are two common adsorption isotherm models, Langmuir and Freundlich isotherm models. Table 17 illustrated that the adsorption of living and free cells can be described by Langmuir model. Because of R^2, the values of R^2 of the Langmuir model (0.9406 – 0.9482) were higher than the

values of correlation coefficients of the Freundlich model (0.0933 – 0.3443). Hence, the adsorption characteristics of paraquat on biochar are obviously described by the Langmuir model.

Influence of contact time on PQ adsorption equilibrium

In order to determine the time required for PQ adsorption equilibrium, the experiments were implemented over 30 hours and samples taken at different intervals. The results show that the equilibrium adsorption of living cells was achieved/ gotten within 30 minutes, while the equilibrium adsorption/capacity of dying cells was achieved within 8 hours in the Figure 49. Moreover, the PQ adsorption capacity of living cells is higher than the PQ adsorption capacity of dying cells. This is confirmed that based on the table 17, the maximum PQ adsorption capacity of living cells is 3.15 (mg/g) is larger than the maximum PQ adsorption capacity of dying cells with 2.41 (mg/g). Therefore, it can be explained by generating extra-cellualar of living *Pseudomonas putida* or EPS – Extra PolySaccharide which interact with PQ. A report by Ahemad and Khan, (2012), the amount of Extra-Poly-Saccharide (EPS) generated by P. putida strain PS9 increased with the increase in herbicide concentrations that were explained by the herbicides and might have acted as inducers of EPS secretion.

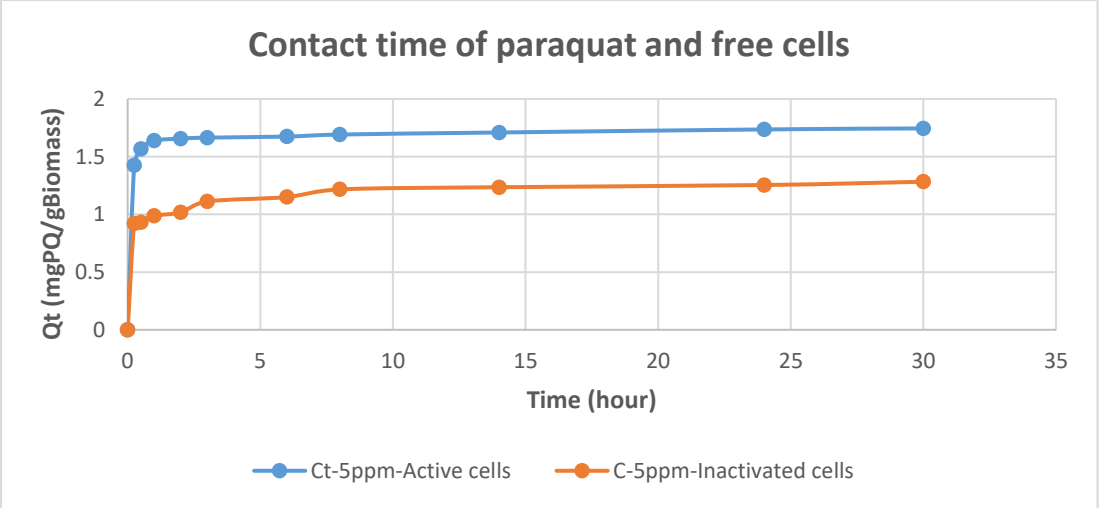

Figure 49 Influence of contact time on PQ adsorption equilibrium

Summary

In the free cells part, the results indicated growth of *Pseudomonas putida* under optimum conditions such as pH and different initial concentrations free cells of *Pseudomonas putida*. The pH is the important factor effecting the growth of *Pseudomonas putida* and impacts on PQ removal in the biodegradation process. The highest PQ removal was at pH 7. The growth of *Pseudomonas putida* free cells was optimal at pH 7.0.

The amount of Extra-Poly-Saccharide (EPS) generated by *Pseudomonas putida* increased with the increase in PQ concentrations. Optimum increase of the EPS was found at 26 ppm of PQ. However, the EPS production was reduced at 58 ppm.

The isotherm adsorption of paraquat removal using living and dying cells of *Pseudomonas putida* can be obviously described by Langmuir model. Moreover, the PQ adsorption capacity of living cells (3.15 mg/g) is higher than the PQ adsorption capacity of dying cells (2.41 (mg/g). The equilibrium adsorption of living cells was achieved/ gotten within 30 minutes, while the equilibrium adsorption/capacity of dying cells was achieved within 8 hours.

PART 3 FIXED CELLS

In the fixed cells part, the results included the following:

A. Corn cob biochar (CCB)

+ Isotherm: Ad, Co, En
+ Kinetic model: Ad, Co, En

B. Coconut fiber biochar (CFB)

+ Isotherm: Ad, Co, En
+ Kinetic model: Ad, Co, En

C. Rice hush biochar (RHB)

+ Isotherm: Ad, Co, En
+ Kinetic model: Ad, Co, En

D. Bagasse biochar (BGB)

+ Isotherm: Ad, Co, En
+ Kinetic model: Ad, Co, En

E. Intermediate products of paraquat

A. Corn cob biochar (CCB)

+ Isotherm: Ad, Co, En

+ Kinetic model: Ad, Co, En

Isotherm - Corn cob biochar

Table 17 shows the isotherm parameters of paraquat removal by fixed cells using different immobilization methods of *Pseudomonas putida*. Langmuir and Freundlich isotherm models were used to test the isotherm parameters of paraquat removal. Table 18 illustrates the adsorption of fixed cells with different immobilization methods of *Pseudomonas putida.* These are described according to the Langmuir model. Because of R^2, the values of R^2 of the Langmuir model (0.990 – 0.974) were higher than the values of the correlation coefficients of the Freundlich model (0.980 – 0.792), the adsorption characteristics of paraquat on biochar are described according to the Langmuir model. Table 18 shows the comparison of Paraquat adsorption by three types of cell immobilization with different paraquat adsorption capacities. The following biochars are arranged according to their order of PQ removal capacity: adsorption method (4.78 mg/g), the covalent binding method (2.66 mg/g), and the entrapment method (1.63 mg/g), respectively. The maximum paraquat removal capacity by fixed cells of *Pseudomonas putida* on CCB using different methods for PQ is the adsorption method with 4.78 (mg/g).

Table 18 Langmuir and Freundlich parameters for PQ removal by fixed cells on CCB with different immobilization methods of *Pseudomonas putida* at pH 7 and room temperature

Types of fixed method	Langmuir parameters			Freundlich parameters		
	Qo (mg/g)	b (L/mg)	R^2	Kf $(mg/g)(L/mg)^{1/n}$	1/n	R^2
Adsorption	4.78	0.29	0.990	1.72	0.29	0.892
Covalent binding	2.66	0.22	0.974	1.20	0.18	0.792
Entrapment	1.63	0.05	0.986	4.00	0.87	0.980

Kinetic models

The kinetic models defined by the Pseudo first-order kinetic and Pseudo second-order equations, as described below:

The pseudo-first-order model was expressed as (Ho and Mc Kay 1998):

$$\text{Log } (Q_e - Q_t) = \text{Log } Q_e - K_1 t$$

The pseudo-second-order model as proposed by Ho and Mc Kay (1998) and used for the study as described in the Equation:

$$\frac{t}{Q_t} = \frac{1}{K_2 Q_e} + \frac{1}{Q_e} t$$

Both models were used to test experimental data for analysis of the PQ removal process kinetics.

Table 18 showed the values of the kinetic parameter in PQ removal by fixed cells of *Pseudomonas putida* using different fixed methods. The Pseudo first-order rate constant (K1) and Qe, cal values (equilibrium adsorption capacity estimated by the Pseudo first-order kinetic) determined from Figure 50 and Figure 51 along with the correlation coefficients are shown in Table 19. The correlation coefficients of the Pseudo first - order kinetic model (0.706-0.912) were smaller than those of the Pseudo second-order kinetic model (0.959-0.998). Moreover, the Qe, cal value identified from the Pseudo-second order model agree with the experimental qe, exp values (equilibrium adsorption capacity at 48h). Therefore, the PQ removal by fixed cells of *Pseudomonas putida* using different fixed methods can fit well the Pseudo-second order kinetic model.

From the parameters in Table 19, the adsorption capacities of PQ is highest at 4.21 mg/g with the covalent binding method. Moreover, the entrapment method (qe=2.72 mg/g) provided a lower amount of paraquat adsorbed at equilibrium than the adsorption method (qe = 3.3 mg/g). This agrees with the results of Chen et al. (2016) who used the pseudo-second order model satisfactorily represented the kinetics of simultaneous adsorption and biodegradation of diesel oil using immobilized

Acinetobacter venetianus on porous material. Interestingly, this finding has the similar trend with study of Ha et al. (2021) that using the bacteria immobilized onto coconut fiber biochar.To explain the highest adsorption capacities of PQ with the covalent binding method, the coverage of alginate can affect the reducing adsorption efficiency due to form by the bonding of Ca+2 ions with polyguluronic portions of the polymer strands, a process known as ionic gelation. This phenomenon can lead to the adsorption capacities of PQ is lowest at 2.72 mg/g and K2 is lowest at 0.14 g/mg hour. Based on study of Ha et al (2021), the possibility of bacteria retention by an adsorption method (40.56%) was less than that by the covalent binding method (60.70%).

Table 19 Values of kinetic parameters of for PQ removal by fixed cells on CCB with different immobilization methods of *Pseudomonas putida*

Types of fixed methods	qe exp (mg/g)	Pseudo first-order kinetic model			Pseudo second-order kinetic model		
		Qe,cal (mg/g)	K1 (1/hour)	R^2	Qe, cal (mg/g)	K2 (g/mg hour)	R^2
Adsorption	3.33	1.30	0.12	0.706	3.30	0.31	0.994
Covalent binding	4.20	1.53	0.07	0.912	4.21	0.26	0.998
Entrapment	2.79	1.73	0.09	0.708	2.72	0.14	0.959

Kinetic models - Corn cob biochar

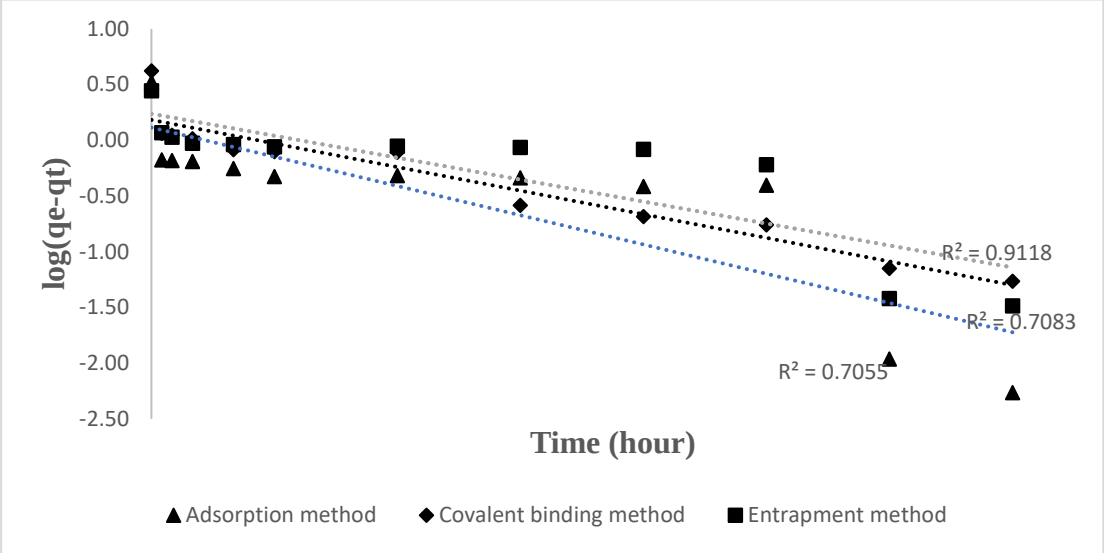

Figure 50 Pseudo first-order kinetic model of PQ removal by fixed cells of *Pseudomonas putida* with different immobilization methods

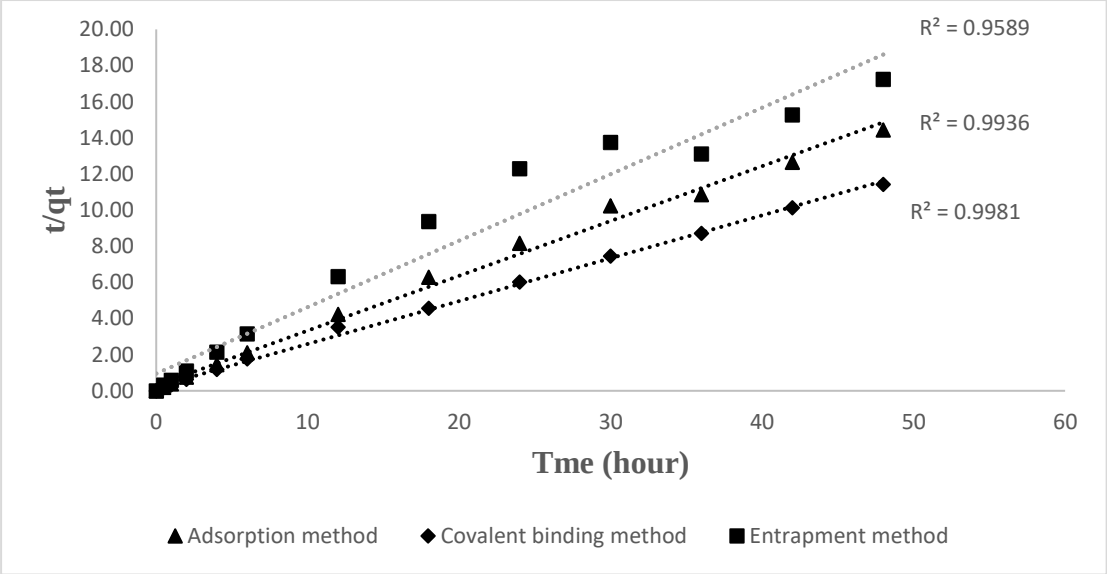

Figure 51 Pseudo second-order kinetic model of PQ removal by fixed cells of *Pseudomonas putida* with different immobilization methods

B. Coconut fiber biochar (CFB)

+ Isotherm: Ad, Co, En

+ Kinetic model: Ad, Co, En

Isotherm - Coconut fiber biochar

Table 20 shows the isotherm parameters of paraquat removal by fixed cells using different immobilization methods of *Pseudomonas putida*. Langmuir and Freundlich isotherm models were used and tested. Table 20 shows that the adsorption of fixed cells with different immobilization methods of *Pseudomonas putida* can be described by the Langmuir model. The values of R^2 of the Langmuir model (0.997 – 0.949) were higher than the values of correlation coefficients of the Freundlich model (0.993 – 0.961). Hence, the adsorption characteristics of paraquat on biochar are clearly described by the Langmuir model. Moreover, Table 20 shows the comparison of Paraquat adsorption using three types of cell immobilization with different paraquat adsorption capacities. The following biochars are arranged according to their order of capacity: adsorption method (6.12 mg/g), Covalent binding method (2.93 mg/g), Entrapment method (2.75 mg/g), respectively. The maximum paraquat adsorption capacity by fixed cells of *Pseudomonas putida* on CFB using different methods for PQ is adsorption method with 6.12 (mg/g).

Table 20 Langmuir and Freundlich parameters for PQ removal by fixed cells on CFB with different immobilization methods of *Pseudomonas putida* at pH 7 and room temperature

Types of fixed methods	Langmuir parameters			Freundlich parameters		
	Qo (mg/g)	b (L/mg)	R^2	Kf $(mg/g)(L/mg)^{1/n}$	1/n	R^2
Adsorption	6.12	0.32	0.985	2.53	0.24	0.961
Covalent binding	2.93	0.55	0.997	1.79	0.13	0.971
Entrapment	2.75	0.04	0.949	4.20	0.58	0.993

Kinetic - Coconut fiber biochar

Table 20 indicates the values of kinetic parameters of for PQ removal by fixed cells on CFB using different immobilization methods of *Pseudomonas putida.* The Pseudo first-order rate constant (K1) and Qe, cal values (equilibrium adsorption capacity estimated by the Pseudo first-order kinetic) determined from Figure 52 and Figure 53 along with the correlation coefficients are shown in Table 21. The correlation coefficients of the Pseudo first-order kinetic model (0.627-0.895) were smaller than those of the Pseudo second-order model (0.984-1.000). More importantly, the Qe, cal value identified from the Pseudo second-order model agree with the experimental qe, exp values, Hence, the PQ removal by fixed cells of *Pseudomonas putida* on CFB using different fixed methods can fit well the Pseudo-second order kinetic model.

Table 21 Values of kinetic parameters of for PQ removal by fixed cells on CFB using different immobilization methods of *Pseudomonas putida*

Types of fixed methods	qe exp (mg/g)	Pseudo first-order kinetic model			Pseudo second-order kinetic model		
		Qe,cal (mg/g)	K1 (1/hour)	R^2	Qe, cal (mg/g)	K2 (g/mg hour)	R^2
Adsorption	5.53	1.82	0.114	0.895	5.56	0.28	0.999
Covalent binding	4.85	2.30	0.086	0.750	4.85	1.78	1.000
Entrapment	3.26	1.92	0.139	0.627	3.25	0.17	0.984

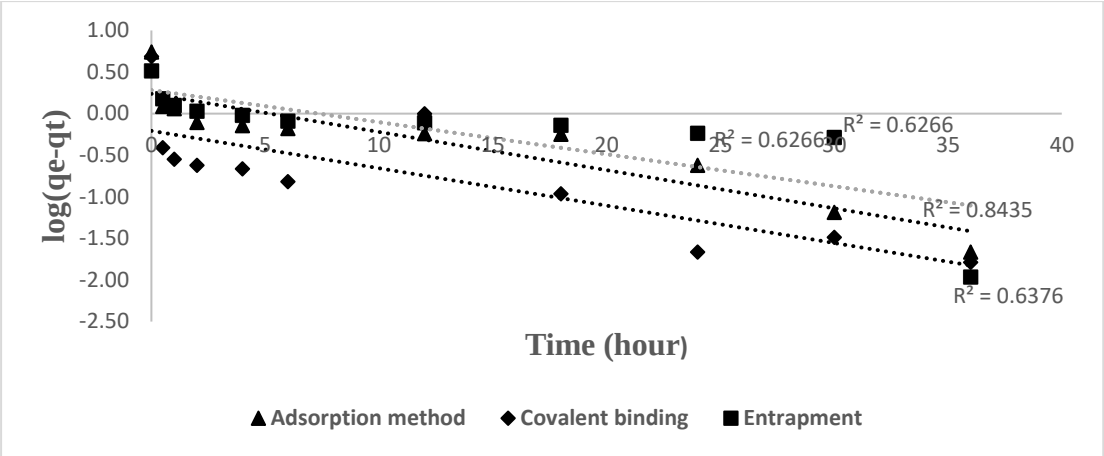

Figure 52 Pseudo first-order kinetic model of PQ removal by fixed cells of *Pseudomonas putida* with different immobilization methods

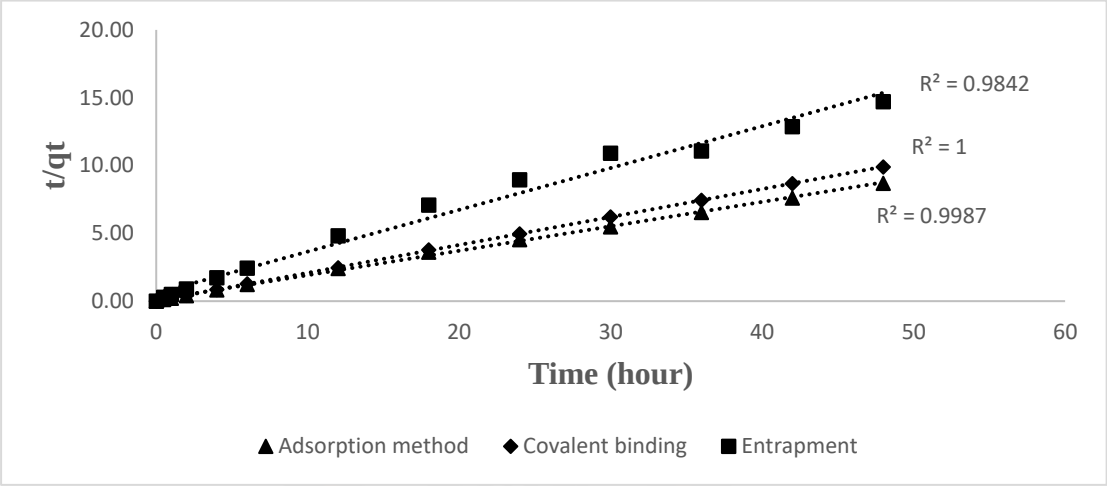

Figure 53 Pseudo second-order kinetic model of PQ removal by fixed cells of *Pseudomonas putida* with different immobilization methods

C. Rice husk biochar (CFB)

+ Isotherm: Ad, Co, En

+ Kinetic model: Ad, Co, En

Isotherm - Rice husk biochar

Table 21 points out the isotherm parameters of paraquat removal by fixed cells on RHB using different immobilization methods of *Pseudomonas putida*. Langmuir and Freundlich isotherm models were used to test the data. Table 22 shows that the adsorption of fixed cells with different immobilization methods of *Pseudomonas putida* can best be described by the Langmuir model. Because of R^2, the values of R^2 of the Langmuir model (0.994 – 0.960) were higher than the values of correlation coefficients than the Freundlich model (0.967 – 0.889). Hence, the adsorption characteristics of paraquat on biochar are more clearly described by the Langmuir model. More interestingly, Table 22 shows the comparison of Paraquat adsorption by three types of cell immobilization with different paraquat adsorption capacities. The following biochars are arranged according to their reducing order of capacity: adsorption method (5.47 mg/g), Covalent binding method (2.85 mg/g), Entrapment method (1.50 mg/g), respectively. The maximum paraquat adsorption capacity by fixed cells of *Pseudomonas putida* on RHB using different methods for PQ is adsorption method with 5.47 (mg/g).

Table 22 Langmuir and Freundlich parameters for PQ removal by fixed cells on RHB using different immobilization methods of *Pseudomonas putida* at pH 7 and room temperature

Types of fixed methods	Langmuir parameters			Freundlich parameters		
	Qo (mg/g)	b (L/mg)	R^2	Kf $(mg/g)(L/mg)^{1/n}$	1/n	R^2
Adsorption	5.47	0.19	0.987	1.54	0.34	0.967
Covalent binding	2.85	0.38	0.994	1.30	0.22	0.889
Entrapment	1.50	0.06	0.960	6.59	0.56	0.930

Kinetic - Rice husk biochar

Table 22 showed the values of kinetic parameters of for PQ removal by fixed cells on RHB using different immobilization methods of *Pseudomonas putida*. The Pseudo first-order rate constant (K1) and Qe, cal values (equilibrium adsorption capacity estimated by the Pseudo-first order kinetic) determined from Figure 54 and Figure 55 along with the correlation coefficients are shown in Table 23. The correlation coefficients of the Pseudo-first order kinetic model (0.679-0.854) were smaller than those of the Pseudo-second order model (0.974-0.999). Moreover, the Qe, cal value identified from the Pseudo-second order model agree with the experimental qe, exp values. Thus, the PQ removal by fixed cells of *Pseudomonas putida* on RHB using different fixed methods can fit well the Pseudo-second order kinetic model.

Table 23 Values of kinetic parameters of for PQ removal by fixed cells on RHB using different immobilization methods of *Pseudomonas putida*

Types of fixed methods	qe exp (mg/g)	Pseudo first-order kinetic model			Pseudo second-order kinetic model		
		Qe,cal (mg/g)	K1 (1/hour)	R^2	Qe, cal (mg/g)	K2 (g/mg hour)	R^2
Adsorption	3.38	1.62	0.070	0.679	3.21	0.14	0.9743
Covalent binding	3.89	1.33	0.098	0.854	3.88	0.37	0.9989
Entrapment	2.73	1.76	0.102	0.808	2.74	0.17	0.9850

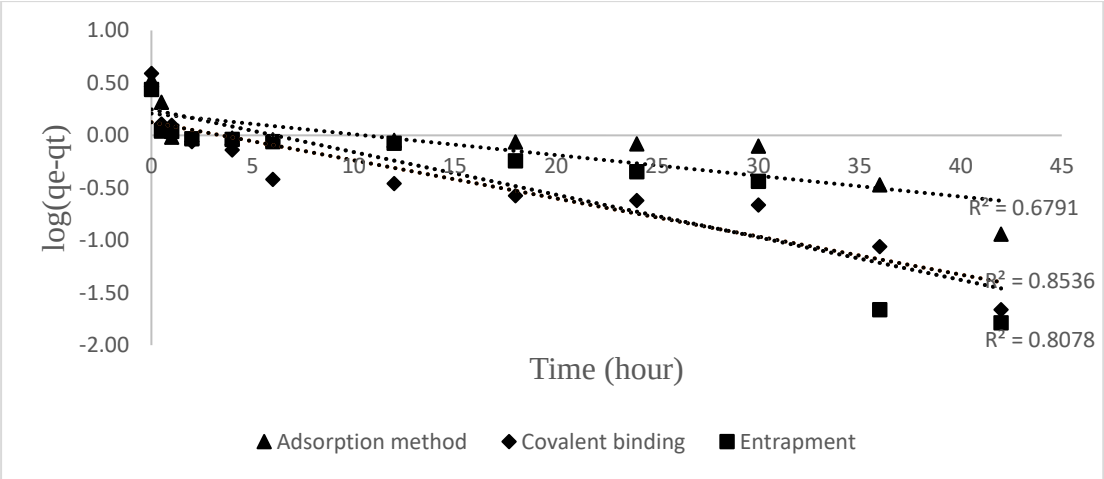

Figure 54 Pseudo first-order kinetic model of PQ removal by fixed cells of *Pseudomonas putida* with different immobilization methods

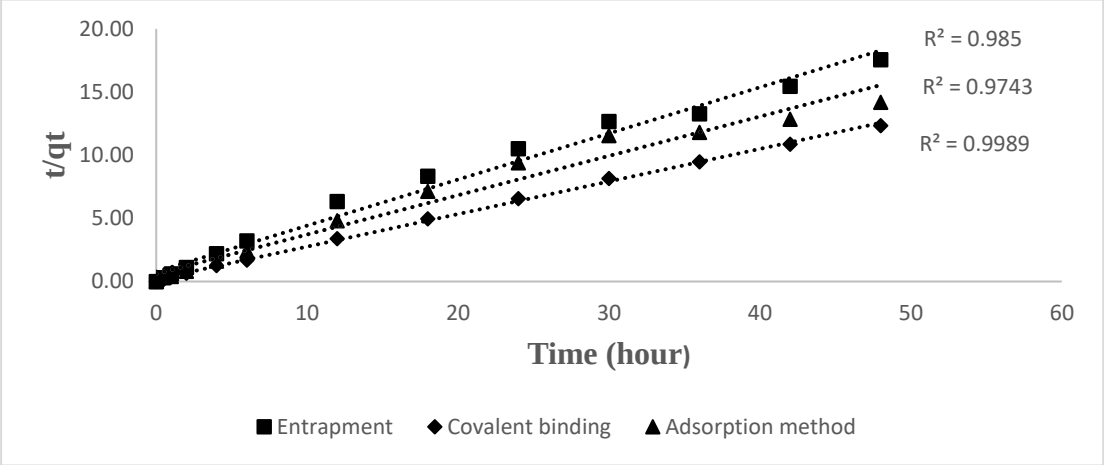

Figure 55 Pseudo second-order kinetic model of PQ removal by fixed cells of *Pseudomonas putida* with different immobilization methods

D. Bagasse biochar (BGB)

+ Isotherm: Ad, Co, En

+ Kinetic model: Ad, Co, En

Isotherm - Bagasse biochar

Table 23 shows the isotherm parameters of paraquat removal by fixed cells on BGB using different immobilization methods of *Pseudomonas putida*. Langmuir and Freundlich isotherm models were used to test the data. Table 24 illustrates that the adsorption of fixed cells with different immobilization methods of *Pseudomonas putida* can be described by Langmuir model. Because of R^2, the values of R^2 of the Langmuir model (0.996 – 0.941) were higher than the values of correlation coefficients of the Freundlich model (0.993 – 0.872). Hence, the adsorption characteristics of paraquat on biochar are obviously described according to the Langmuir model. Furthermore, Table 24 shows the comparison of Paraquat adsorption by three types of cell immobilization with different paraquat adsorption capacities. The following biochars are arranged according to their reducing order of capacity: adsorption method (4.88 mg/g), Covalent binding method (2.84 mg/g), Entrapment method (2.31 mg/g), respectively. The maximum paraquat adsorption capacity by fixed cells of *Pseudomonas putida* on BGB using different methods for PQ is adsorption method with 4.88 (mg/g).

Table 24 Langmuir and Freundlich parameters for PQ removal by fixed cells on BGB with different immobilization methods of *Pseudomonas putida* at pH 7 and room temperature

Types of fixed methods	Langmuir parameters			Freundlich parameters		
	Qo (mg/g)	b (L/mg)	R^2	Kf $(mg/g)(L/mg)^{1/n}$	1/n	R^2
Adsorption	4.88	0.24	0.996	1.61	0.30	0.984
Covalent binding	2.84	0.23	0.978	1.24	0.20	0.872
Entrapment	2.31	0.04	0.941	7.07	0.64	0.993

Kinetic – Bagasse biochar (BGB)

Table 24 indicates values of kinetic parameters of for PQ removal by fixed cells on BGB using different immobilization methods of *Pseudomonas putida.* The Pseudo-first and second order rate constant (K1), (K2) and Qe, cal values determined from Figure 56 and Figure 57 along with the correlation coefficients are shown in table 25. The correlation coefficients of the Pseudo-first order kinetic model (0.503-0.858) were smaller than those of the Pseudo-second order model (0.948-0.999). Moreover, the Qe, cal value identified from the Pseudo-second order model agree with the experimental qe, exp values. Therefore, the PQ removal by fixed cells of *Pseudomonas putida* on BGB using different fixed methods can fit well the Pseudo-second order kinetic model

Table 25 Values of kinetic parameters of for PQ removal by fixed cells on BGB using different immobilization methods of *Pseudomonas putida*

Types of fixed methods	qe exp (mg/g)	Pseudo first-order kinetic model			Pseudo second-order kinetic model		
		Qe,cal (mg/g)	K1 (1/hour)	R^2	Qe, cal (mg/g)	K2 (g/mg hour)	R^2
Adsorption	2.97	1.08	0.166	0.858	3.00	0.62	0.9996
Covalent binding	3.76	1.38	0.077	0.819	3.74	0.32	0.9986
Entrapment	2.73	1.40	0.084	0.503	2.65	0.12	0.9483

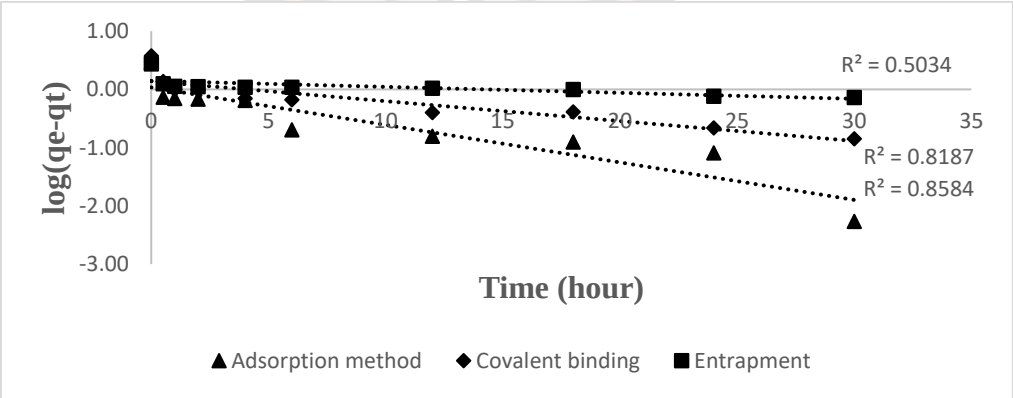

Figure 56 Pseudo first-order kinetic model of PQ removal by fixed cells of *Pseudomonas putida* with different immobilization methods

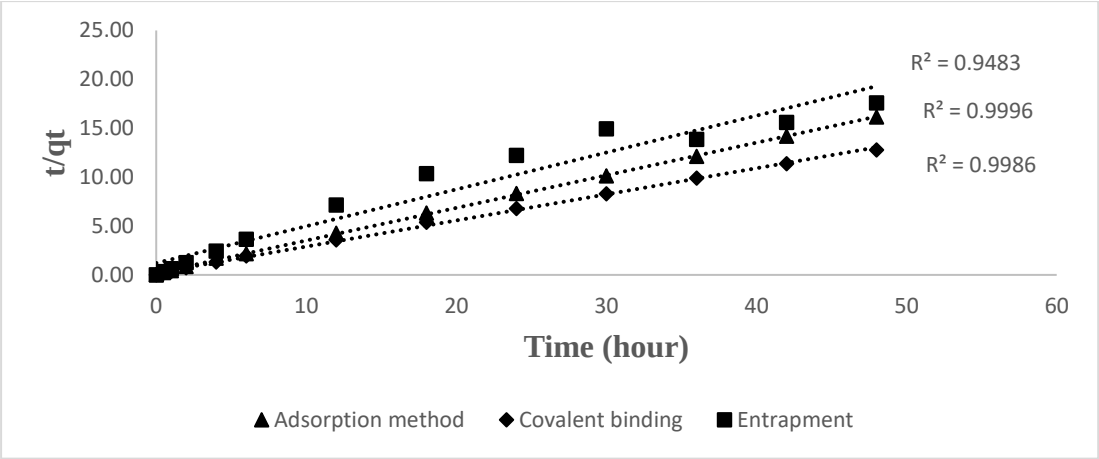

Figure 57 Pseudo second-order kinetic model of PQ removal by fixed cells of *Pseudomonas putida* with different immobilization methods

E. Intermediate products of paraquat

The intermediate products in Figure 58 such as 4,4-bipyridyl (*m*/*z* 155) and malic acid (*m*/*z* 133) are detected in the effluent of samples (free cells, fixed cells on CCB, CFB, BGB, RHB using entrapment, covalent binding and adsorption methods) was collected at 35 h experimental period for analysis Paraquat products by GC/MS. The experiment was set up at the optimal operational concentration of Paraquat being 25.73 mg/L. Compared to the original chemical structure, the results indicated that Paraquat was degraded into different by-products under decomposition by *Pseudomonas putida*.

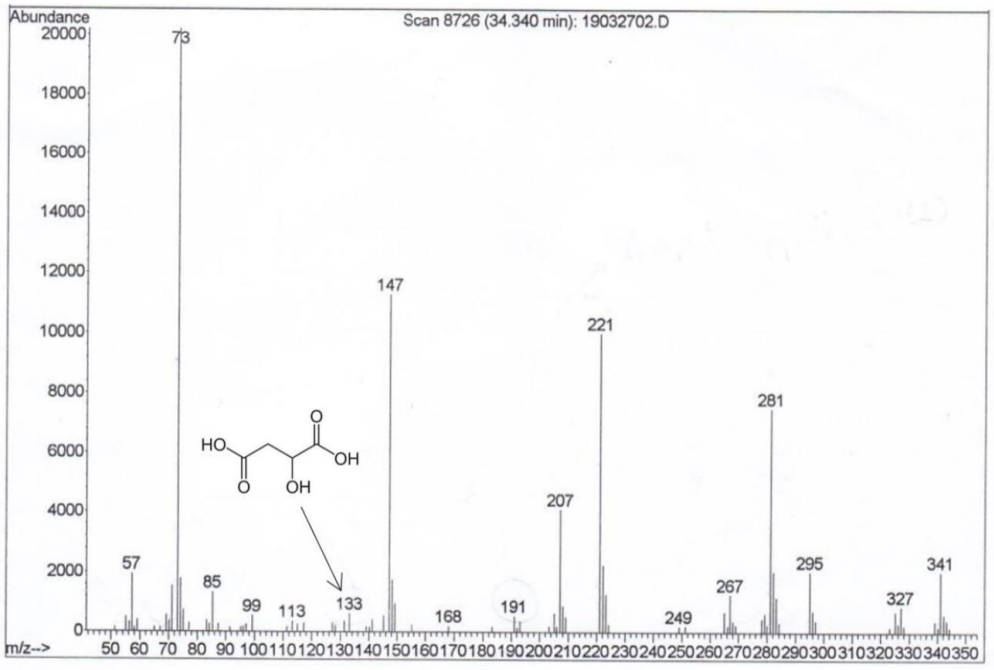

(a)

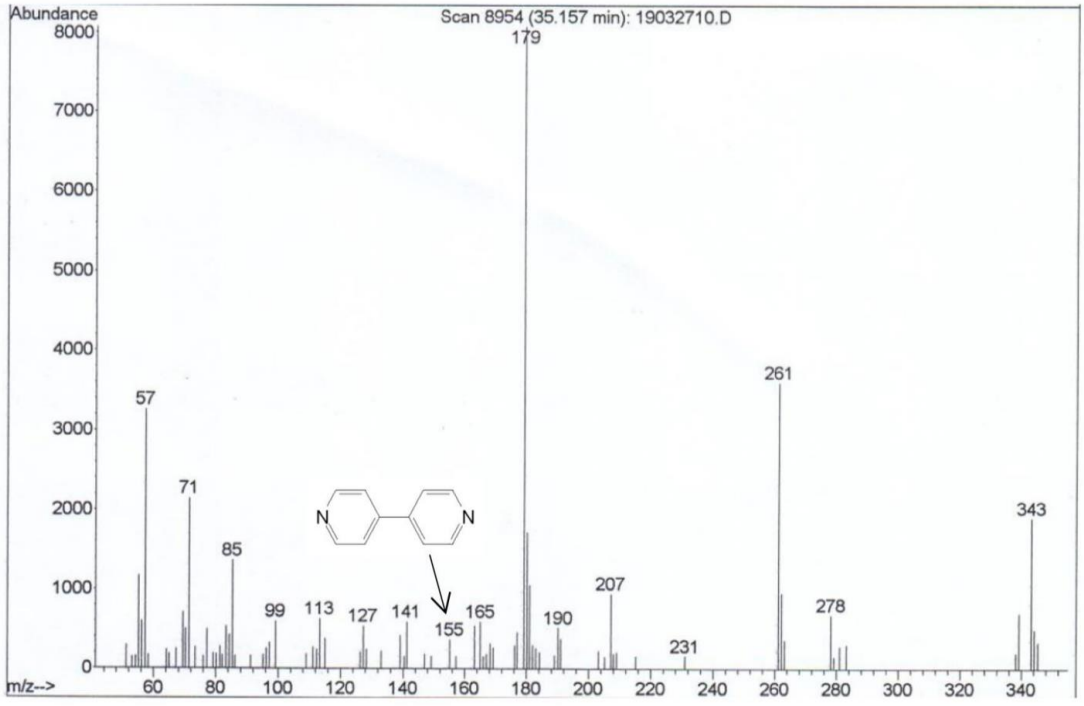

(b)

Figure 58 Paraquat biodegradation metabolic intermediates: (a) malic acid; (b) 4,4'-bipydidyl

The below Figure 59 shows the degradation pathway of PQ by cell-immobilized biochar. Firstly, Paraquat molecular was subjected to demethylation to form monoquat, and then either process releases the methyl group of mono Paraquat to from 4,4-bipyridyl at the fragment m/z 155 g mol^{-1} (Huang et al. 2019, Ha et al., 2021). The second degradation route resulted ring fragmentation products have been identifed as malate, succinate, N-formylglycine, oxalate, formate, and methylamine, which indicated that Malate was formed by the oxidative ring cleavage (Dean, 1999; Dinis-Oliveira et al. 2008). The Malate produced the Malic acid at the fragment m/z 133 g mol^{-1} (Ha et al., 2021). Finally, byproducts can be mineralized to CO_2, NH_3, and H_2O.

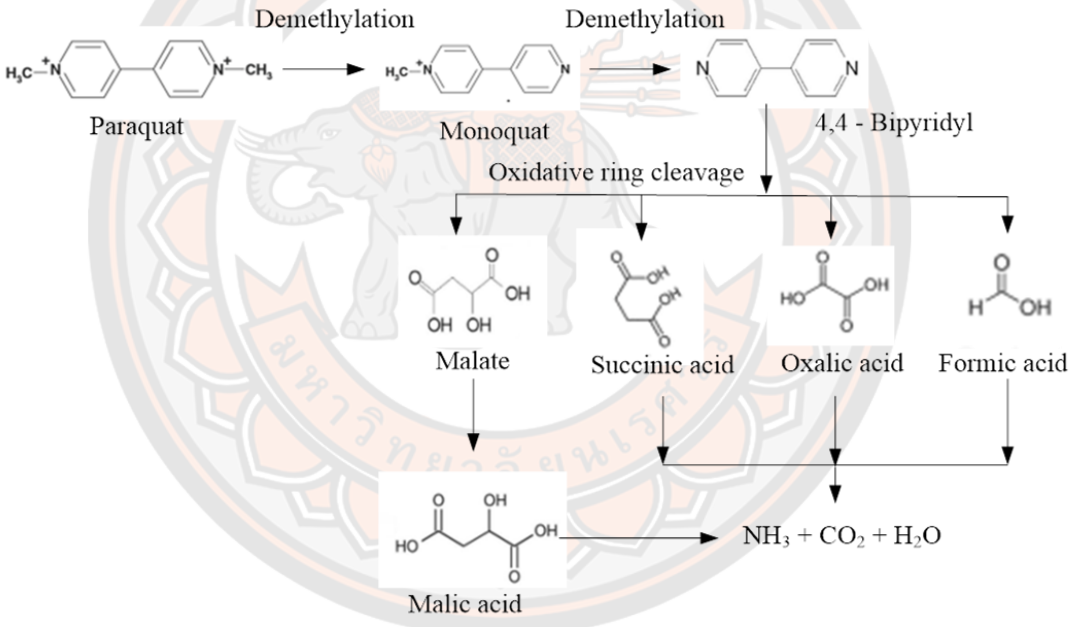

Figure 59 Tentative pathway of Paraquat biodegradation

CHAPTER V

CONCLUSIONS

Part 1

In part A, the corn cob biochar obtained from optimal pyrolysis conditions at 200^0C during 6 hours could have adequate characteristics with suitable surface morphology, suitable functional groups for paraquat adsorption with maximum capacity 71.83 (mg/g). The kinetic and isotherm data was fitted and well explained by the Pseudo-second-order and Langmuir models, which indicated that the adsorption capacity decreased with increasing pyrolysis temperatures and decreasing pyrolysis time. The dominant adsorption mechanisms of paraquat on biochar possibly contributed to hydrogen bonding and pore filling. Therefore, this biochar can become an alternative and economic adsorbent for Pesticide removal in agricultural water treatment.

In part B, the isotherm data was explained by the Langmuir model. The paraquat adsorption capacities of the biochar were determined in order: CFB > CCB > RSB > BGB which are based on the surface area and total pore volume. The kinetic data suited the Pseudo-second-order model which is a chemisorption process. The intra-particle diffusion model was used to assess the kinetic rate of paraquat adsorption. Film diffusion has a role in the adsorption process. The adsorption mechanisms could be pore filling, diffusion, hydrogen bonding, π-π and electrostatic interactions. CFB has the highest adsorption capacity (12.72 mg/g), and can be an alternative adsorbent.

Part 2

In the free cells part, the results indicated growth of *Pseudomonas putida* under optimum conditions such as pH and different initial concentrations free cells of *Pseudomonas putida*. The pH is the important factor effecting the growth of *Pseudomonas putida* and impacts on PQ removal in the biodegradation process. The highest PQ removal was at pH 7. The growth of *Pseudomonas putida* free cells was optimal at pH 7.0.

The amount of Extra-Poly-Saccharide (EPS) generated by *Pseudomonas putida* increased with the increase in PQ concentrations. Optimum increase of the EPS was found at 26 ppm of PQ. However, the EPS production was reduced at 58 ppm.

The isotherm adsorption of paraquat removal using living and dying cells of *Pseudomonas putida* can be described according to the Langmuir model. Moreover, the PQ adsorption capacity of living cells (3.15 mg/g) is higher than the PQ adsorption capacity of dying cells (2.41 (mg/g). The equilibrium adsorption of living cells was achieved/ gotten within 30 minutes, while the equilibrium adsorption/ capacity of dying cells was achieved within 8 hours.

Part 3

In the fixed cells part, the present study has successfully evaluated growth of *Pseudomonas putida* under optimum conditions such as pH and different initial concentrations free cells of *Pseudomonas putida*. The pH is the important factor effecting the growth of *Pseudomonas putida* free cells and impacts on the highest PQ removal in the biodegradation process with optimal at pH 7.0. The amount of Extra-Poly-Saccharide (EPS) generated by *Pseudomonas putida* increased with the increase in PQ concentrations with the optimum increase of the EPS at 26 ppm of PQ. The isotherm adsorption of paraquat removal using living and dying cells of *Pseudomonas putida* can be described according to the Langmuir model. Moreover, the PQ adsorption capacity of living cells (3.15 mg/g) is higher than the PQ adsorption capacity of dying cells (2.41 (mg/g). The characteristics of bacteria and biochar were studied using SEM, BET. The immobilized cells of *Pseudomonas putida* on corn cob biochar using the covalent bonding method was the best immobilization cell method with PQ removal at 4.21 mg/g in the adsorption method, the covalent bonding method and the entrapment methods. The degradation pathways of paraquat under microorganisms were found out. The study encircles paraquat removal from contaminated environments through biochar adsorption and microbial degradation. The discovery of these intermediate products sheds light on the specific degradation pathways of paraquat and may provide valuable information for developing effective strategies for the remediation of paraquat contaminated environments.

REFERENCES

REFFERENCES

Admad, M., Rajapaksha, A.U; Lim, J.E., Zhang, M., Bolan, N., Mohan, D., Vithanage, M., Lee, S.S., & Ok, Y.S. (2014). Biochar as a sorbent for contaminant management in soil and water: A review. *Chemosphere, 99,* 19-33.

Agrow. (1998). *Agrow reports.* Richmond, UK: PJP publications.

Ahemad, M., & Khan, M. S. (2012). Evaluation of plant-growth-promoting activities of rhizobacterium Pseudomonas putida under herbicide stress. *Ann Microbiol 62,* 1531-1540.

Ahmad, A. L., Loh, M. M., & Aziz, J. A. (2007). Preparation and characterization of activated carbon from oil palm wood and its evaluation on Methylene blue adsorption. *Dyes and Pigments, 75*(2), 263-272

Akin, C (1987). Biocatalysis with immobilized cells. Biotechnolgy and Genetic Engineering Reviews – Vol. 5

Amondham.W., Parkpian. P., Polprasert. C., DeLaune. R. D.,& Jugsujinda, A. (2006). Paraquat adsorption, degradation, and remobilization in tropical soils of Thailand. *Journal of Environmental Science and Health Part B, 41*, 485-507.

Apiwat. T., Usavadee. T., & Padet. S., (2015). *Pesticides used in Thailand and toxic effects to human health. Medical Research Archives. Issue 3.* N.P.: n.p.

Aragão Börner, R., Zaushitsyna, O., Berillo, D., Scaccia, N., Mattiasson, B., & Kirsebom, H. (2014). "Immobilization of Clostridium acetobutylicum DSM 792 as macroporous aggregates through cryogelation for butanol production". *Process Biochemistry, 49.*

Association of Official Agricultural Chemists. (2000). *Official methods of analysis of AOAC international* (17th ed.). AOAC International, Arlington, VA, USA.

Agricultural Toxic Substances Division. (2000). *Annual Research Report*. Department of Agriculture, Bangkok, Thailand.

Bagby, M. O., & Widstrom, E. W. (1987). Biomass uses and conversions. In *Corn: Chemistry and Technology* (ed.) S. A. Waston & P. E. Ramstad (pp. 575-590). American Association of Cereal Chemists, MN.

Ban, K., Hama, S., Nishizuka, K., Kaieda, M., Matsumoto, T., & Kondo, A. (2002). Repeated use of whole-cell biocatalysts immobilized within biomass support particles for biodiesel fuel production. *Journal of Molecular Catalysis B: Enzymatic, 17,* 157-165.

Bellinaso, M. L., Greer, C. W., Peralba, M. C., Henriques, J. A., & Gaylarde, C. C. (2003). Biodegradation of the herbicide trifluralin by bacteria isolated from soil. *FEMS Microbiol Ecol, 43*, 191–194

Bicki, Thomas J. (1989). *Pesticides and groundwater. Land and Water. Conserving Natural Resources in illinois.* May 1989

Blackburn, R. (2004). Natural polysaccharides and their interactions with dye molecules: Applications in effluent treatment. *Environ. Sci. Technol. 38,* 4905-4909.

Brewer, C.E., Schmidt-Rohr, K., Satrio, J. A., & Brown, R. C. (2009). Characterization of biochar from fast pyrolysis and gasification systems. *Environ Prog Sustain Energy, 28,* 386–396.

Brownawell, B. J., Chen, H., Collier, J. M., & Westall, J. C. (2014). Adsorption of organic cations to natural materials. *Environ. Sci. Technol, 24,* 1234–1241.

Brownsort, P. A. (2009). *Biomass pyrolysis processes: performance parameters and their influence on biochar system benefits* (Master's thesis). Nicolson: The University of Edinburg.

Burns, R. G., & Audus, L. J. (1970). Distribution and breakdown of paraquat in soil. *Weed Res., 10,* 49–58.

Cao, X., Ma, L., Gao, B., & Harris, W. (2009). Dairy-Manure derived biochar effectively sorbs lead and atrazine. *Environ. Sci. Technol, 43,* 3285 - 3291

Carrott, S. P. J. M., & Carrott, M. M. L. R. (2007). Lignin-from natural adsorbent to activated carbon: A review. *Bioresource Technology, 98,* 2301-2312.

Carson. R. (1964). *Silence spring*. Greenwich, CN: Fawcett Publications.

Cassidy, M. B., Lee, H., & Trevors, J. T. (1996). Environmental applications of immobilized microbial cells: a review. *Journal of Industrial Microbiology, 16,* 7-101.

Chatterjee, R., Sajjadi, B., Chen, W. Y., Mattern, D. L., Nathan, H., Raman, N. V., & Dorris, A. (2020). *Effect of Pyrolysis Temperature on Physico Chemical Properties and Acoustic-Based Amination of Biochar for Efficient CO2 Adsorption. Front. Energy Res.* Retrieved November, 25, 2020, from https://doi.org/10.3389/fenrg.2020.00085

Cheah, U., Kirkwood, R., & Lum, K. (1998). Degradation of Four commonly used pesticides in Maylaysian agricultural soils. *Journal of Agricultural and Food Chemistry, 46,* 1217 – 1223.

Chen, B., Yuan, M., & Qian, L. (2012). Enhanced bioremediation of PAH-contaminated soil by immobilized bacteria with plant residue and biochar as carriers. *J Soil Sediments, 12,* 1350-1359.

Chen, B. L., Zhou, D. Q., & Zhu, L. Z., (2008). Transitional adsorption and partition of nonpolar and polar aromatic contaminants by biochars of pine needles with different pyrolytic temperatures. *Environmental Science and Technology, 42,* 5137-5143.

Chen, C., Lehmann, J., Thies, J. E.., Burton, S. D., & Engelhard, M. H. (2006). Oxidation of black carbon by biotic and abiotic processes. *Organic Geochemistry, 37,* 1477-1488.

Chen, C., Zhou, W., Lin, D., (2015). Sorption characteristics of N-nitrosodimethylamine onto biochar from aqueous solution. *Bioresour. Technol, 179,* 359–366.

Chen, C. M., & Lua, A. C. (2000). Lung toxicity of paraquat in the rat. *Toxicol. Environ. Health (A), 59,* 477.

Chen, X., Chen, G., Chen, L., Chen, Y., Lehmann, J., McBride, M. B., & Hay, A. G. (2011). Adsorption of copper and zinc by biochars produced from pyrolysis of hardwood and corn straw in aqueous solution. *Bioresource Technology, 102*(19), 8877-8884

Chun, Y., Sheng, G., Chiou, C. T., & Xing, B. (2004). Compositions and sorptive properties of crop residue-derived chars. *Environmental Science & Technology, 38,* 4649-4655.

Clausen, L., Fabricius, I., & Madson, L. (2001). Adsorption of Pesticides onto Quartz, Calcite, Kaolinite, and α-Alumina. *Journal of Environmental Quality, 30*, 846 – 857.

Coates, J. (2000). Interpretation of Infrared Spectra, A practical Approach. In *Encyclopedia of Analytical Chemistry*, R.A, Meyers (Ed.). Ohn Wiley & Sons Ltd, Chichester. 10815-10837.

Cobb, A. H., & Reade, J. P. H. (2010). *Herbicides and Plant Physiology* (2nd ed.). Chichester, West Sussex, UK: Wiley-Blackwell.

Cocenza, D. S., Moraes, M. A., Beppu, M. M., & Fraceto, L. F. (2012). *Water Air Soil Pollution, 223,* 3093 - 3104

Colburn. T., Dumanoski. D., & Myers. J. P (1996). *Our stolen future: are we threatening our fertility intelligence and survival? – a scientific detective story*. New York: Dutton Books.

Compant, S., Cle´ment, S., & Sessitsch. A. (2010). Plant growth-promoting bacteria in the rhizo-and endosphere of plants: their role, colonization, mechanisms involved and prospects for utilization. *Soil Biol Biochem, 42*, 669–678

Crini, G., Gimbert, F., Robert, C., Martel, B., Adam, O., Morin-Crini, N., Griorgi, F. D., & Bodot, P. M., (2008). The removal of Basic Blue 3 from aqueous solutions by chitosan-based adsorbent: Batch studies. *Journal of Hazardous Materials, 153,* 96-106.

Cunningham, C. J., Ivshina, I. B., Lozinsky, V. I., Kuyukina, M. S., & Philp, J. C. (2004). Bioremediation of diesel-contaminated soil by microorganisms immobilised in polyvinyl alcohol. *Int Biodeter Biodegr, 54*, 167–174

de Keizer A. (1990). Adsorption of paraquat ions on clay minerals: electrophoresis of clay particles. *Progr in Colloid Polym Sci., 83*, 118–126

de Wild, P., van de Laan, R., Kloekhorst, A., & Heeres, E. (2009). *Lignin Valorisation for Chemicals and (Transportation) Fuels via (Catalytic) Pyrolysis and Hydrodeoxygenation*. Wiley InterScience. DOI 10. 1002/ep/10391

Dervakos, G. A., & Webb, C. (1991). On the merits of viable-cell immobilization. *Biotech. Adv., 9,* 559-612.

Draoui, K., Denoyel, R., Chgoura, M., & Rouquerol, J. (1999). Adsorption of paraquat on minerals. A thermodynamic study. *Journal of Thermal Analysis and Calorimetry. 58*, 597-606

Dzionek, A., Wojcieszynska, D., & Guzik, U. (2016). Natural carriers in bioremediation: A review. *Electronic Journal of Biotechnology, 23*, 28-36.

Elsayed, B., B., & El-Nady, M., F. (2013). Bioremediation of pendimethalin-contaminated soil. *African Journal of Microbiology Research, 7*(21), 2374-2588.

Elsayed, C. S., Karthick, N. A., Thilagam, R., Chandralekha, A., Raghavarao, K. S. M. S., & Gnanamani,A. (2017). Efficacy of free and encapsulated Bacillus lichenformis strain SL10 on degradation of phenol: A comparative study of degradation kinetics. *Journal of Environmental Management, 197*, 373-383.

Fiol, N., & Villaescusa, I. (2009). Determination of sorbent point zero charge: usefulness in sorption studies. *Environmental Chemistry Letters, 7*(1), 79-84.

Fogler, H. S. (1999). *Elements of Chemical Reaction Engineering* (3rd ed.). New Jersy: Prentice Hall.

Foster, D. M., Rachwal, A. J., & White, S. L. (1991). New treatment processes for pesticides and chlorinated organics control in drinking water. *Water and Environmental Journal, 1,* 466-477.

Funke, A., & Ziegler, F. (2010). Hydrothermal carbonization of biomass: A summary and discussion of chemical mechanisms for process engineering. *Biofuels bioprod. Biorefin. 4*, 160-177.

Gai, X., Wang, H., Liu, J., Zhai, L., Liu, S., Ren, T., & Liu, H. (2014). Effects of feedstock and pyrolysis temperature on biochar adsorption of ammonium and nitrate. *Plos one, 9*(12), 1-19.

Gavrilescu, M (2005). Fate of pesticides in the environment and its bioremediation. *Eng Life Sci, 5,* 497-526.

Ghavi, A., Bagherian, G., & Vahidian, R. H. (2021). Degradation of paraquat herbicide using hybrid AOP process: statistical optimization, kinetic study, and estimation of electrical energy consumption. *Environ Sci Eur, 33,* 117.

Giardiana, Hill, I. R., & Wright, S. J. L. (1978). *Pesticide Microbiology: Microbiological Aspects of Pesticide Behavior in the Environment.* London: Academic Press.

Giardina, M. C., M. T. Giardi, & G. Filacchioni. (1980). 4-Amino-2-chloro-1,3,5-triazine: A new metabolite of atrazine by a soil bacterium. *Agric. Biol. Chem, 44*, 2067-2072.

Guiseley, K. B. (1989). Chemical and physical properties of algal polysaccharides used for cell immobilization. *Enzyme Microbiol Technol, 11*, 706-716.

Gupta, P. K. (2004). Pesticide exposure – Indian scene. *Toxicology, 198,* 83–90.

Gwenzi, W., Chaukura, N., Noubactep, C., & Mukome, F. N. D. (2017). Biochar-based water treatment systems as a potential low-cost and sustainable technology for clean water provision. *J. Environ. Manag, 197,* 732-749.

Hamadi, N. K., Swaminathan, S., & Chen, X. D. (2004). Adsorption of Paraquat dichloride from aqueous solution by activated carbon derived from used tires. *Journal of Hazardous Materials, B112,* 133-141.

Hamdaoui, O. (2006). Batch study of liquid-phase adsorption of methylene blue using cedar sawdust and crushed brick. *Journal of Hazardous Material, B135,* 264-273

Hao, F., Zhao. X., Ouyang, W., Lin, C., Chen, S., Shan, Y., & Lai, X. (2013). Molecular structure of Corncob-derived Biochars and the Mechanism of Atrazine sorption. *Agronomy, Soils & Environmental Quality*, *105,* 3.

Hassler, J. W. (1963). *Activated carbon*. New York: Chemical.

Herbert, L., Hosek, I., Kripalani, R. (2012). *The characterization and comparison of biochar produced from a decentralized reactor using forced air and natural draft pyrolysis*. California: Materials Engineering Department. California Polytechnic State University, San Luis Obispo.

Herman, P. L., Behrens, M., Chakraborty, S., Crastil, B. M., Barycki, J., & Weeks, D. P. (2005). A three component dicamba O-demethylase from Pseudomonas maltiphilia strain DI-6: gene isolation, characterization and heterologous expression. *J Biol Chem, 280,* 24759– 24767.

Ho, Y. S., & McKay, G. (1998). A comparison of chemisorption kinetic models applied to pollutant removal on various sorbents. *Trans I Chem E, 76,* Part B, November 1998

Huang, Y., Zhan, H., Bhatt, P., & Chen, S., (2019). *Paraquat Degradation from Contaminated Environments: Current Achievements and Perspectives. Frontiers in Microbiology*, 01754.

Husband, R. (2001), *Paraquat Dichloride: Physical and Chemical Properties of Pure Material, Unpublished Study From Syngenta Crop Protection, Jealott's Hill Research Centre, Bracknell, Berkshire, UK, Report no. RJ3167B, Syngenta* File No. PP148/1116.

Hwang, C., Ban, Y. M, Lee, C. H., Chung, C. H., & Ahn, I. S. (2008). Adhesion of Pseudomonas putida NCIB 9816-4 to a naphthalene-contaminated soil. *Colloid. Surface, B, 62*, 91-96.

Inyang. M, & Dickenson. E (2015). The potential role of biochar in the removal of organic and microbial contaminants from potable and reuse water: A review. *Chemosphere, 134*, 232-240.

Jeyaratnam, J, Lun, K., C., & Phoon, W. O. (1987). Survey of acute pesticide poisoning among agricultural workers in the four Asian countries. *Bulletin of the World Health Organization, 65*, 521-527.

Jin, J., Sun, K., Wu, F., Gao, B., Wang, Z., Kang, M., Bai, Y., Zhao, Y., Liu, X., & Xing, B., (2014). Single-solute and bi-solute sorption of phenanthrene and dibutyl phthalate by plant- and manure-derived biochars. *Sci. Total Environ, 473–474, 3*08–316.

John, R. P., Tyagi, R. D., Brar, S. K., Surampalli, R. Y., & Prévost, D. (2011). Bio encapsulation of microbial cells for targeted agricultural delivery. *Critical Reviews in Biotechnology, 31*(3), 211–226

Johnsen, K., Jacobsen, C. S., Torsvik, V., & Sorensen, J. (2001). Pesticide effects on bacterial diversity in agricultural soils-a review. *Biol Fertil Soils, 33,* 443–453

Kalinke, C., Mangrich, A. S., Marcolino, L. H., & Bergamini, M. F. (2016). Biochar prepared from castor oil cake at different temperatures: A voltammetric study applied for Pb^{2+}, Cd^{2+} and Cu^{2+} ions preconcentration. *Journal of Hazardous Materials, 318,* 526-532.

Karpouzas, D. G., & Walker, A. (2000). Factors influencing the ability of Pseudomonas putida strain epl and epll to degrade the organophosphate ethoprophos. *J. Appl. Microbiol, 89,* 40 – 48.

Kasozi, G. N., Zimmerman, A. R., Nkedi-Kizza, P., & Gao, B. (2010). Catechol and humic acid sorption onto a range of laboratory-produced black carbons (Biochars). *Environ. Sci. Technol*, *44*(16), 6189–6195.

Kearns, J. P., Wellborn, L. S., Summers, R. S., & Knappe, D. R. U. (2014). 2,4-D adsorption to biochars: Effect of preparation conditions on equilibrium adsorption capacity and comparison with commercial activated carbon literature data. *Water Research, 62,* 20-28.

Keiluweit, M., Nico, P.S., Johnson, M.G., & Kleber, M. (2010). Dynamic molecular structure of plant biomass-derived black carbon (biochar). *Environmental Science and Technology, 44,* 1247 – 1253.

Kinney, T. J., Masiello, C. A., Dugan, B., Hockaday, W. C., Dean, M. R., Zygourakis, K., & Barnes, R. T. (2012). Hydrologic properties of biochars produced at different temperatures. *Biomass and Bioenergy, 41,* 34-43.

Kong, S. H., Lam, S. S., Yek, P. N. Y., Liew, R. K., Ma, N. L., Osman, M. S., & Wong. C.C. (2019). Self-purging microwave pyrolysis: an innovative approach to convert oil palm shell into carbon-rich biochar for methylene blue adsorption. J. Chem. Technol. *Biotechnol, 94,* 1397–1405.

Krzesin´ska, M., & Zachariasz, J. (2007). The effect of pyrolysis temperature on the physical properties of monolithic carbons derived from solid iron bamboo. *Journal of Analytical and Applied Pyrolysis*, *80*(1), 209-215.

Kumar, R., Jain, S. K., Misra, R. K., Kachchwaha, M., & Khatri, P. K. (2012). Aqueous heavy metals removal by adsorption on beta-diketone-functionalized styrene-divinylbenzene copolymeric resin. *Int J Environ Sci Technol, 9,* 79-84.

Kuyukia. M. S., Korshunova. I. O., Rubtsova. E. V., & Ivshina. I. B. (2013). *Methods of microorganism immobilization for Dynamic Atomic-Force studies.* N.P.: n.p.

Kyriakopoulos, G., Xiarchos, I., & Doulia, D. (2017). Removal of pesticides from aqueous solutions by adsorption. In *3rd European Conference on Pesticides and Related Organic Micropollutants in the Environment.* N.P.: n.p.

Lehmann, J., & Joseph, S. (2009). *Biochar for environmental management: Science and technology*. Routledge-Earthscan.

Leung, K., Cassidy. M. B., Holmes., S. B., Lee, H., & Trevors, J. T. (1995). Survival of κ-carrageenan-encapsulated Pseudomonas aeruginosa UG2Lr in forest soil monitored by polymerase chain reaction and spead plating. *FEMS Microbiology Ecology, 16,* 71-82.

Li, C., Zhu, X., He, H., Fang, Y., Dong, H., Lü, J., Li, J., & Li, Y. (2019). Adsorption of two antibiotics on biochar prepared in air-containing atmosphere: influence of biochar porosity and molecular size of antibiotics. J. *Mol. Liq., 274*, 353–361.

Lian, F., & Xing, B. (2017). Black carbon (biochar) in water/soil environments: molecular structure, sorption, stability, and potential risk. *Environ. Sci. Technol*, *51*, 13517–13532.

Libra J. A., K. S. Ro, C. Kammann, A. Funke, N. D. Berge,…& Y. Neubauer. (2011). Hydrothermal carbonization of biomass residuals: a comparative review of the chemistry, processes and applications of wet and dry pyrolysis. *Biofuels, 2*, 71–106.

Liu, N., Zhu, M., Wang, H., & Ma, H. (2016). Adsorption characteristics of Direct Red 23 from aqueous solution by biochar. *J. Mol. Liq, 223,* 335-342

Liu, N., Charrua, A. B., Weng, C. H., Yuan, X., & Ding, F. (2015). Characterization of biochars derived from agriculture wastes and their adsorptive removal of atrazine from aqueous solution: A comparative study. *Bioresource Technology, 198*, 55-62.

Liu, W., Zhonga, Z., Wangb, S., & Luob, Z., (2011). Interactions of biomass components during pyrolysis: A TG-FTIR study. *Journal of Analytical and Applied Pyrolysis, 90,* 213-218.

Liu, W. J., Zeng, F. X., Jiang, H., Zhang, X. S. (2011). Preparation of high adsorption capacity bio-chars from waste biomass. *Bioresource Technology, 102,* 8247-8252.

Liu, X., Tan, Y., Zeng, G., Wang, X., Hu, X., Gu, Y., & Yang, Z. (2015). Application of biochar for the removal of pollutants from aqueous solutions. *Chemosphere, 125,* 70-85.

Loh, K.-C., & Cao, B. (2008). Paradigm in biodegradation using Pseudomonas putida-A review of proteomics studies. *Enzyme Microbial. Technology, 43,* 1–12

Luo, Z., Yao, B., Yang, X., Wang, L., Xu, Z., Yan, X., Tian, L., Zhou, H., & Zhou, Y. (2022). Novel insights into the adsorption of organic contaminants by biochar: A review. *Chemosphere, 287,* 132113

MacCarthy, P., & Djebbar, K. K.(1986). Removal of paraquat, diquat, and amitrole from aqueous solution by chemically modified peat. *J Environ Qual, 15,* 103–107

Manyà J. J. (2012). Pyrolysis for biochar purposes: a review to establish current knowledge gaps and research needs. *Environ Sci Technol, 46,* 7939–7954.

Marcus. A. (1980). Environmental Protection Agency. In J. Q. Wilson, *The politics of regulation.* New York: Basic Books.

Marien, C. B. D., Pivert, M. L., Azais, A., Bra, I. C., Drogui, P., Dirany, A., & Robert, D. (2018). Kinetics and mechanism of Paraquat's degradation: UV-C photolysis vs UV-C photocatalysis with TiO2/SiC foams. *Journal of Hazardous Materials.*

Martani, E., Yanti, N. A., & Sebastian M. (2006). Biodegradation of Paraquat in Peat Soil by Micrococcus sp. S-2 and Achromobacter sp. *SM-1. J. Tanah Trop., 12,* 49-54.

Martwong, E., Chuetor, S., & Junthip, J. (2021). Adsorption of Paraquat by Poly (Vinyl Alcohol)- Cyclodextrin Nanosponges. *Polymers, 13,* 4110. https://doi.org/10.3390/polym13234110

Mattiasson, B., & Hahn-Hägerdal, B. (1982). Micro-environmental effects on metabolic behavior of immobilized cells: a hypothesis. *Eur J Appl Microbiol Biotechnol, 16,* 52–55.

McConnel. R., Pacheco A. F., & Murray, D. L. (1993). Hazards of closed pesticide mixing and loading systems: The paradox of protective technology in the third world. *British Journal of Industrial Medicine, 49,* 615-620.

Michelsen, D. L., Gideon, J. A., Griffith, G. P., Pace, J. E., & Kutat, H. L. (1975). *Removal of soluble mercury from waste water by complexing techniques. US Dept. Industry, Office of Water Research and Technology.* Bull No 74.

Mierzwa-Hersztek, M., Gondek K., & Baran, A. (2016). Effect of poultry litter biochar on soil enzymatic activity, ecotoxicity and plant growth. *ApplSoil Ecol, 105,* 144 -150

Mohammadi, A., & Nasernejad, B. (2009). Enzymatic degradation of anthracene by the white rot fungus Phanerochaete chrysosporium immobilized on sugarcane bagasse. *J Hazard Mater, 161*, 534–537.

Mohan, D., Sarswat, A., Ok,Y.S.C.U(2014). Pittman. Organic and inorganic contaminants removal from water with biochar, a renewable, low cost and sustainable adsorbent – a critical review. *Bioresour. Technol, 160*, 191–202.

Mohan, D., Pittman, C. U., & Steele. P. H. (2006). Pyrolysis of wood/biomass for bio-oil: a critical review. *Energy Fuels, 20*, 848–889.

Murray, D. L., & Taylor. P. L (2000). Claim no easy victories: Evaluating the pesticide industry's global safe use campaign. *World development, 28*(10), 1735-1749.

Najafpour, G. (1990). Immobilization of microbial cells for the production of organic acids. *Journal of Sciences, Islamic Republic of Iran, 1*(3), 172-176.

Narine, D. J., Guy, R. D. (1982). Binding of diquat and paraquat to humic acid in aquatic environments. *Soil Sci., 133,* 356–363.

Neogi, S., Sharma, V., Khan, N., Chaurasia, D., Ahmad, A., Chauhan, S., Singh, A., You, S., Pandey, A., & Bhargava, P.C. (2022). Sustainable biochar: A facile strategy for soil and environmental restoration, energygeneration, mitigation of global climate change and circular bioeconomy. *Chemosphere, 293,* 133474

Nguyen, T., Cho, H., Poster, D., & Ball, W. (2007). Evidence for a pore-filling mechanism in the adsorption of aromatic hydrocarbons to a natural wood char. Environ. *Sci.Technol, 41*(4), 1212–1217.

Nguyen, T. H. Ha, Nguyen, C. Toan, Kajitvichyanukul Puangrat. (2021). *Enhanced paraquat removal from contaminated water using cell-immobilized biochar. Clean Technologies and Environmental Policy.* https://doi.org/10.1007/s10098-020-01996-8

Nikolajeva, V., Griba, T., & Petriņa, Z. (2012). Factors influencing adhesion of Pseudomonas putida on porous clay ceramic granules. *EEB, 10,* 77–80.

Nuithitikul, K., Srikhun, S., & Hirunpraditkoon, S. (2010). Kinetics and equilibrium adsorption of Basic Green 4 dye on activated carbon derived from durian peel: Effects of pyrolysis and post-treatment conditions. *Journal of the Taiwan Institute of Chemical Engineers, 41*(5), 591-598.

Ortiz-Hernández ML, Sánchez-Salinas E. (2010). Biodegradation of the organophosphate pesticide tetrachlorvinphos by bacteria isolated from agricultural soils in México. *Rev Int Contam Ambient, 26,* 27–38

Panwar, N. L., Pawar, A., Salvi, D. B. L. (2019). Comprehensive review on production and utilization of biochar. *SN Appl. Sci. 1,* 168.

Perkins, J. H. (1982). *Insects experts and the insecticide crisis: the quest jot new pest management strategies*. New York: Plenum Press.

Pignatello, J., Kwon, S., & Lu, Y. (2006). Effect of natural organic substances on the surface and adsorptive properties of environmental black carbon (char): attenuation of surface activity by humic and fulvic acids. *Environ. Sci.Technol, 40*(24), 7757–7763.

Pukcothanung, Y., Siritanon, T., & Rangsriwatananon, K.,(2018). The efficiency of zeolite Y and surfactant-modified zeolite Y for removal of 2, 4-dichlorophenoxyacetic acid and 1, 1’-dimethyl-4, 4’-bipyridinium ion. Micropor. Mesopor. *Mat. 258,* 131–140. Doi:10.1016/j.micromeso. 2017.08.035

Qambrani, N. A., Rahman, M. M., Won, S., Shim, S., & Ra, C., (2017). Biochar properties and eco friendly applications for climate change mitigation, waste management, and wastewater treatment: A review. Renew. *Sustain. Energy Rev, 79,* 255–273.

Quilliam, R. S., Glanville, H. C., Wade, S. C., & Jones, D. L. (2013). Life in the 'charosphere'-Does biochar in agricultural soil provide a significant habitat for microorganisms?. *Soil Biol. Biochem., 65*, 287-293.

Regkouzas, P., & Diamadopoulos, E. (2019). Adsorption of selected organic micro-pollutants on sewage sludge biochar. *Chemosphere, 224*, 840–851.

Ribeiro, A. R., Nunes, O. C., Pereira, M.F., & Silva, A. M., (2015). An overview on the advanced oxidation processes applied for the treatment of water pollutants defined in the recently launched Directive 2013/39/EU. *Environment International, 75*, 33-51.

Rodea-Palomares, I., Makowski, M., Gonzalo, S., Gonzalez-Pleiter, M., Leganes, F., & Fernandez-Pinaz, F. (2015). Effect of PFOA/PFOS pre-exposure on the toxicity of the herbicides 2,4-D, Atrazine, Diuron and Paraquat to a model aquatic photosynthetic microorganism. *Chemosphere, 139*, 65-72.

Rosenstock, L. (1991). *Chromic central nervous system effects of acute organophosphate pesticide intoxication*. Lancet.

Ross, M. A., & Lembi, C. A. (1999). *Applied Weed Science* (2nd ed.). New Jersey: Prentice-Hall.

Sadeghfar, F., Ghaedi, M. (2021). Chapter 12. Photocatalytic treatment of pollutants in aqueous media. Interface Sci. *Technol*, *32*, 725-759.

Saffari, M., Karimian, N., Ronaghi, A., Yasrebi, J., & Ghasemi-Fasaei, R. (2015). Stabilization of nickel in a contaminated calcareous soil amended with low-cost amendments. *Journal of Soil Science and Plant Nutrition, 15*(4), 896-913

Samonin, V. V, & Elikova, E. E. (2004). A study of the adsorption of bacterial cells on porous materials. *Microbiology*, *73*(6), 696-670.

Sannino, F., Iorio, M., De Martino, A., Pucci,M., Brown, C.D., & Capasso, R (2008). Remediation of waters contaminated with ionic herbicides by sorption on polymerin. *Water Res, 42*, 643–652

Santolini, E., Bovo, M., Barbaresi, A., Torreggiani, D., & Tassinari, P. (2022). Turning Agricultural Wastes into Biomaterials: Assessing the Sustainability of Scenarios of Circular Valorization of Corn Cob in a Life-Cycle Perspective. *Appl. Sci., 11*(14), 6281; https://doi.org/10.3390/app11146281

Santos, M. S. F., Alves, A., & Madeira, L. M. (2011). Paraquat removal from water by oxidation with Fenton's reagent. *Chem. Eng. J, 175,* 279-290

Scheele, C. W. (1773). *Chemische Abhandlung von der Luft und dem Feuer; see: Ostwald's Ž. Klassiker der exakten Wiss. 58 (1894). H. Kayser, Wied. Ann. Phys. 12 (1881) 526. H. Kayser, Wied. Ann. Phys. 14 (1881) 450.*

Senseman, S. A. (2007). *Herbicide Handbook* (9th ed.). Champaign, Illinois: Weed Science Society of America.

Shaheen, S., Niazi, N.K., Hassan, N. E., Bibi, E., Wang, I., Tsang, H., Daniel, C.W., Ok, Y.S., Bolan, N., & Rinklebe, J. (2019). Wood-based biochar for the removal of potentially toxic elements in water and wastewater: A critical review. *Int. Mater. Rev., 64,* 216–247.

Sharma, R. K., Wooten, J. B., Baliga, V. L., Lin, X., Chan, W. G., & Hajaligol, M. R. (2004). Characterization of chars from pyrolysis of lignin. Fuel. 83, 1469-1482.

Shi, W., Guo, F., Wang, H., Liu, C., Fu, Y., & Yuan, S. (2018). Carbon dots decorated magnetic ZnFe2O4 nanoparticles with enhanced adsorption capacity for the removal of dye from equeous solution. *Applied Surface Science, 433,* 790-797.

Singh, B. K., Kuhad, R. C. (1999). Biodegradation of lindane by the white-rot fungus Trametehirsutus. Lett. Appl. Microbiol., 28, 238-241.

Singh, B. K., & Kuhad, R. C. (2000). Degradation of the pesticide lindane by white-rot fungi Cyathus bulleri and Phanerochaete sordida. *Pest Manag. Sci., 56,* 142-146.

Singh, B. K., Walker, A., Morgan, J.A.W., & Wright, D.J. (2003a). Role of soil pH in the development of enhanced biodegradation of fenamiphos. *Applied and Environmental Microbiology, 69,* 7035–7043.

Singh, B. K., Walker, A., Morgan, J. A.W., & Wright, D. J. (2003b). Effect of soil pH on the biodegradation of chlorpyrifos and isolation of a chlorpyrifos-degrading bacterium. *Applied and Environmental Microbiology, 69,* 5198–5206.

Singh, B. K., Walker, A., Morgan, J. A. W., & Wright, D. J. (2004). Biodegradation of chlorpyrifos by Enterobacter strain B-14 and its use in bioremediation of contaminated soils. *Applied and Environmental Microbiology, 70,* 4855–4863.

Singh, B. K., Walker, A., & Wright, D. J. (2002). Degradation of chlorpyrifos, fenamiphos and chlorothalonil alone and in combination and their effects on soil microbial activity. *Environmental Toxicology and Chemistry, 21,* 2600–2605.

Singh, B. K., Walker, A., & Wright, D. J. (2005). Cross-enhancement of accelerated biodegradation of organophosphorus compounds in soils: dependence on structural similarity of compounds. *Soil Biology & Biochemistry, 37,* 1675–1682.

Singh, B. K., Walker, A., & Wright, D. J. (2006). Bioremedial potential of fenamiphos and chlorpyrifos degrading isolates: Ifluence of different environmental conditions. *Soil Biology and Biochemistry, 38*, 2682–2693.

Skipper, H. D., C. M. Gilmour, & W. R. Furtick. (1967). Microbial versus chemical degradation of atrazine in soils. *Soil Sci. Soc. Am. Proc., 31,* 653-656.

Slade. P., & Smith, A. E. (1965). Photochemical degradation of diquat. *Nature, 213,* 919-920.

Smith, S. N., Lyon, A. J. E., & Sahid, Ismail BIN. (1976). The Breakdown of Paraquat and Diquat by Soil Fungi. *New Phytologist, 77*(3), 735.

Sohi, S., Krull, E., Lopez-Capel, E., & Bol, R. (2010). A review of biochar and its use and function in soil. Adv Agron, 105, pp. 47–82.

Solanki, A., & Boyer, T. H. (2017). Pharmaceutical removal in synthetic human urine using biochar. Environ. *Sci: Water Res. Technol, 3*, 553 – 565.

Srivastava. V., Weng, C. H., Singh, V. K., Sharma, Y. C. (2011). Adsorption of Nickel ions from aqueous solutions by Nano alumina: Kinetic, Mass transfer, and Equilibrium studies. *Journal of Chemical and Engineering data, 56,* 1414-1422.

Sun, J., Fuhong, H., Yinghua, P., & Zhenhua, Z. (2016). Effects of pyrolysis temperature and residence time on physicochemical properties of different biochar types. *Acta Agriculturae Scandinavica, Section B — Soil & Plant Science,* 12-22

Sun, K., Jin, J., Keiluweit, M., Kleber, M., Wang, Z., Pan, Z., & Xing, B. (2012). Polar and aliphatic domains regulate sorption of phthalic acid esters (PAEs) to biochars. *Bioresour. Technol, 118,* 120–127.

Tan, X., Liu Y., Zeng, G., Wang, X., Hu, X., Gu, Y.,0- Yang, Z., (2015). Application of biochar for the removal of pollutants from aqueous solutions. *Chemosphere, 125,* 70-85.

Tantriratna, P., Wirojanagud, W., Neramittagpong, S., Wantala, K., & Grisdanurak, N. (2011). Optimization for UV-photocatalytic degradation of paraquat over titanium dioxide supported on rice husk silica using Box-Behnken design. *Indian Journal of Chemical Technology, 18,* 363-371.

Tran, H. N., Wang, Y. F., You, S. J., & Chao, H. P. (2017). Insights into the mechanism of cationic dye adsorption on activated charcoal: The importance of π–π interactions. *Process Safety and Environmental Protection, 107,* 168-180.

Tsai, W.T., Chang, C.Y., & Lee, S.L. (1997). Preparation and characterization of activated carbons from corn cob. *Carbon, 35,* 1198-1200.

Tsai, W. T., & Chen, H. R. (2013). Adsorption kinetics of herbicide paraquat in aqueous solution onto a low-cost adsorbent, swine-manure-derived biochar. Int. J. Environ. *Sci. Technol, 10,* 1349-1356.

Tsai, W. T., Hsien, K. J., Chang, Y. M., & Lo, C. C. (2005). Removal of herbicide paraquat from an aqueous solution by adsorption onto spent and treated diatomaceous earth. *Bioresource Technology, 96,* 657-663.

Tsai, W. T., & Lai, C.W. (2006). Adsorption of herbicide paraquat by clay mineral regenerated from spent bleaching earth. *Journal of Hazardous Materials B134,* 144-148.

Tsai, W. T., Lai, C. W., & Hsien, K. J. (2003). Effect of particle size of activated clay on the adsorption of paraquat from aqueous solution. *Colloids and Surfaces, 263,* 29-34.

Tsai, W. T., Lai, C. W., & Hsien, K. J. (2003). The effects of pH and salinity on kinetics of paraquat sorption onto activated clay. *Colloids and Surfaces, 224,* 99-105.

Tsai, W. T., Lai, C. W., & Hsien, K. J. (2004). Adsorption kinetics of herbicide paraquat from aqueous solution onto activated bleaching earth. *Chemosphere 55,* 829 – 837.

Tu, C. M., & Bollen, W. B. (1968). Interaction between paraquat and microbes in soil. *Weed Research, 8,* 38-45.

Uchimiya, M., Wartelle, L. H., & Boddu, V. M. (2012). Sorption of triazine and organophosphorus pesticides on soil and biochar. *Agricultural and food chemistry, 60,* 2989−2997.

United States Environmental Protection Agency (EPA). (2011). *Finalization of Guidance on Incorporation of Water Treatment Effects on Pesticide Removal and Transformations in Drinking Water Exposure Assessments*. Washington, D.C.: Office of Pesticide Programs U.S. Environmental Protection Agency,

Upton, B. R., Hendley, P., & Skidmore, M. W. (1985). *Paraquat: Hydrolytic Stability in Water at pH 5, 7 and 9,* Unpublished Study Submitted by ICI Plant Protection Division, Jealott's Hill Research Centre, Bracknell, Berkshire, UK, Report no. RJ0436B, Syngenta File no. PP148/0666.

Vassilev, S. V., Baxter, D., Andersen, L. K., Vassileva, C.G., & Morgan, T.J. (2012). An overview of the organic and inorganic phase compostion of biomass. *Fuel 94,* 1-33.

Vyavahare, G., Jadhav, P., Jadhay, J., Patil, R., Aware, C., Patil, D., Gophane, A., Yan, Y.H., & Gura, R. (2019). Strategies for crystal violet dye sorption on biochar derived from mango leaves and evaluation of residual dye toxicity. *J. Clean. Prod, 207,* 296-305.

Wang, S., Wang, K., Dai, C., Shi, H., & Li, J. (2015). Adsorption of Pb^{2+} on amino-functionalized core-shell magnetic mesoporous SBA-15 silica composite. *Chem. Eng. J., 262,* 897-903.

Wang, Y., & Liu. R. (2017). Comparison of characteristics of twenty-one types of biochar and their ability to remove multi-heavy metals and methylene blue in solution. Fuel Process. *Technol., 160,* 55–63.

Warnock, D.D., Lehmann, J., Kuyper, T. W., Rillig, M. C. (2007). Mycorrhizal responses to biochar in soil–concepts and mechanisms. *Plant Soil, 300,* 9-20.

Weber, J. J., Metcalf, R. L., & Pitts, J. N. (1972). *Adsorption in physicochemical processes for water quality control.* NY: Wiley Interscience.

Weber, J. B., Best, J. A., & Witt, W.W. (1974). Herbicide residues and weed species shifts on modified-soil field plots. *Weed Science, 22,* 427–433.

Weber, W.J., Jr., E. (1984). Evolution of a Technology. *Journal of the Environmental Engineering Division, American Society of Civil Engineers, 110* (EE5), 889-917

Weng. (2014). Effective removal of copper ions from aqueous solution using base treated black tea waste. *Ecol. Eng, 67,* 127-133.

WHO. (1990). *The public health impact of pesticides use in agriculture*. Geneva: World Health Organization.

Wolff, M. S. (1993). Blood levels of organochlorine resudues and risk of brast cancer. *Journal of the National Cancer Institute, 85,* 648-652.

World Health Organization (WHO). (1984). *Environmental health criteria for parquet and diquat. Interantional programe on chemical safety.* Environmental health criteria 39

Xiao, F., & Pignatello, J. J. (2015). Interactions of triazine herbicides with biochar: Steric and electronic effects. *Water Research, 80,* 179-188.

Yadav, O. O., Hossain, F., Karjagi, C. G., Kumar, B., Zaidi, P. H., Jat, S.L., Chawla, J.S., Kaul, J., Hooda, K.S Kumar, P., Yadava, P., & Dhillon, B.S. (2015). Generic improvement of maize in India: retrospect and prospects. *Agric Res, 4*, 325-338.

Yamada. Y. (2004). *Report of FAO/WHO Meeting on Pesticide Residues*. Rome.

Yang, H., Yan, R., Chen, H., Lee, D. H., & Zheng, C. (2007). Characteristics of hemicellulose, cellulose and lignin pyrolysis. *Fuel, 86,* 1781-1788.

Yavari, S., Malakahmad, A., & Sapari, N.B. (2015). Biochar efficiency in pesticides sorption as a function of production variables – a review. *Environ Sci Pollut Res, 22,* 13824-13841.

Yin, Z., Liu, Y., Tan, X., Jiang, L., Zeng, G., Liu, S., Tian, S., Liu, S., Liu, N., & Li, M. (2019). Adsorption of 17β-estradiol by a novel attapulgite/biochar nanocomposite: characteristics and influencing factors. *Process Saf. Environ. Protect, 121,* 155–164.

Zauscher, F., Chalela, G., & Kopytko, M. (2002). Biodegradation of two commercial herbicides (Gramoxone and Matancha) by the bacteria Pseudomonas putida. *Electron. J. Biotechn. 5,* 182-195. Doi: 10.2225/vol5-issue2-fulltext-1

Zaushitsyna, O., Berillo, D., Kirsebom, H., & Mattiasson, B. (2013). Cryostructured and Crosslinked Viable Cells Forming Monoliths Suitable for Bioreactor Applications. *Topics in Catalysis*, *57*(5), 339.

Zhang, G., Zhang, Q., Sun, K., Liu, X., Zheng, W., & Zhao, Y. (2011). Sorption of simazine to corn straw biochars prepared at different pyrolytic temperatures. *Environment Pollution, 159,* 2594-2601.

Zhang, P., Sun, H., Yu, L., & Sun, T. (2013). Adsorption and catalytic hydrolysis of carbaryl and atrazine on pig manure-derived biochars: impact of structural properties of biochars. *J. Hazard. Mater, 244,* 217–224.

Zhang, X., Gao, B., Zheng, Y., Hu. X., Creamer, A.F., Annable, M.D., & Li, Y. (2017). Biochar for volatile organic compound (VOC) removal: sorption performance and governing mechanisms. *Bioresour. Technol, 245,* 606 -614.

Zhang, Y., Liu, G., Chen, L., & Zheng, H. (2016). Adsorption of chlorpyrifos on giant reed derived biochars. Paper presented at the International conference on civil, transportation and environment (ICCTE 2016), *Atlantis Press*, 1015-1018.

Zhao, L., Cao, X., Masek, O., & Zimmerman, A. (2013). Heterogeneity of biochar properties as a function of feedstock sources and production temperatures. *J Hazard Mater, 256,* 1-9.

Zheng, H., Zhang, Q., Liu, G., Luo, X., Li, F., Zhang, Y., & Wang, W. (2019). Characteristics and mechanisms of chlorpyrifos and chlorpyrifos-methyl adsorption onto biochars: influence of dashing and low molecular weight organic acid (LMWOA) aging and coexistence. *Sci. Total Environ. 657,* 953–962.

Zhou, L., Liu, Y., Liu, S., Yin, Y., Zeng, G., Tan, X., Hu, X., Hu, X., Jiang, L., Ding, Y., Liu, S., & Huang, X. (2016). Investigation of the adsorption-reduction mechanisms of hexavalent chromium by ramie biochar of different pyrolytic temperatures. *Bioresource Technology, 218,* 315-359.

Zhu, C., Wang, L., & Chen, W. (2009). Removal of Cu (II) from aqueous solution by agricultural by-product: peanut hull. *Journal of Hazardous Material, 168,* 739-746.

Zhu, D., Kwon, S., & Pignatello, J. (2005). Adsorption of single-ring organic compounds to wood charcoals prepared under different thermochemical conditions. *Environ. Sci. Technol*, *39*(11), 3990–3998.

Zhu, D., & Pignatello, J. (2005). Characterization of aromatic compound sorptive interactions with black carbon (charcoal) assisted by graphite as a model. Environ. *Sci. Technol, 39*(7), 2033–2041.